

https://dspace.org/

The accumulation of heavy metals in sedimentary deposits in the Fleurhof and Russel Stream Dams of the Central Rand, Johannesburg

Ndasi, Moses Babila

2008-10-23T11:01:35Z
http://hdl.handle.net/10539/5807

Downloaded from a DSpace repository. https://dspace.org/

University of the Witwatersrand, Johannesburg.

THE ACCUMULATION OF HEAVY METALS IN SEDIMENTARY DEPOSITS IN THE FLEURHOF AND RUSSEL STREAM DAMS OF THE CENTRAL RAND, JOHANNESBURG.

Moses Babila Ndasi

A Research Report submitted to the Faculty of Science, University of the Witwatersrand Johannesburg, in partial fulfilment of the requirements of the Degree of Masters of Science.

October, 2007

Johannesburg.

DECLARATION

I hereby declare that this report is my own, unaided work. It is being submitted for the degree of Masters of Science at the University of the Witwatersrand, Johannesburg. It has not been submitted before for any degree or examination in any other University.

_____

Signature of Candidate

This ---------- Day of---------- 2007.

DEDICATION

“ Yes, he’s my son, and I will sponsor his education up to the University…” I can’t actually remember which year this was, but I remember I was at secondary school, and she was saying these challenging words, one winter morning, to one of my aunts because they had a quarrel. And she kept to her promise. That’s why I am dedicating this piece of work and all its fruits to her, my beloved mum,

Mama Prudencia Mbongeh,

the most-determined woman I have ever known in my life so far.

ACKNOWLEDGEMENTS

I would like to express my indebtedness to all those who contributed directly or indirectly to the success of this project.

I would especially like to thank Prof. M.J. Viljoen and Prof. T. S. McCarthy who reviewed and commented on the entire manuscript with good faith, incredible patience and guidance as my supervisors. I equally thank Prof. Kim Hein and Prof. Paul Dirks for their useful comments.

Special thanks go to Prof. J.H Annegarn, my pace-setter at Wits, for his wise counsel, advice and encouragements.

This project wouldn't have gone this far if not for the incredible financial support of URAMIN Inc. Particularly I want to thank Mr George Roach for offering me a bursary and Marco for assisting with the modelling software (Geo-station). Special thanks also go to Mrs Fiona Neville, Mrs Laura and the rest of the URAMIN staff for their kind support and advice.

Crown Gold Recovery Ltd, particularly Mr Willie Laing, and Patrick, are thanked for providing gold value distribution data collected during the evaluation of the stream and dam sediment prior to mining and information on the Central Rand.

I also wish to thank Dr. H.Tutu for carrying out ICP-OES analysis as well as giving good and faithful field assistance, the Council for Geosciences in Pretoria for carrying out ICP-MS analysis, Mrs. S. Farrel for undertaking XRF analysis, Mrs Lyn Whitfield, Mrs Dianne Du Toit and Mrs Wendy for assisting with cartography and Dr. Frederick Mphephu for his mentorship and field guidance.

I can't forget to say thanks to Mr Walton Imrie, Mr. Chris Picken and Mr John Stockley, who provided me work with Shanta Gold that got me supplementary finance and time to catch up with studies. May they extend my gratitude to their families as well?

Sincere thanks also go to many of my relatives and friends who showed me love and gave me courage in this venture which though may look simple, was both intriguing and challenging. These include my beloved mum, Mama Prudencia Mbongeh; my Dad Mr. Kum Fidelis; my beloved fiancée, Anne L.; my friends, Eddie B.; B. Steve, Fefe, Nandi K., Thandi M, T. Roseline; Magdo Assey; Nelson Fultang; Sama Aloysius; Jude Eze; Ni Emmanuel Fomba, and all my brothers and sisters, namely; Ndasi Eugene; Ndasi Mary; Kum Beltha; Kum Carine; Ngole Dohmua; my son, Ndasi Williams Fritx; my niece, Ndasi Clivette; as well as those whose names I have not mentioned.

If this project has any merits, they are due to the wise counsel and contributions of the above-mentioned people. Its shortcomings whether of style or arrangement, errors of facts or interpretation are all mine.

ABSTRACT

Exploitable auriferous conglomerates were first discovered on the farm Langlaagte in the Central Rand area of the Witwatersrand Basin in 1886. This led to a rush for gold and the establishment of the early mines around Johannesburg, providing the nucleus for the gold-mining industry, which subsequently played a dominant role in the economy of South Africa. In order to recover the mineral wealth, huge quantities of rock were mined, transported, crushed, milled and processed and the bulk of the fine residue transported to the mine waste disposal areas or tailings dumps. Approximately 240 mine tailings dumps have been registered in the Witwatersrand Basin, with 103 in the Central Rand.

Fleurhof Dam (on Rand Leases) and Russel Stream dam (on Crown Mines) are some of the dams that were built at the turn of the 20th century on boggy wetlands and vleis to serve as water reservoirs for mines of the Central Rand. These dams have accumulated tailings eroded from surrounding tailings dumps for over 100 years. The main aim of this study is to investigate the distribution and concentration of metals in the dam sediments and compare their geochemistry and mineralogy. Cross-sections of the exposed face of the dam deposits were drawn, and these portray considerable similarities in the stratigraphic sequences, with much of the sediment being mud.

Samples were collected from a series of profiles through the sedimentary accumulation, where exposed. The samples were analyzed by various methods (e.g. ICP-OES, ICP-MS, XRF) for a range of major and trace

elements and also examined by XRD. Results show very high concentrations of metals in the dam sediments. The concentrations of metals in the dam sediments were observed to be higher than in the surrounding tailings dumps from where they have been derived by run-offs. This observation means that dam sediments are traps to heavy metals entrained by surface waters from tailings dumps. The major element (mineral) with the greatest abundance is SiO_2, suggesting that the sediments are silica enriched, followed by Al_2O_3 and Fe_2O_3. Metal concentration particularly gold, is higher where the clay content is higher. Minerals that occur in greater abundance include quartz and pyrophylite. Other minerals that occur in smaller proportions are illite, muscovite, pyrite and uraninite, a reflection of the mineralogy of the Witwatersrand conglomerates.

Sediment thickness and gold value data obtained by Crown Gold Recoveries were also modelled and integrated into this study. Thickness models show that sediments are thicker along the main river channels. More gold occurs in the finer, thinner sediments of the prodelta than in coarser thicker sediments of the bar back. High concentrations of gold in these sediments have been proven to be economically viable in both the Fleurhof and Russel Stream dams. In Fleurhof Dam, reprocessing of silt sediments by Crown Gold Recovery yielded an average of two grams Au per ton (2 g/t Au), but with values up to 30 g/t Au in areas along the delta front. Reserve calculations on the Russel Stream sediments (still unmined) gave a total estimated gold content of 6.4 tons (206,452 ounces) at an average grade of 0.8 g/t Au.

TABLE OF CONTENTS

Content	Page
Declaration	i
Dedication	ii
Acknowledgements	iii
Abstract	v
Table of contents	vii
List of figures	xi
Chapter one-Introduction	1
Chapter two-Aim and objectives	9
Chapter three-Location of study areas	10
Chapter four-Geology of the Central Rand	12
Chapter five-Study methodology of Fleurhof Dam	15
V.1. Mapping and Sampling of Fleurhof Dam sediments	15
V.2. Sediment thickness isopach and gold value isochon	16
V.3. Stratigraphic logging and profiling of Fleurhof Dam	16
V.4. Mineralogical analysis of Fleurhof Dam sediments	17
V.4.A). X-Rays Diffraction (XRD)	17
V.4.B). Reflectance spectroscopy	17
V.5. Geochemical analysis of Fleurhof Dam sediments	18
V.5.A). X-Ray Fluoresecence analysis	18
V.5.B). ICP-OES analysis	18
V.6. Normative calculations of Fleurhof Dam sediments	20

Content **Page**

Chapter six-Results and discussions of Fleurhof Dam study 21

VI.1. Sedimentology of Fleurhof Dam sediments 21

VI.1.i. Sediment thickness 21

VI.1.ii. Longitudinal Section of Fleurhof Dam sediments 25

VI.1.iii. Stratigraphic columns of Fleurhof Dam sediments 27

VI.1.iv. Depositional style and sediementation of Fleurhof dam deposit 30

VI.2. Gold value distribution in Fleurhof Dam sediments 32

VI.3. Mineralogy Fleurhof Dam sediments 36

VI.3.A. X-Ray diffraction analysis 36

VI.3.B. Reflectance spectroscopy 38

VI.4. Geochemistry of Fleurhof Dam sediments 40

VI.4.A. Major Elements 40

VI.4.A.i. X-Ray Fluorescence (XRF) analysis 40

VI.4.B. Trace elements 47

VI.4.B.i.). X-Rays Fluorescence (XRF) analysis 47

VI.4.B.i. ICP-OES analysis 55

Chapter seven-Study methodology of Russel Stream dam 63

VII.1. Mapping and sampling of Russel Stream dam sediments 63

VII.2. Sediment thickness isopach and gold value isochon 64

VII.3. Stratigraphic logging and profiling of Russel Stream dam 65

Content **Page**

VII.4. Mineralogical analysis of Russel Stream dam sediments 65

VII.4.A). X-Rays Diffraction (XRD) 65

VII.5. Geochemical analysis of Russel Stream dam sediments 65

VII.5.A). X-Ray Fluoresecence analysis 65

VII.5.B). ICP-MS analysis 66

VII.6. Normative calculations of Russel Stream dam sediments 66

Chapter eight-Results and discussions of Russel Stream dam study 67

VIII.1. Sedimentology of Russel Stream dam sediments 67

VIII.1.i. Sediment thickness 67

VIII.1.ii. Longitudinal Section of Fleurhof Dam sediments 69

VIII.1.iii. Stratigraphic columns of Russel Stream dam 71

VIII.1.iv. Depositional style and sediementation of Russel Stream deposit 73

VIII.2. Gold value distribution in Russel Stream dam sediments 73

VIII.3. Mineralogy Russel Stream dam sediments 77

VI.3.A. X-Ray diffraction analysis 77

VIII.4. Geochemistry of Russel Stream dam sediments 78

VIII.4.A. Major Elements 78

VI.4.A.i. X-Ray Fluorescence (XRF) analysis 79

VIII.4.B. Trace elements 84

VIII.4.B.i.). X-Rays Fluorescence (XRF) analysis 84

VIII.4.B.i. ICP-MS analysis 89

Content **Page**

Chapter nine-Discussion and Conclusions 94

IX.1. Study methodology 94

IX.2. Sedimentology 95

IX.3. Mineralogy 96

IX.4. Geochemistry 97

IX.4.i. Major Elements 97

IX.4.i. Trace elements 97

References 99

Appendix A. Analytical quality 102

A.1. XRF and ICP-OES analyses of Fleurhof Dam sediments 102

A.2. XRF and ICP-MS analyses of Russel Stream sediments 105

LIST OF FIGURES

Figure 1. Google Earth picture showing location of Fleurhof Dam and Russel Stream dam in relation to tailings dumps, the Upper Klipspruit Stream tailings dumps sampling points and the Fleurhof Township. (Google Earth, 29 May, 2007).

Figure 2. Locality map of study areas and occurrence of tailings and slimes dumps, the main drainages of the Central Rand and stream sediment sampling points of the upper Klipspruit, modified from Mphephu, (2001).

Figure 3. Central Rand Goldfield; Geology and mining leases (Mphephu, 2001).

Figure 4. Isopach map of sediment thickness (m) in the Fleurhof Dam (modified from Ndasi, 2004).

Figure 5. Cross sections along lines a) U-V; b) W-X; c) Y-Z on figure 4, shows the changes in sediment thickness and water depth from the dam wall toward the river mouth of the Fleurhof Dam, due to depositional control factors such as velocity, sediment load and accommodation space.

Figure 6. Photograph of a section of the exposed unprocessed sediment in Fleurhof Dam (Photo by Ndasi M.B., 06/10/2003)

Figure 7. Stratigraphic profile of the exposed unmined sediment of the Fleurhof Dam

Figure 8. Stratigraphic columns of profiles A,E and H of the Fleurhof Dam sediments.

Figure 9. Idealised sedimentological model for a Mississippi type distributory modified into Fleurhof Dam setting (modified from Dag et al., 1982).

Figure 10. Diagram showing depositional architecture and progradation, with on-lapping sediment (modified from Galloway, 1989).

Figure 11. Isochon map of gold grade (g/t Au) in the Fleurhof Dam sediments. Areas greater than 5g/t Au persist southwards and terminate in a 120m long east-northeast trending, high grade (>10 g/t Au) distal delta front, which extends over a distance of about 250m. An easternmost (south-southeast) trending shoot also has high grades (>10 g/t Au) over variable thicknesses extending over 50m.

Figure 11. Isopach map of gold grade in the Fleurhof Dam sediments. The gold content distribution follows a similar pattern as the gold grade in relation to sediment thickness and channel axes and high grade shoots. Higher gold contents occur where sediments are thinner and vice-versa.

Figure 13. Ternary plots of major elements for profiles A, E, H and stream sediments and tailings from surrounding tailings dumps of the Fleurhof deposit. This indicates the relative abundance of silica (quartz), aluminium (pyrophylite) and clay-rich (illite) minerals in the sediments.

Figure 14. Ternary plots of major minerals for profiles A, E and H of Fleurhof Dam.

Figure 15. Comparative graphs of selected metals to illustrate the relation between metal concentration and stratigraphy along profile A in Fleurhof Dam sediments.

Figure 16. Comparative graphs of selected metals to illustrate the relation between metal concentration and stratigraphy along profile E in Fleurhof Dam sediments.

Figure 17. Comparative graphs of selected metals to illustrate the relation between metal concentration and stratigraphy along profile H in Fleurhof Dam sediments.

Figure 18. Correlation plots of a) Mn vs Cu for profile E; b) Mn vs Ni for profile E; c) Fe vs Ni for profile A; d) Fe vs Cu for profile E for Fleurhof Dam.

Figure 19. Diagram showing valley silt deposit in dams A, B and C on Russel Stream (Willie, 2005).

Figure 20. Isopach map of sediment thickness (m) along Russel Stream in Dam B. The diagram shows a region of greater than 12m of sediment fill just below and behind the dam wall. An axial zone following the original river course contains sediments in excess of 10m over a distance of 250m.

Figure 21. Isopach map of sediment thicknesses (m) along Russel Stream in Dam C. Dam C occurs downstream of Dam B and shows a similar pattern with an axial zone of greater than 8m thickness.

Figure 22. Stratigraphic section of the exposed unmined face of the Russel Stream dam sediments.

Figure 23. Stratigraphic columns of profiles RS1, RS2, RS3, RS4 and RS5 of the Russel Stream dam sediments.

Figure 24. Isochon of gold grade (g/t Au) in the Russel Stream sediments (Dam B). An area averaging 1g/t Au and trending north – south straddles the dam wall and runs over a distance of about 300m with an average width of 100m. These are in close association with areas of maximum sediment thickness.

Figure 25. Isochon of gold grade (g/t Au) in the Russel Stream sediments (Dam C). Not much high grade ore exists in Dam C.

Figure 26. Ternary plots of major elements for profiles a):RS1; b): RS2; c): RS3; d): RS4 and e): RS5 of Russel Stream Dam B. The ternary plots indicate the dominance of quartz in the samples as seen in the average concentration of major elements in Table 10.

Figure 27. Ternary plots of major minerals for profiles a): RS1; b): RS2; c): RS3; d): RS4 and e): RS5 of Russel Stream Dam B.

Figure 28 Comparative graphs of metals concentration along profile RS1 from along Russel Stream.

Figiure 29. Comparative graphs of metals concentration along profile RS2 from along Russel Stream.

Figiure 30. Comparative graphs of metals concentration along profile RS3 from along Russel Stream.

CHAPTER ONE

INTRODUCTION

Mining is second only to agriculture as the world's oldest and most important industry, and primitive societies have largely depended upon mined products, as illustrated by the nomenclature of those epochs: Stone Age, Bronze Age and Iron Age, a sequence which also shows the increasing complexity of society's relation with mining (Down and Stocks, 1977). Over the centuries, man's use of minerals has been characterized by an increased variety of minerals used, for a greater range of purposes and an increased sophistication of the methods of locating, wining and processing those minerals (Ibid). Arising from these trends have been several consequences including a number of important effects on the environment such as the effects of tailings disposal.

South Africa holds the world's largest reserves of ores of platinum-group metals (PGMs), (87.7%), manganese (80%), chrome (72.4%), gold (40.1%), and alumino-silicates (37.4%) and is also prominent in terms of titanium, vanadium, zircon, vermiculite and fluorspar (DME, 2005). Despite the decline in gold output in South Africa during the last two decades, the gold mining industry still makes a major contribution to the economy of South Africa. Sales of primary mineral products accounted for 28.7% of South Africa's total export revenue during 2004, while the contribution of gold decreased to 9.3% from 11.2% in 2003. The declining trend over the last two decades in both these indicators has been the result of the contraction in the gold-mining industry,

increased local beneficiation and relatively lower commodity rand prices across the board. However, the inclusion of various processed mineral products, such as ferro-alloys, aluminium and carbon and stainless steel, would arguably raise the contribution of the minerals sector to above 35%.

Exploitable auriferous conglomerates were first discovered in the Central Rand area of the Witwatersrand basin. The discovery of the rich Main Reef leader in 1886 on the farm Langlaagte led to a gold rush and the establishment of the early mines in the Johannesburg area, providing the nucleus for the gold-mining industry, which subsequently played a dominant role in the economy of South Africa. In order to recover the mineral wealth, huge quantities of rock were mined, transported, crushed, milled and processed and the bulk of the fine residue transported to the mine waste disposal areas or tailings dumps. Mining has been continuous for 120 years in the Johannesburg region and because of this, many mine tailings disposal sites including slimes dams, sand dumps and rock dumps have been established. Approximately 240 mine tailings dumps have been registered in the Witwatersrand Basin, with 103 in the Central Rand.

Water, necessary for milling and cyanidation operations for the Central Rand mines, was obtained by conserving water in reservoirs or dams in the summer rainfall period (Hatch, F and Chalmers, J., 1895). These dams were constructed across vleis or boggy water courses which occur on, or in, the neighbourhood of most properties. The dams were often constructed of earthwork, the material being obtained from the bed or sides of the vleis. The

earth, generally containing a fair proportion of clayey matter was trammed to the dam wall, which was constructed with a core of puddle clay along the central portion, the core being 2 or 3 feet (0.75-1 metre) in thickness and extending some few feet into the bed rock (Ibid).

At the turn of the 20th century (106 years ago) the Fleurhof Dam was built on the upper Klipspruit a few hundred metres south of Florida Lake (Fig.1). The Fleurhof Dam was the first and only masonry (concrete) dam in the district that was built at the time by Rand Mines for the Geldenhuis Deep and other properties. This dam is 12 m deep and about 450 m in length, the capacity being estimated at 700,000,000 gallons (2,590,000,000 litres) (Hatch and Chalmers, 1895). Tailings materials have accumulated in the Fleurhof Dam for more than 100 years, due to erosion from the Rand Leases, Bantjies and other old tailings dumps around the Fleurhof Dam. This has formed a thick layer of sediment, averaging 2m thick, but up to 7m in some areas, part of which Crown Gold Recovery has reprocessed.

At almost the same time, similar events took place in the Crown Mines neighbourhood, when a number of dams were built along the Russel (former Booysens) stream, serving small mines which were later consolidated to become Crown Mines Ltd in 1909 (Laing, 2005, personal communication). The Crown Reef dam was situated immediately east of a mine road currently known as Crownwood road and the Russel Stream dam was constructed some several hundred metres to the west of this.



Fig. 1: Google Earth picture showing location of Fleurhof Dam and Russel Stream dam in relation to tailings dumps, the Upper Klipspruit Stream tailings dumps sampling points and the Fleurhof Township (TDA, TDC, TDD, TDE and TDB1 = tailings dump sampling points) (Google Earth, 29 May, 2007).

Silting up of the Russel Stream dams occurred with mine material originating from the tailings disposal sites of small mines operating in the area. These mines with names such as “Crown Reef G.M.Co Ltd, Crown Deep Ltd and others were in close proximity to the dams, rivers and other drainage systems (Fig.2)

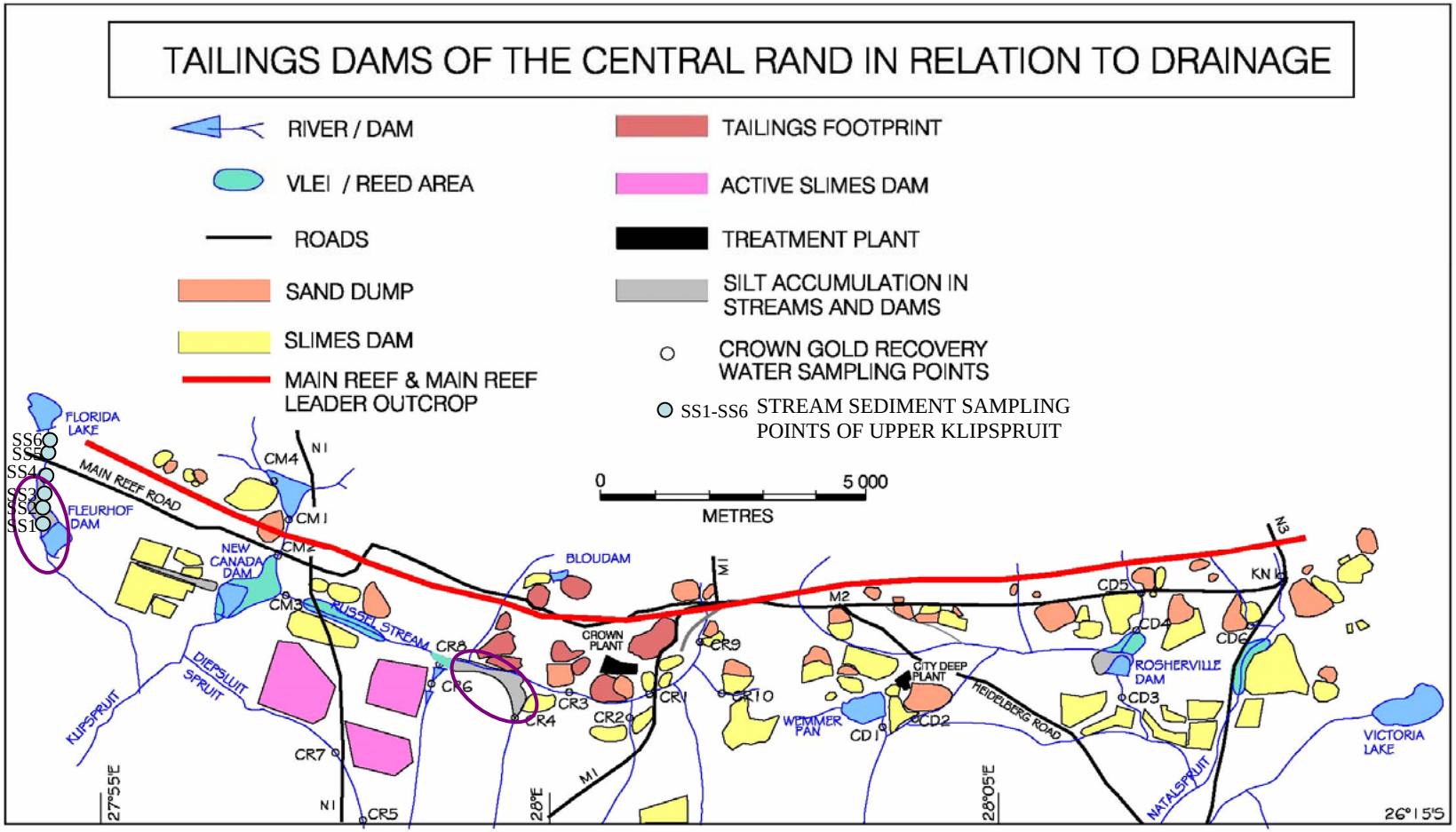


Fig.2: Locality map of study areas and occurrence of tailings and slimes dumps, the main drainages of the Central Rand and stream sediment sampling points of the upper Klipspruit. CR = Crown Mines, CD = City Deep. (Modified from Mphephu, 2001).

As siltation of the dams continued, the stream was displaced and its original course changed slightly northward. Current reclamation has partly uncovered the old stream and dam positions. The thickness of sediments in the Russel Stream dam ranges from 2m to 12m and this deposit is now referred to as valley silt by Crown Gold Recovery. Silts of the Crown Reef dam have been almost totally removed by Crown Gold Recovery while that of the Russel Stream dam is still largely untouched.

Tailings are finely crushed rock particles and mineral wastes remaining after the extraction of valuable components that are produced and deposited in slurry form on tailings dumps. During rainfall, as erosion of poorly managed tailings dumps occurs, the tailings are washed away by rain waters. Sulphide minerals in the tailings particularly pyrite are prone to rapid oxidation and this leads to the formation of acid mine drainage (AMD). As a result, contained heavy metals are leached and dissolved in the water. Both tailings and mobilised metals are transported by streams into the dams. The dams thus act as sinks for sediments. Recent studies (Tutu, 2005) have shown that dams also clean up the acidic waters passing through, suggesting that heavy metals as well as sediments are accumulated in the dam. This includes high concentrations of gold in both the Fleurhof and Russel Stream dam sediments. In Fleurhof Dam, according to data obtained from Crown Gold Recovery, reprocessing of silty sediment by Crown Gold Recovery yielded an average of two grams per ton (2 g/t Au), but with values up to 30 g/t Au in places. Calculations done on gold value distribution data obtained from Crown Gold Recovery on the Russel Stream sediments (still

unmined) suggests 6.4 tons (206,452 ounces) of gold at an average grade of 0.8 g/t Au.

Reprocessing of the sediment in the Fleurhof Dam exposed a section through the deposit, revealing a well-layered stratigraphy representing more than one hundred years of sedimentation, providing an opportunity to examine both sediment and metal accumulation in a mine dam. This exposure provided the motivation for the study in the Fleurhof Dam situated on the Rand Leases (Volgelstruisfontein) G.M. Co; located on the farms Roodepoort 237 and Volgelstruisfontein 231 (Ndasi, 2004).

The Fleurhof Dam study was started as a BSc. Hons degree project in 2004, during which the Stratigraphic profile of the Fleurhof Dam sediments was established, and the isopach map of sediment thickness and isochon map of gold grade and gold content constructed. Ndasi, 2004 observed and concluded that the sediment in the Fleurhof dam was enriched in heavy metals such as Fe, Ni, Co, As, Cu, Zn and Cd. The geochemistry and mineralogy of the sediments have been largely reviewed. In addition, the depositional style of the sediments has been examined and cross-sections drawn to portray the sediment thickness from the dam wall to the river-mouth (prodelta to delta front). A similar exposure of sediments in the Russel Stream dam has been made by a relatively recent erosion channel of the stream, which has cut a section through the northern flank of the sedimentary accumulation, bearing a similarity in stratigraphy to the sediments of the Fleurhof Dam. This similarity in stratigraphy inspired a comparative study on the Russel stream deposit to investigate and confirm the hypothesis that dam sediments are trap sites for heavy metals entrained from surrounding tailings

dumps. The Fleurhof dam study is presented separately in a first section, and the Russel Stream study in a second section, and the results compared in the conclusion.

Samples were collected from a series of profiles through the exposed sedimentary accumulation in both dams. The samples were analyzed for a range of major and trace elements and also examined mineralogically. Results show very high concentration of metals in these sediments. Sediment thickness and gold value data obtained from Crown Gold Recoveries were also modelled and integrated into this study.

CHAPTER TWO

AIM AND OBJECTIVES

The inspiration for this study came from the observation of the general similarities in the stratigraphy of the exposed faces of the sediments of the Fleurhof and Russel Stream dams. The main aim of this study was to investigate the distribution and concentration of metals in the dam sediments. The objectives were therefore:

- To map and draw stratigraphic profiles of both deposits in order to portray the similarities and differences in their stratigraphic sequences.
- To document the abundances and distribution of selected heavy metals in dam sediments.
- To compare metal abundances in the dam sediments with abundances in the sediment source (tailings dumps) to establish whether metals are relatively concentrated in the dams.
- To use data obtained by Crown Gold Recoveries to model and portray sediment thickness and gold value distribution in both deposits.

CHAPTER THREE

LOCATION OF STUDY AREA

The Central Rand goldfield extends for a distance of 45 km, east – west, in the region south of Johannesburg. This area forms part of the northern margin of the Witwatersrand Basin and is bounded in the east by the East Rand Goldfield and on the west by the West Rand Goldfield (Mphephu et al., 2003). Fleurhof Dam is situated on the Rand Leases (Volgelstruisfontein) G.M. Co Property; located on the farms Roodepoort 237 and Volgelstruisfontein 231 (Fig. 1). Russell Stream flows in an east – west direction to the south of Crown treatment plant and north of Gold Reef City on Crown Mines (Fig. 1). The mean annual precipitation of the Gauteng Highveld is about 672 mm, falling mainly during the summer months in the form of heavy thunderstorms. A windy season from August to October precedes the summer rains and is responsible for considerable erosion from exposed tailings dumps and serious air pollution. The northern part of the area forms the east-west watershed between the Crocodile River catchments in the north and the Klip River catchments in the south. The south-western streams, including those around the Fleurhof Dam and Russel Stream, drain into the Klipspruit, while in the east streams drain into the Natalspruit (Fig.2). The Klipspruit and the Natalspruit both drain into the Klip River, which in turn flows into the Vaal River. A subtle N-S watershed between the Natalspruit and the Klipspruit occurs immediately to the west of Wemmer pan (Fig.2). Many tailings dumps of the Central Rand lie in close proximity to these drainage systems and to wetlands and dams including the Klipspruit wetland, New Canada dam, Rosherville dam, Russel Stream and Fleurhof Dam (Mphephu, 2001), the last two being the foci of this

study. Figure 1 is a Google Earth picture showing location of Fleurhof Dam and Russel Stream valley silts, while figure 2 is a locality map of the study areas (Fleurhof Dam Russel Stream silts) in relation to some tailings dumps with respect to their type (sand or slimes) and status in terms of active or footprint remaining after gold reprocessing operations. The drainage systems and dams of the Central Rand with the Fleurhof and Russel Stream silt deposits (highlighted in red) are also shown in figure 2.

CHAPTER FOUR

GEOLOGY OF THE CENTRAL RAND

The Central Rand Group forms the upper succession of sediments of the Witwatersrand Supergroup and contains most of the auriferous conglomerate deposits (Anthony, 1998). The name has been derived from the goldfield, the Central Rand Goldfield. It has well defined structural and sedimentological boundaries and therefore exists as both a geographical and geological entity. In the west, the Central Rand Goldfield terminates against the Roodepoort fault, which strikes in an east-westerly direction. On the north-western side of the fault, the lower West Rand Group beds have been upthrown into a horst, which lies between the Roodepoort and Witpoortje faults (the Witpoortje gap), and in the east it's defined by an anticlinal structure with poor conglomerate development (the Boksburg gap) (Mphephu, 2001).

The Central Rand Group consists predominantly of coarse-grained subgreywacke with less than 10% conglomerate, silt and minor lava (Tankard et al., 1982). The overall depositional setting is that of a series of fan delta complexes prograding into a closed basin, perhaps containing a lake or inland sea. Burke et al. (1986) suggested that the overall tectonic setting is that of a foreland basin related to collisional tectonics in the area of the Limpopo River to the north. The depositional age of this group is 2914 to 2714 ma (Robb and Meyer, 1995).

The Central Rand group contains six major auriferous conglomerate layers, two of which have been extensively mined (Main Reef Leader and South Reef), three

patchily mined (Main Reef, Bird Reef and Kimberley Reef), with one low grade reef (Elsburg Reef) remaining largely unmined (Pretorius, 1964; Hallbauer, 1986; Werdmuller, 1986; Robb and Meyer, 1995; Mphephu, 2001;). The outcrop of these reefs and their geological setting on the Central Rand in relation to the Fleurhof and Russel Stream dams is shown in figure 3.

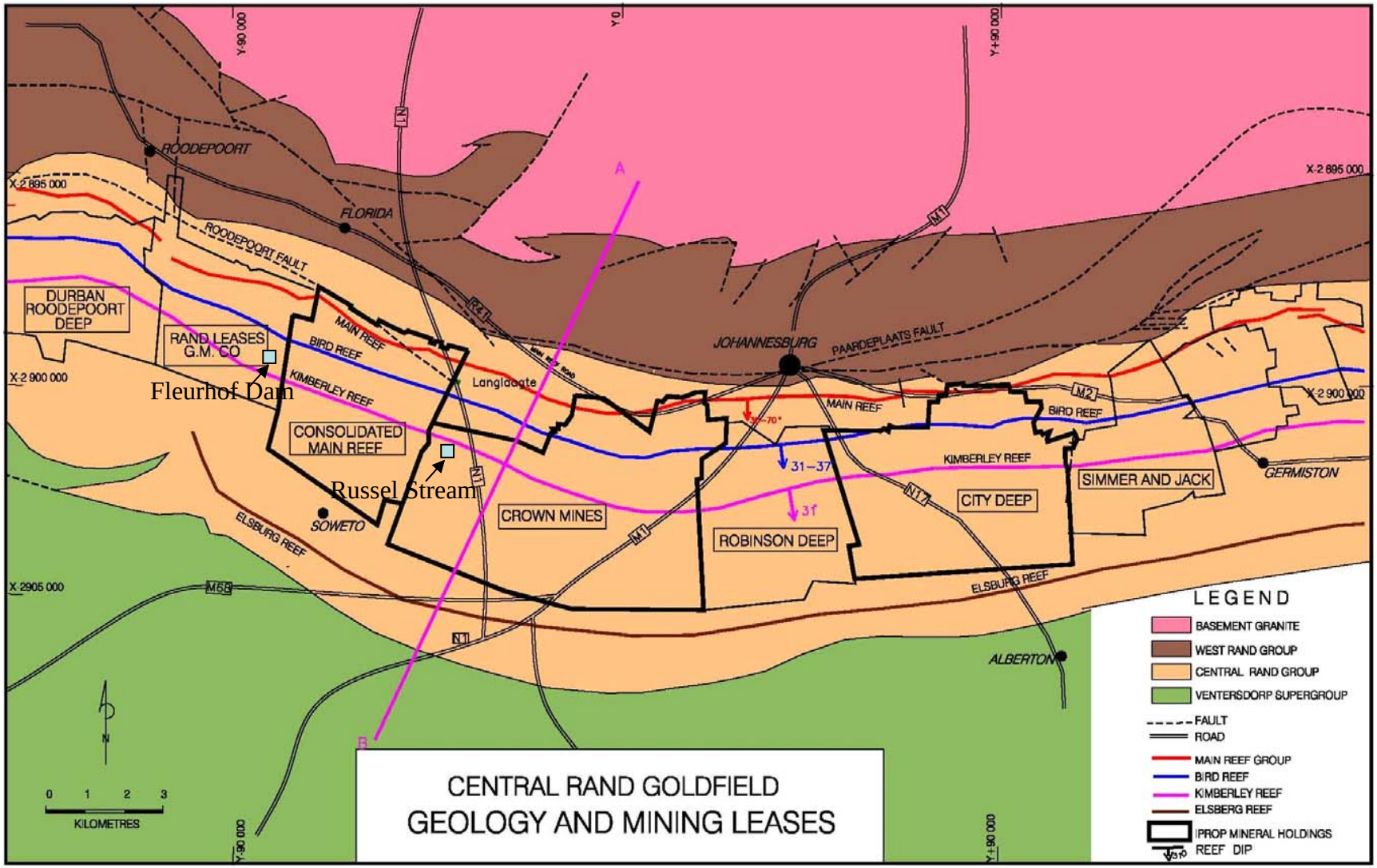


Fig.3: Central Rand Goldfield; Geology and mining leases (after Mphephu, 2001).

CHAPTER FIVE

STUDY METHODOLOGY OF FLEURHOF DAM

V.1. MAPPING AND SAMPLING OF FLEURHOF DAM SEDIMENTS

In 2001 the Fleurhof Dam was drained of water and the tailings sediment accumulated in the dam was sampled on a grid pattern by Crown Gold Recovery. Good gold values were recorded as a result of which much of the sediment below the water level was mined and reprocessed. Mining started near the dam wall in the south and stopped in the northern part of the dam roughly where reed beds of the feeder stream commences. This left a vertical exposed face of sediment and it was this exposure that was mapped and sampled. Coordinates of station points were taken across the length of the exposed face using a GARMIN III GPS. After accurate levelling of points along the profile a geological section of the exposed sedimentary accumulation was compiled and is discussed in section VI.1.iii. The thicknesses of layers were measured using a tape measure. The top of a peat layer at the base of the sediments, possibly originally the grass-covered surface of the dam floor, was taken as the datum and corrections were made for elevations. Three vertical stratigraphic columns labelled A, E and H representative of the various layers of the deposit were also drawn and are discussed in section VI.1.ii.

Samples of sediment were collected from each layer of the stratigraphic columns across the sections mapped. Samples were taken from the top to the bottom of each layer in order to obtain a representative section of the whole thickness of every layer. Tailings dump samples were also collected from surrounding mine tailings dumps, as well as stream sediments along the bed of the upper Klipspruit stream as far as Florida Lake, for a comparative study. Each sample was dried at a temperature of 110ºC for seven hours, milled and then analysed geochemically and mineralogically (Ndasi, 2004).

V.2. SEDIMENT THICKNESS ISOPACH AND GOLD VALUE ISOCHON OF FLEURHOF DAM SEDIMENTS

Drilling data obtained by Crown Gold Recoveries prior to mining were used to model sediment thickness and gold value distribution of the Fleurhof Dam deposit.

V.3. STRATIGRAPHIC LOGGING AND PROFILING OF FLEURHOF DAM SEDIMENTS

Stratigraphic logging and profiling was based on physical observation of the sediments and the main criteria used to differentiate between different layers were colour, texture and internal layering (banding). Based on these criteria the different layers were described and stratigraphic profiles drawn.

V.4. MINERALOGICAL ANALYSIS OF FLEURHOF DAM SEDIMENTS

V.4.A). X-RAY DIFFRACTION (XRD) ANALYSIS

Powder from each sample was placed on a metal slide (a slurry made from selected samples was left to settle on a slide and dried in the open) and XRD was undertaken in the School of Geosciences at the University of the Witwatersrand, Johannesburg, to determine the mineralogical composition of the samples using a Phillips X-ray diffractometer.

V.4.B). REFLECTANCE SPECTROSCOPY

Some samples such as samples F3A, F1E, F3E, F1H and F3H produced poor XRD results. These samples were thought to contain poorly crystalline hydrous ferric minerals. Most hydrous minerals are polymorphic and usually amorphous, making XRD an unsuitable method for their detection (Gordon, 2004).

. These samples and other selected samples were re-analysed using a method called reflectance spectroscopy using a device called Terraspec. This method uses the energy in the visible (0.4 – 0.7μm), near infrared (0.7 – 1.3μm) and short wave infrared (1.3 – 2.5μm) wavelength regions of the electromagnetic spectrum to analyse materials based on their absorption spectra (Ibid).

V.5. GEOCHEMICAL ANALYSIS OF FLEURHOF DAM SEDIMENTS

V.5.A). X-RAYS FLUORESCENCE (XRF)

Geochemical analysis for major and trace elements was done by X-Ray Fluorescence (XRF). The powder from each sample was pressed into pellets and analysed for trace elements. Glass beads were made from the powder of each sample fused with Lithium metaborate for major elements analysis. Mrs. Sharon Farrel of the School of Geosciences in the University of the Witwatersrand undertook XRF analysis.

V.5.B). INDUCTIVELY COUPLED PLASMA-OPTICAL EMISSION SPECTROSCOPY (ICP-OES)

ICP was used to analyse for a number of metals such as Au and U that could not be analysed by XRF, and also to check for the accuracy of XRF (analytical quality).

Inductively Coupled Plasma-Optical Emission Spectroscopy (ICP – OES) was completed for the Fleurhof Dam samples by Tutu of the School of Chemistry at the University of the Witwatersrand, Johannesburg. With ICP OES, the concentrations of metals in samples were determined using a Spectro-Ciros ICP-OES with coupled charge detection (CCD). Calibration was undertaken using certified standards (Industrial Analytical). Analysis of a 1ppm standard gave an instrument capability index of 1.55 (for n = 10), meaning that the instrument is of medium capability. The capability index, Cp, shows how well

a process or instrument is able to meet specifications. It is obtained from the quotient of allowable range/6*standard deviation. A Cp value less than 1 implies that the process is unsatisfactory; a value between 1 and 1.6 implies that the process of medium relative capability while a value greater than 1.6 implies that the process is of high capability (Tutu, and Cukrowska, 2004).

.

Sediments and tailings dumps materials were digested with aqua regia (a 3:1 mixture of hydrochloric and nitric acids). Digestion was completed using an Anton Paar Multiwave 3000 SOLV Microwave Sample Preparation System. Fractionated metal portions in the samples were extracted using the BCR three-step sequential extraction procedure and then determined using the ICP-OES. Sample centrifugation was done using an MSE Mistral 1000 Centrifuge.

The most important anions were determined using the Metrohm 761 Compact Ion Chromatograph with a Metrosep A Supp 5 (6.1006.520) 150 x 4.0 mm analytical column. All solutions were prepared with purified water obtained by passing deionised water through a Milli-Q-water purification system. All chemicals were of analytical grade obtained from Aldrich, Industrial Analytical and Merck (Tutu and Cukrowska, 2004).

V.6. NORMATIVE CALCULATIONS ON FLEURHOF DAM SEDIMENTS

Normative calculations were done for selected major elements; SiO_2, Al_2O_3, K_2O and Fe_2O_3. In these calculations the concentration of the above elements were recalculated as mineral percentages in order to obtain quantitative estimate of the sample mineralogy. Minerals chosen as representatives of the above major elements and calculated were quartz, pyrophylite, illite and hematite respectively and this was portrayed on ternary plots.

CHAPTER SIX

RESULTS AND DISCUSSION OF FLEURHOF DAM STUDY

VI.1. SEDIMENTOLOGY OF FLEURHOF DAM SEDIMENTS

VI.1.i. SEDIMENT THICKNESS.

Data collected by Crown Gold Recovery prior to reprocessing were used as a guide to contour thickness variation of the distal portion of the deposit. The isopach map in figure 4 reveals a delta system with a major tongue of maximum sedimentary deposition along river distributaries and their tributaries (deposition axes). This is defined by a region of greater than 4m thick. In the upper unmined proximal sector of this depository system (bar back or delta top) sediment thickness is greater than 6m in the axial region of the depositional system. Two subsidiary distributaries or channel branches can be discerned on the east side of the main channel axis. To the east, west and southe of the main distributory system, sediment thickness reduces 2 m in the prodelta region. The section lines U-V, W-X and Y-Z are sections drawn in figures 5a), b) and c) to illustrate the relationship between sediment thickness, water depth and gold grade. Section U-V traverses the bar back where sediment thickness is greatest (max. thickness = 7 m, max. water depth = 3 m); W-X traverses the bar front (max. thickness = 5 m, max. water

depth = 9 m) and Y-Z traverses the prodelta region where sediment thickness is smallest (max. thickness = 4m, max. water depth = 10m). Sediments are thinner in regions of deeper waters and vice-versa.

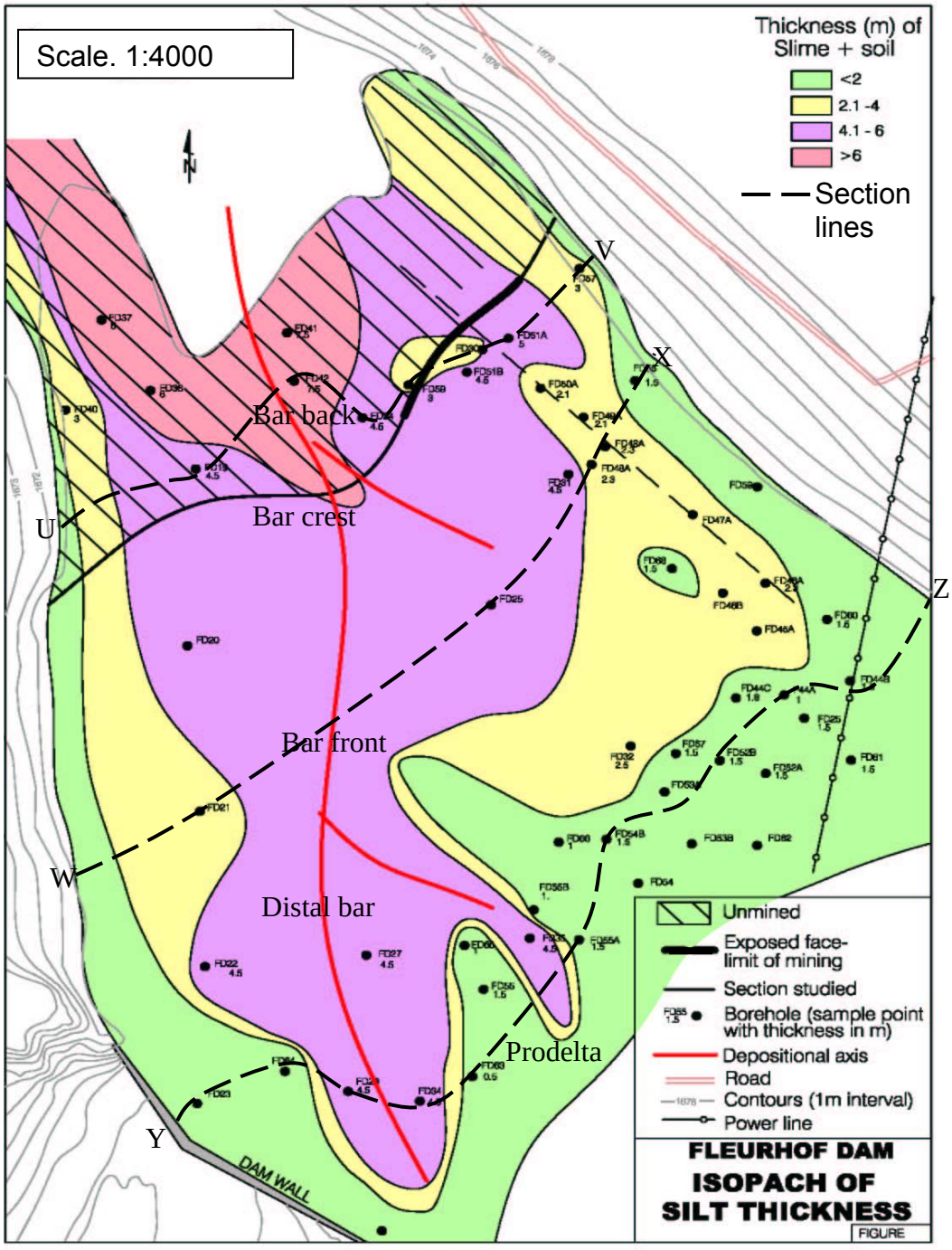


Fig. 4: Isopach map of sediment thickness (m) in the Fleurhof Dam. (The map shows the average thicknesses of the various layers in the sediments. The thicknesses of various layers were obtained from vertical boreholes drilled by

Crown Gold Recovery prior to mining. The map was obtained from Crown Gold Recovery (2004), and hand-contoured. The contoured map was then digitised using GIS software by Mrs Lyn Whitfield and Mrs Dianne Du Toit of the School of Geosciences, University of the Witwatersrand, Johannesburg).

The isopach map shows that the thickness of sediments decrease, in general, from the proximal part of the dam (bar back) toward the deeper water area near the dam wall (distal bar or mid delta) in the prodelta region as shown on profiles in figures 5a), b) and c). There is also an increase in thickness from the sides toward the centre of the dam along the main channel. Fleurhof Dam is a man-made dam that was built across the upper Klipspruit to retain mine water and the deepest area of the dam occurs along the old stream course towards the centre. Water depth thus decreases outward from the centre to the sides and from the prodelta region to the bar back where sediment thickness is highest as illustrated in sections U-V, W-X and Y-Z in figures 5a), b) and c), which are sections showing the relationship between water depth and sediment thickness across the dam. The gold grades shown in these sections are average grades from gold value data obtained from Crown Gold Recovery. Vertical boreholes were drilled using an auger to the bedrock and the average gold grade of the various horizontal layers were used to portray a horizontal gold value occurrence as discussed in section VI.2.

Section U-V traverses the bar back (delta top) where the dam is largely filled up by sediments and having the greatest thickness. Here the sediments are covered by reeds. Line W-X traverses the bar front in the middle of the dam

where sediments are about 4m thick and covered by water, while line Y-Z traverses the prodelta region where sediments are finest and thickness is least.

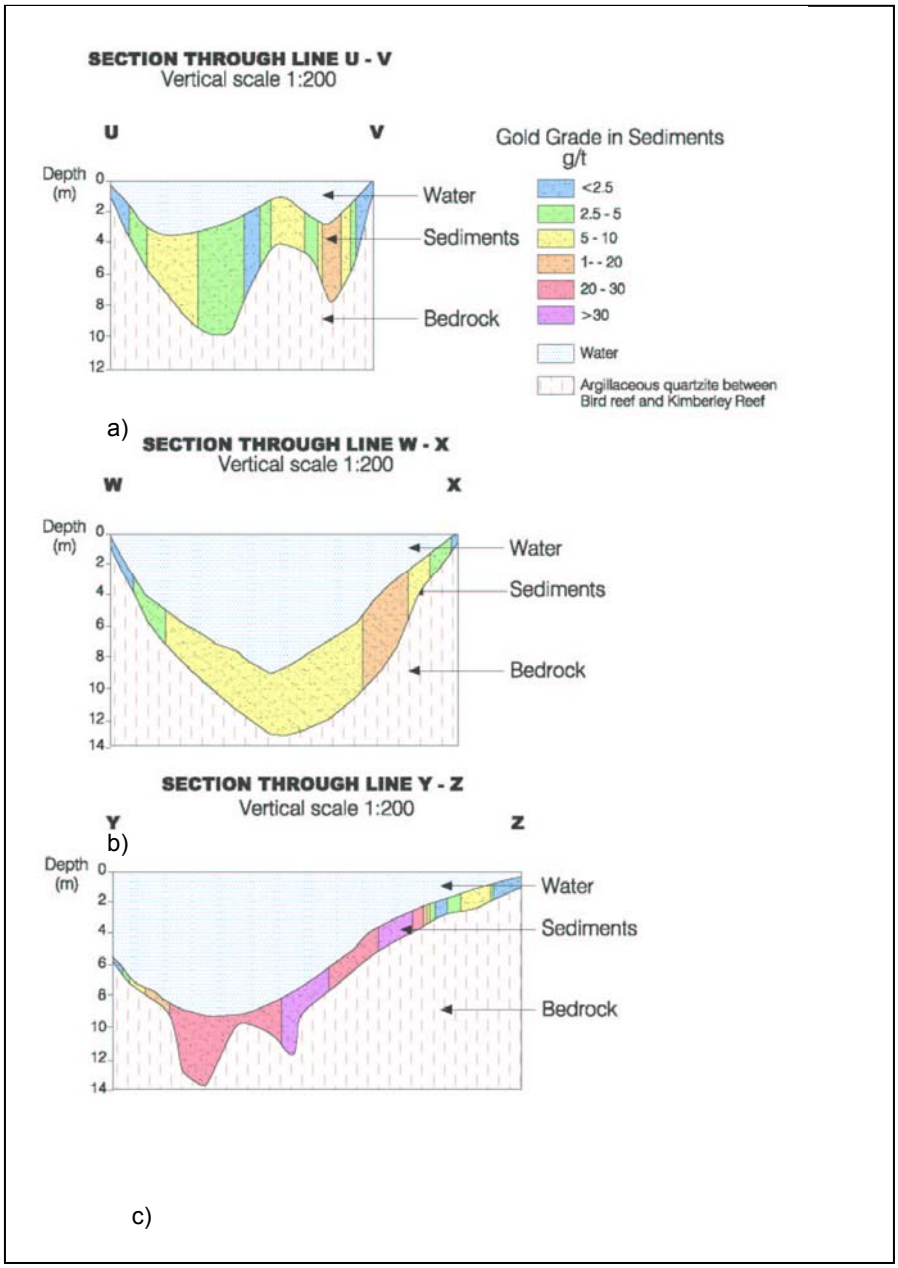


Fig. 5. Cross sections of a) line U-V; b) W-X; c) Y-Z. Sections were hand contoured and digitised using power point.

VI.1.ii. LONGITUDINAL SECTION OF FLEURHOF DAM.

The sediments in Fleurhof Dam have been largely reprocessed by Crown Gold Recovery following the draining of the dam. Mining started from the dam wall and proceeded upstream. From the incomplete reprocessing of the sediment a section through the deposit was left exposed revealing a well-layered stratigraphy representing more than one hundred years of sedimentation. Figure 6 is a photograph of the exposed unmined face of the Fleurhof Dam sediments. It is a section of this exposure that was mapped (Fig.7), sampled and studied for its mineralogy and geochemistry.



Fig.6. Photograph of a section of the exposed unprocessed sediment in Fleurhof Dam.

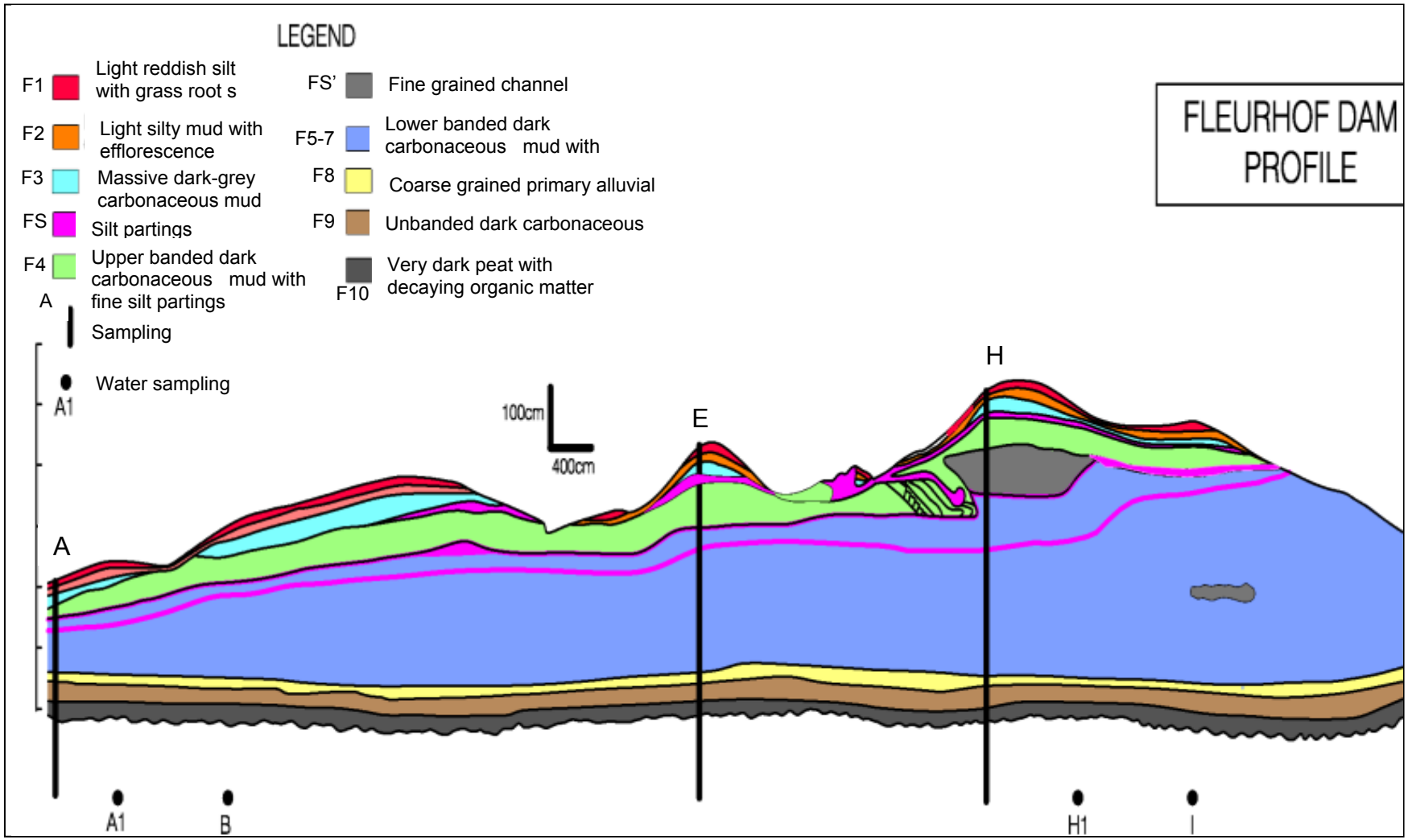


Fig.7. Stratigraphic profile of exposed face of unmined sediment in the Fleurhof Dam (Ndasi, 2004).

VI.1.iii. STRATIGRAPHIC COLUMNS OF FLEURHOF DAM

The stratigraphy of the exposed face of the sediments in the Fleurhof Dam was established from the construction of vertical profiles at varying intervals along the face, (Fig.8). The section shown in figure 8, page 28, represents a continuous stratigraphic section of the Fleurhof Dam Based on extrapolation between the vertical profiles A, E and H. Most of the sediments are mud and silt and the following stratigraphy was established along the studied section with the following layers occurring from bottom to top:

F10: a very dark (charcoal coloured) peat layer with decaying organic material that lies on a bed rock of argillaceous quartzite. This probably represents decomposed materials of the original surface before sedimentation.

F9: a dark unbanded carbonaceous mud.

F8: a coarse grained reddish-brown primary alluvial sand and grit. This would probably have been eroded from the bedrock and brought into the dam as basal sediments.

F5-7: a lower banded carbonaceous mud with larger but less numerous silt partings and bands. Layers 5-7 were sampled and described as one on the basis of characteristic similarity.

FS': a fine grained channel sand

FS: a very fine grained fluvial inter-band sand

F4: an upper dark banded carbonaceous mud layer with thin silt partings

F3: a massive light-grey banded carbonaceous mud with very thin but numerous silt partings and bands

F2: a light brown silt with roots also encrusted with efflorescence on the face

F1: Reddish brown clay soil with grass roots and usually encrusted by efflorescence on the top, and sometimes having bands of fine-grained sand. It is covered by reeds.

Figure 6 shows the three vertical stratigraphic profiles labelled A, E and H of the Fleurhof Dam sediments drawn using colour, texture and grain size as criteria for logging. The manner in which Samples as represented in figure 8 have been collected from the dam is as follows: samples F1A, F1E and F1H are taken from the same layer F1 in such a way that each sample is a representative of the entire layer within the corresponding profile. The section studied is 137m in length and varies in thickness from 2m to 6m, being thickest at the main distributory channel. Layers are consistent throughout the studied section except for some areas in the middle of the section that have been eroded by distributary channels of the river. Lines A, E and H are the lines of vertical profiles (stratigraphic columns) from where samples were collected.

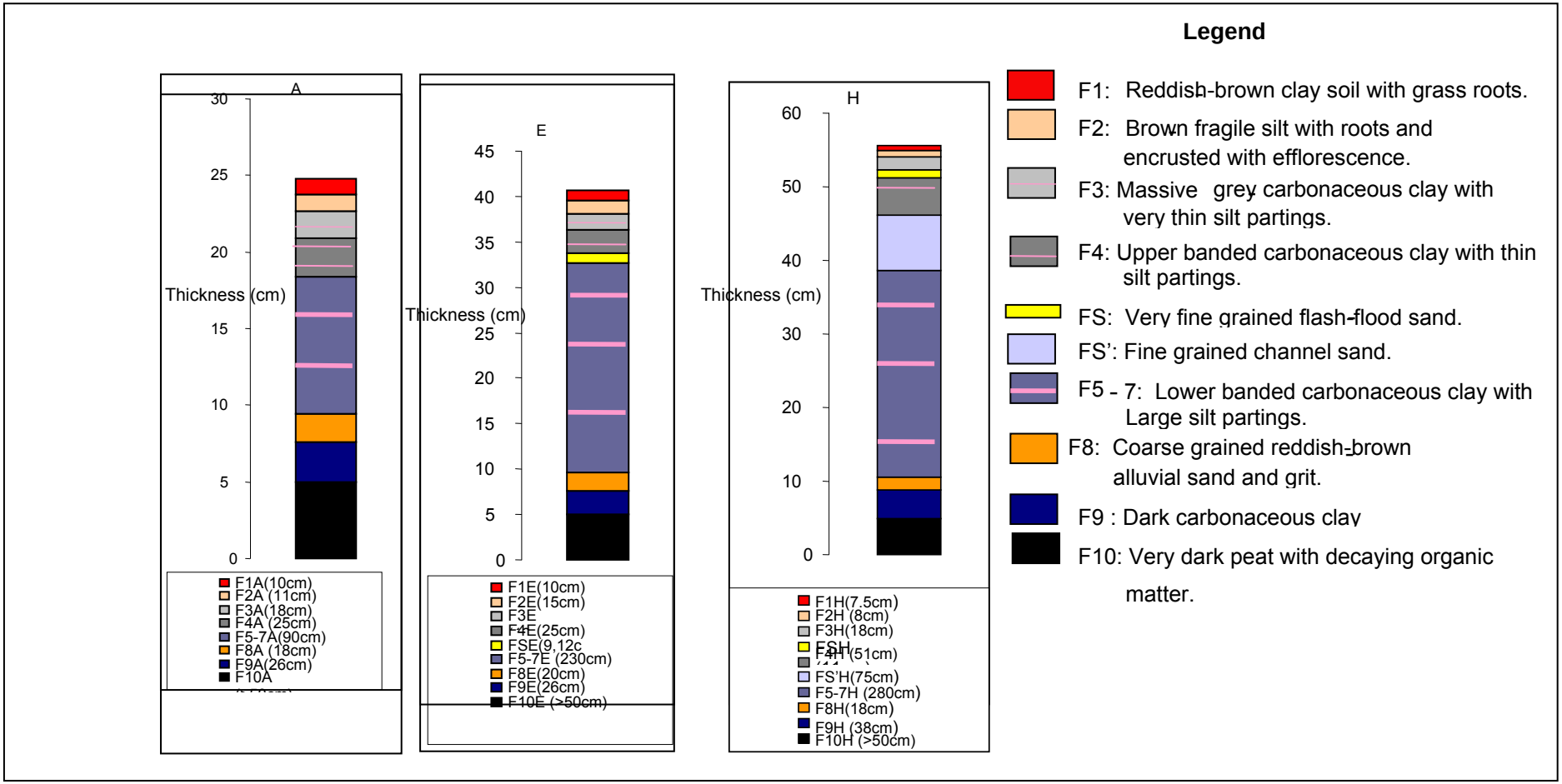


Fig.8: Stratigraphic columns showing sample localities of profiles A, E and H of Fleurhof Dam (modified from Ndasi, 2004). Sample number (e.g. F1A) represents an entire layer within the corresponding profile from which it is collected.

VI.1.iv. DEPOSITIONAL STYLE AND SEDIMENTATION OF FLEURHOF DAM DEPOSIT

The depositional style of the sediments in the Fleurhof Dam is that of a prograding delta. A delta is defined as a deposit built by a terrestrial feeder system, typically alluvial, into a lake or sea (Colella, and David, 1990) or a dam, such as the Fleurhof Dam. The result is a localized, often irregular progradation of the shoreline, controlled directly by the feeder system, with possible by-basinal processes, such as the action of waves (Ibid). Fleurhof Dam is fed by the upper Klipspruit River, which has transported sediments eroded from surrounding tailings dams of the Rand Leases and the Bantjies mines just downstream and south of Florida Lake, and deposited there into a standing water body (Fig. 1). As the dam fills up with sediments a progradation of the shoreline occurs from the river mouth towards the dam wall with finer suspended material being carried some distance out from the river mouth and spread over a wide area to form the prodelta mud. Coarser sediments are deposited closer to the river mouth where water depths are shallower (Blatt, et al., 1980). Facies thus changes with an upward coarsening mode from the thinner non-channelised prodelta characterised by a sheet flood deposition with finer facies toward the bar back of the dam where the channel sand becomes more conspicuous.

Figure 9 is a diagram illustrating the depositional style in the Fleurhof Dam, while figures 5a), b) and c) shows the changes in sediment thickness and water depth

as discussed in section VI.1.i. This is controlled by factors such as velocity, sediment load and accommodation space.

Progradatonal geometries occur when sediment supply exceeds the rate of topset accommodation volume and facies migrate basinward. This results in an on-lapping of sediments, as illustrated in figure 10. As the dam continues to fill up, accommodation space becomes less and more sediments tend to deposit backward forming a wedge of sediments. In the Fleurhof Dam the sediments had built up to the water level and then became colonised by reeds. The river might divert its course or form minor tributaries that form multiple sedimentary axes or channels. The sediments were deposited slightly dipping toward the delta front with well-defined strata, in an approximately 1200m wide amphitheatre-shaped dam.

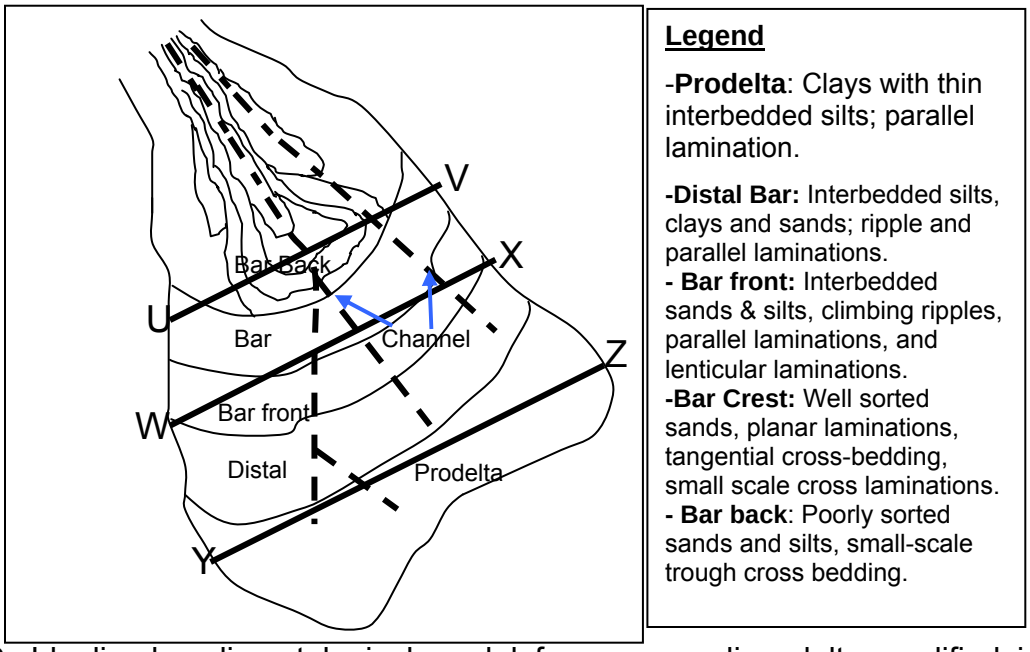


Fig. 9. Idealised sedimentological model for a prograding delta modified into Fleurhof Dam setting from Dag et al., (1982).

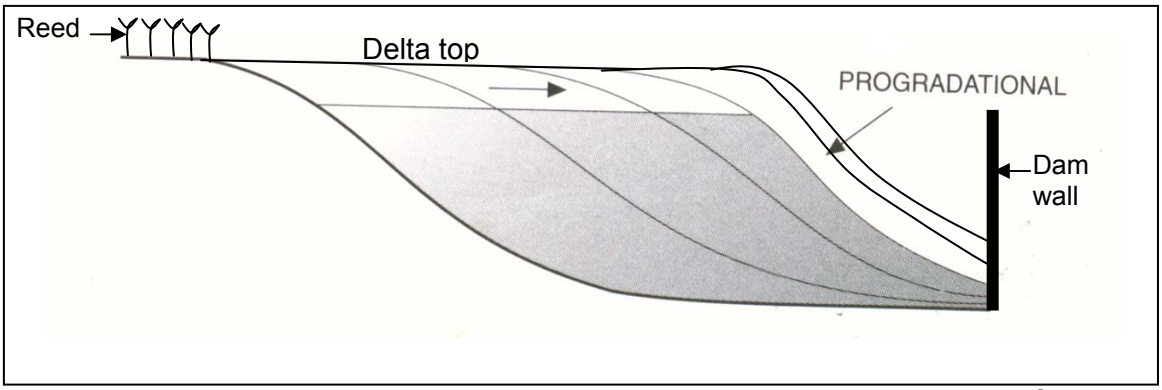


Fig 10. Diagram showing depositional architecture and progradation of a delta formed in a dam (modified from Galloway, 1989).

VI. 2. GOLD VALUE DISTRIBUTION IN FLEURHOF DAM SEDIMENTS

Data collected during the evaluation of the sediment prior to reprocessing by Crown Gold Recovery, were used to contour gold value distribution in the Fleurhof Dam sediments. These values were obtained from vertical boreholes drilled by Crown Gold Recovery prior to mining. The maps were obtained from Crown Gold Recovery (2004), and hand-contoured. The contoured maps was then digitised using GIS software by Mrs Lyn Whitfield and Mrs Dianne Du Toit of the School of Geosciences, University of the Witwatersrand, Johannesburg.

The vertical distribution of Au is discussed in Section 6.4 and illustrated in figures 15, 16 and 17. The vertical distribution shows two main peaks, one at the bottom and another at the top of the sedimentary deposit. The higher values in the lower, distal sediments are seen in a plan distribution of grades, with the highest grades

occurring at the distal most (southern) part of the dam where the sediments are finest, and decreases toward the delta front (Fig.11). Thus gold is associated with deposition of the fine mud and entrained to the distal organic-rich sediments near the dam wall, while other metals were deposited in the shallow water in the reed bed at the delta top. Higher gold grades also occur in the thinner sediments flanks of the dam, especially in the broader eastern flank of the prodelta. Bulk cores were analysed by Crown Gold Recovery. The area of higher grade commences immediately north of the exposed face. From here to the south values rise to over 5 g/t Au over a distance of 110 m. Areas greater than 5g/t Au persist southwards and terminate in a 120 m long east-northeast trending remarkable high grade (>10 g/t Au) distal delta front that extends over a distance of about 250 m. An easternmost (south-southeast) trending shoot also has high grades (>10 g/t Au) over variable thicknesses extending over 50 m. Lower grade areas (<2.5 g/t Au) occur toward the distal area and along the flanks of the deposit.

The gold content (in centimetre gram per ton- cmg/t Au) distribution follows a similar pattern as the gold grade in relation to sediment thickness and channel axes and high grade shoots. Higher gold contents occur where sediments are thinner and vice-versa. Figure 12 is an isopach map of gold content distribution. Gold values presented in figures 11 and 12 are average values of the various layers of the sediments in the dam. In general, highest gold grades were realised in the thinnest and finest sediments of the prodelta and values decrease toward the delta front where sediments are thickest (Fig. 5).

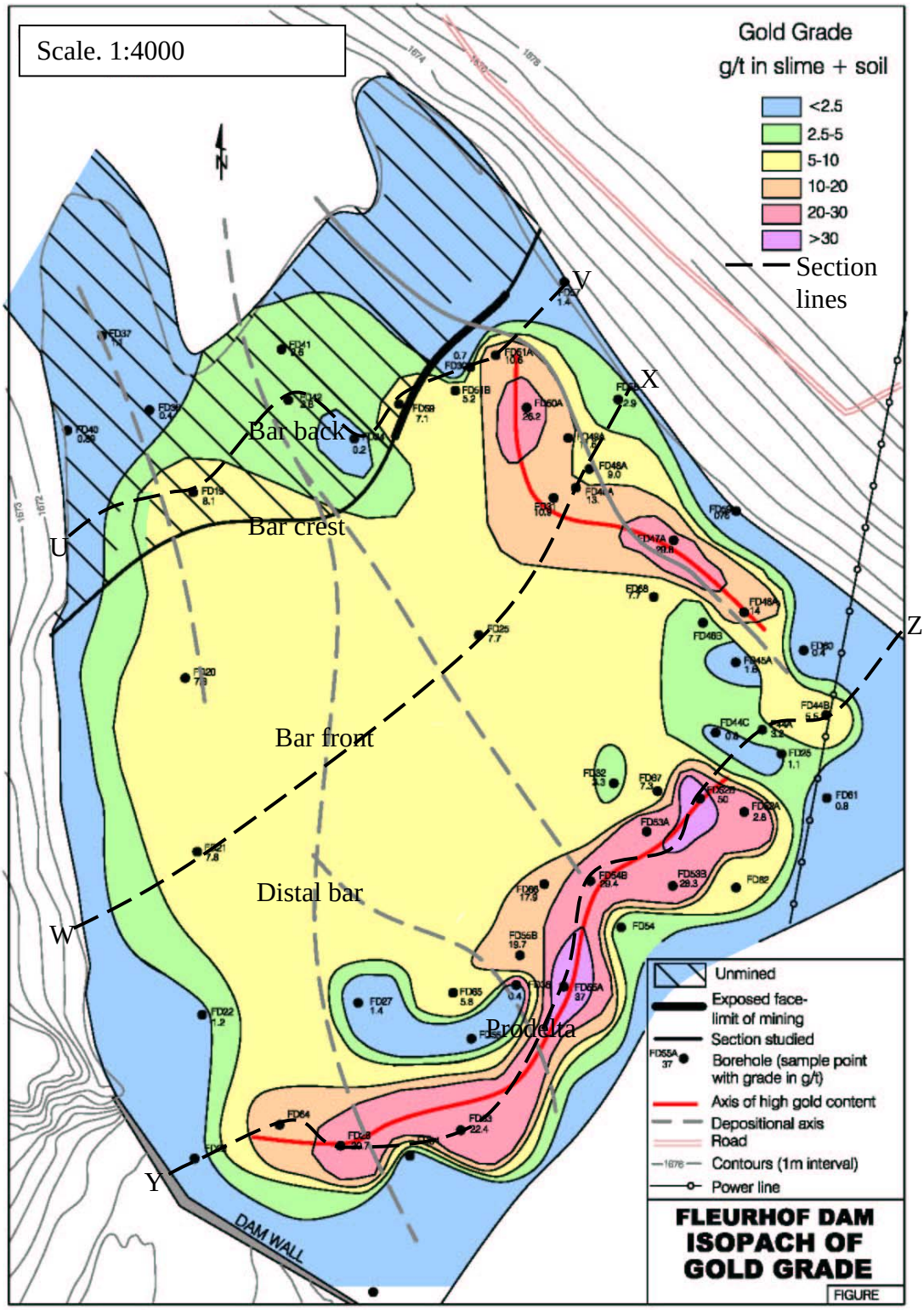


Fig.11. Isochon map of gold grade (g/t Au) in the Fleurhof Dam sediments.

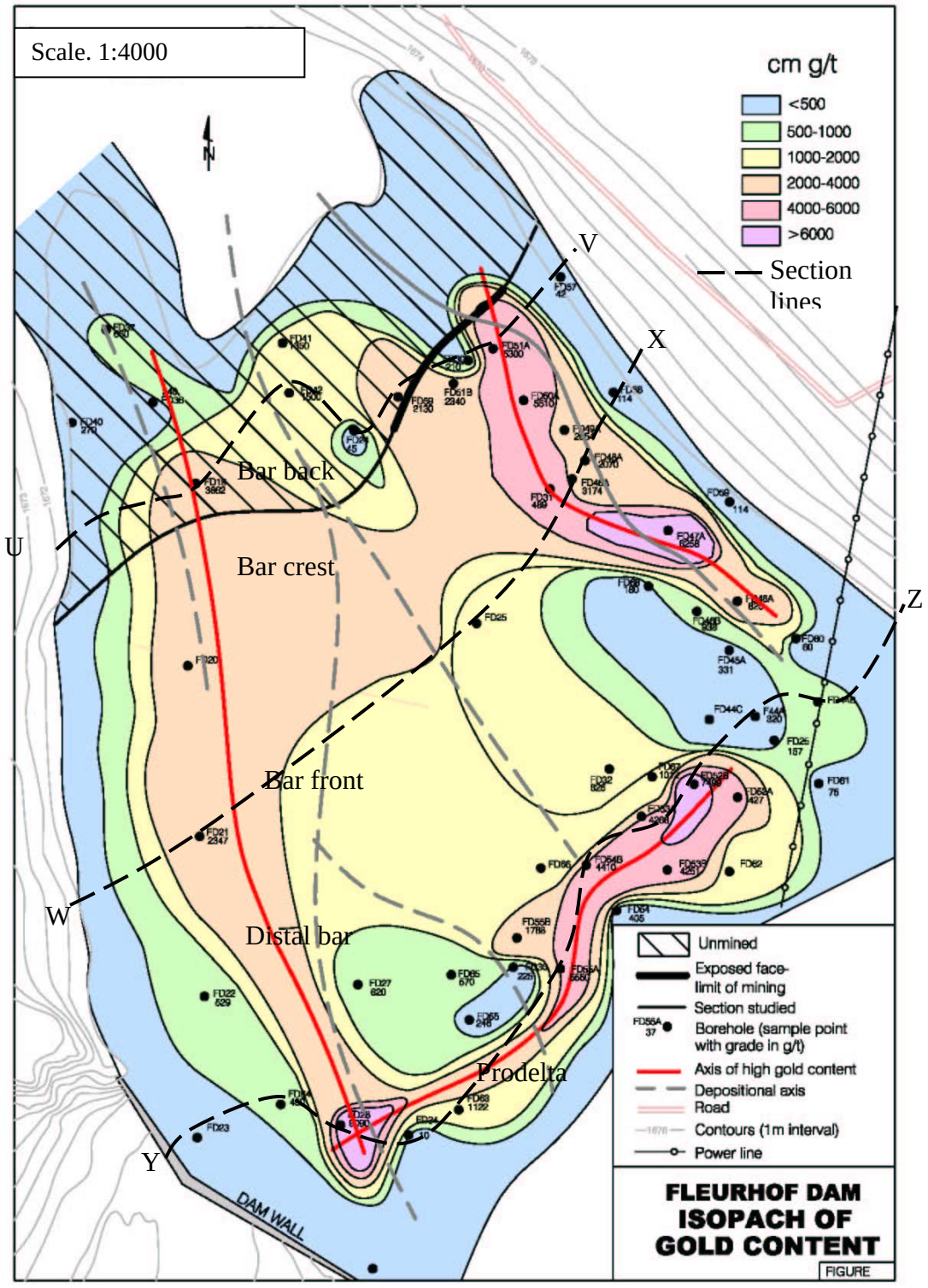


Fig. 12. Isopach map of gold content (cmg/t Au) in the Fleurhof Dam sediments.

VI.3. MINERALOGY OF FLEURHOF DAM SEDIMENTS

VI.3.A. X-RAY DIFFRACTION (XRD)

The minerals obtained from XRD analysis for Fleurhof Dam samples are shown in the Table 1 below (Ndasi, 2004).

Table 1. Minerals obtained from XRD analysis for Fleurhof Dam samples. For sample localities see figure 6.

Sampling points	Sediment type	Minerals determined
F1A	Reddish brown clay	Quartz , Pyrophilite,
F2A	Brown fragile silt	Quartz, Pyrophilite, illite
FA3	Massive carbonaceous clay	Poor XRD results
F4A	Upper banded clay	Quartz, Pyrophilite, illite
F5A	1st lower banded clay	Quartz, Pyrophilite, illite
F6A	2nd lower banded clay	Quartz, Pyrophilite, illite
F7A	3rd lower banded clay	Quartz, Pyrophilite, illite
F8A	Alluvial sand	Quartz, Pyrophilite,
F9A	Dark carbonaceous clay	Quartz, Pyrophilite,
F10A	Very dark peat	Quartz, Pyrophilite,
F1E	Reddish brown clay	Poor XRD results
F2E	Brown fragile silt	Quartz, Pyrophilite
F3E	Massive carbonaceous clay	Poor XRD results
FSE	Fine grained flash-flood sand	Quartz, Pyrophilite
F4E	Upper banded clay	Quartz Pyrophilite, illite
F5E	1st lower banded clay	Quartz Pyrophilite, illite
F6E	2nd lower banded clay	Quartz Pyrophilite, illite
F7E	3rd lower banded clay	Quartz Pyrophilite, illite
F8E	Alluvial sand	Quartz, Pyrophilite
F9E	Dark carbonaceous clay	Quartz, Pyrophilite
F10E	Very dark peat	Quartz, Pyrophilite
F1H	Reddish brown clay	Poor XRD results
F2H	Brown fragile silt	Quartz, Pyrophilite, illite
F3H	Massive carbonaceous clay	Poor XRD results
FSH	Fine grained flash-flood sand	Quartz, Pyrophilite
F4H	Upper banded clay	Quartz, Pyrophilite, illite
FS'H	Fine grained channel sand	Quartz, Pyrophilite
F5H	1st lower banded clay	Quartz, Pyrophilite, illite
F6H	2nd lower banded clay	Quartz, Pyrophilite, illite
F7H	3rd lower banded clay	Quartz, Pyrophilite, illite

Sampling points	Sediment type	Minerals determined
F8H	Alluvial sand	Quartz, Pyrophilite
F9H	Dark carbonaceous clay	Quartz, Pyrophilite
F10H	Very dark peat	Quartz, Pyrophilite
TDA	Tailings	Quartz, Pyrophilite
TDB1	Tailings	Quartz, Pyrophilite
TDC	Tailings	Quartz, Pyrophilite
TDD	Tailings	Quartz, Pyrophilite
TDE	Tailings	Quartz, Pyrophilite
SS1	Stream sediments	Quartz, Pyrophilite, muscovite
SS2	Stream sediments	Quartz, Pyrophilite, muscovite
SS3	Stream sediments	Quartz, Pyrophilite, muscovite
SS4	Stream sediments	Quartz, Pyrophilite, muscovite
SS5	Stream sediments	Quartz, Pyrophilite, muscovite
SS6	Stream sediments	Quartz, Pyrophilite, muscovite

Quartz is the most abundant mineral with a relative abundance of >75% and almost 100% in very sandy and silty samples such as FSE, FSH, FS'H and F8. Quartz is present in all samples. Second to quartz in abundance is pyrophylite. Other minerals that occur in smaller proportions are illite, muscovite, pyrite, uranite, and this reflects very well the mineralogy of the rocks of the Witwatersrand conglomerate reefs. Quartz and muscovite would have been derived from the conglomerate and quartzite constituent, pyrophylite from the breakdown of aluminous minerals while illite would probably be derived during weathering. In all three profiles, illite is more prominent in samples F4A, F4E, F4H, F5-7A, F5-7E and F5-7H. These samples represent the banded mud of the deeper waters. F1A, F1E and F1H is the top-most layer that is partially oxidised and contains very little clay. F2A, F2E, F2H, F3A, F3E and F3H also close to the surface would have had much of their mud washed down to deeper levels. F8A, F8E and F8H is a sandy layer and would allow easy leaching because of its high porosity. Samples F9A, F9E, F9H, F10A, F10E and F10H still contain a lot of

organic materials and are rather more peaty than clayish. Samples TDA, TDB1, TDC, TDD and TDE are samples from surrounding tailings dams and they reflect no illite content. SS1-SS6 are stream sediment samples. They contain muscovite that has probably been trapped by stream bed vegetation.

VI.3.B. REFLECTANCE SPECTROSCOPY

Samples FA3, FE1, FE3, FH1 and FH3 in Table 1 produced poor XRD results. These samples were thought to contain some hydrous ferric minerals. XRD could not detect hydrous ferric minerals since the principle behind this method is the determination of minerals from crystal structures. Most hydrous minerals are poorly crystalline or amorphous, making XRD an unsuitable method for their detection. These and other selected samples were re-analysed by reflectance spectroscopy and the results are shown in Table 2 below.

Table 2. Results of reflectance spectroscopy for selected samples

Sample points	Sediment type	Minerals determined
F1A	Reddish brown clay	Quartz, Pyrophilite, cyanotrichite
F2A	Brown fragile silt	Quartz Pyrophilite, smectite
F3A	Massive carbonaceous clay	Fourgerite, green rust, goethite
F7A	3rd lower banded clay	Illite, muscovite, Quartz, Pyrophilite
F8A	Alluvial sand	Quart, Pyrophilite, cyanotrichite
F9A	Dark carbonaceous clay	Quart, Pyrophilite, cyanotrichite
F10A	Very dark peat	Quartz, Pyrophilite, clays
F1E	Reddish brown clay	Green rust, Quartz
F3E	Massive carbonaceous clay	Ferrihydrite, Quartz, AlOH
FSE	Fine grained flash-flood sand	Quartz, Pyrophilite, caynotrichite
F6E	2nd lower banded clay	Pyrophilite, smectite, cyanotrichite, Quartz
F1H	Reddish brown clay	Quartz, smectite, amorphous Fe

Sample points	Sediment type	Minerals determined
F3H	Massive carbonaceous clay	Ferrihydrite, Quartz, AlOH
FS'H	Fine grained channel sand	Pyrophilite, mix FeO(SO4), cyanotrichite, Quartz
F8H	Alluvial sand	Cyanotrichite, Pyrophilite, Quartz
SS2	Stream sediments	Pyrophilite, mica, cyanotrichite
SS4	Stream sediments	Ferrhydrite, Pyrophilite, cyanotrichite
SS5	Stream sediments	Quartz, Pyrophilite, cyanotrichite
TDB1	Tailings	Pyrophilite, Quartz, cyanotrichite
TDC	Tailings	Cyanotrichite, quartz, illite

The results of reflectance spectroscopy maintains quartz as the most abundant mineral, but polymorphic and amorphous minerals such as cyanotrichite (probably related to the cyanide of treatment plants), ferrihydrite that could not be detected by XRD are identified by this method. These minerals however occur in very low proportions. This method also revealed that samples F3A, F1E, F3E, F1H and F3H did not contain pyrophylite, an indication that helped in the normative calculations of minerals (Table 3.i).

VI.4. GEOCHEMISTRY OF FLEURHOF DAM SEDIMENTS

VI.4.A). MAJOR ELEMENTS

VI.4.A.i. X-Ray Fluorescence (XRF) analysis.

The concentration of major elements obtained from XRF analysis of samples from surrounding tailings dams, stream sediments and the Fleurhof Dam sediments are shown in Table 3. Measurements are in %.

Table 3i), XRF results of major element analysis of samples from surrounding tailings dams samples (for localities of sampling points see figure 1). TD in column 1 corresponds to 'tailings dump'.

Sample	Na_2O	MgO	Al_2O_3	SiO_2	K_2O	CaO	TiO_2	Fe_2O_3	S	MnO	P_2O_5
TDA	0.41	0.53	9.61	83.46	0.89	0.16	0.26	3.64	1.03		
TDB1	0.40	0.60	13.12	76.84	0.95	0.06	0.27	6.98	0.78		
TDC	0.54	0.73	14.10	76.04	1.53	0.12	0.34	5.74	0.46	0.07	
TDD	0.18	0.53	7.89	87.20	0.57	0.22	0.33	2.56	0.53		
TDE	0.29	0.63	12.80	80.30	0.67	0.16	0.30	4.24	0.61		
Total	1.83	3.02	57.53	403.83	4.60	0.72	1.50	23.16	3.40	0.07	0.00
Avg	0.37	0.60	11.51	80.77	0.92	0.14	0.30	0.46	0.68	0.01	0.00

Table 3ii), XRF results of major elements from stream sediments samples (for localities of sampling points see figure 2). SS in column 1 corresponds to 'stream sediment'.

Sample	Na_2O	MgO	Al_2O_3	SiO_2	K_2O	CaO	TiO_2	Fe_2O_3	S	MnO	P_2O_5
SS1	0.23	0.56	8.49	86.20	0.62	0.08	0.31	2.71	0.80		
SS2	0.62	1.06	20.26	67.42	1.71	0.35	0.38	7.63	0.14	0.24	0.19
SS3	0.37	0.60	15.31	77.77	0.50	0.49	0.45	4.13	0.12		0.25
SS4	0.35	0.66	15.92	76.13	0.60	0.16	0.44	5.66	0.08		
SS5	0.30	0.43	13.51	80.92	0.75	0.07	0.31	3.49	0.23		
SS6	0.27	0.41	25.54	65.21	1.20	0.13	0.49	6.72	0.04		
Total	2.15	3.70	99.04	453.64	5.39	1.29	2.38	30.34	1.41	0.24	0.44
Avg	0.36	0.62	16.51	75.61	0.90	0.21	0.40	5.06	0.23	0.04	0.07

Table 3iii), XRF results of major elements from Fleurhof Dam deposit samples.

For sample localities see figure 8.

Sample	**Sediment type**	**Na_2O**	**MgO**	**Al_2O_3**	**SiO_2**	**K_2O**	**CaO**	**TiO_2**	**Fe_2O_3**	**S**	**MnO**	**P_2O_5**
F1A	Reddish brown clay	0.44	1.09	13.86	75.23	1.00	0.19	0.28	6.19	1.64	0.07	
F2A	Brown fragile silt	0.57	1.93	18.58	55.91	1.28	1.64	0.22	17.32	2.26	0.28	
F3A	Massive carbonaceous clay	0.46	4.38	25.12	35.28	1.20	3.51	0.16	24.83	4.50	0.56	
F4A	Upper banded clay	0.63	1.47	17.82	64.04	1.08	0.59	0.28	12.16	1.36	0.12	0.27
F5A	1st lower banded clay	0.49	0.91	16.75	71.26	1.54	0.16	0.35	7.49	1.04		
F6A	2nd lower banded clay	0.53	0.90	16.88	70.23	1.54	0.22	0.31	8.45	0.95		
F7A	3rd lower banded clay	0.46	0.76	18.19	69.92	1.27	0.34	0.45	7.84	0.76		
F8A	Alluvial sand		0.42	9.78	85.71	0.39	0.12	0.36	2.50	0.73		
F9A	Dark carbonaceous clay	0.32	0.49	16.27	75.93	0.79	0.15	0.49	5.08	0.48		
F10A	Very dark peat	0.60	0.71	18.62	67.95	1.04	0.41	0.59	8.01	2.07		
F1E	Reddish brown clay	0.17	0.62	26.17	40.11	0.70	0.26	0.35	29.10	2.47		
F2E	Brown fragile silt	0.38	0.72	13.03	75.67	1.02	0.40	0.30	7.58	0.81	0.09	
F3E	Massive carbonaceous clay	0.45	3.58	24.66	34.49	1.15	2.72	0.14	27.99	4.82		
FSE	Fine grained flash-flood sand	0.28	0.65	9.68	82.00	0.71	0.15	0.27	5.24	1.03		
F4E	Upper banded clay	0.59	1.44	17.61	66.39	1.11	0.43	0.25	10.22	1.88	0.08	
F5E	1st lower banded clay	0.55	1.04	15.73	72.75	1.44	0.38	0.31	6.50	1.30		
F6E	2nd lower banded clay	0.60	1.09	17.14	68.84	1.46	0.50	0.31	8.45	1.62		
F7E	3rd lower banded clay	0.51	0.93	16.47	69.11	1.32	1.30	0.40	7.64	2.25	0.08	
F8E	Alluvial sand	0.22	0.61	10.54	85.41	0.38		0.44	1.72	0.69		
F9E	Dark carbonaceous clay		0.82	20.04	69.92	1.08	0.32	0.61	6.04	0.92		
F10E	Very dark peat	0.28	0.85	12.04	70.19	0.52	1.52	0.50	9.29	4.59	0.13	0.22
F1H	Reddish brown clay	0.28	0.52	25.57	41.57	0.69	0.13	0.37	26.11	2.70		
F2H	Brown fragile silt	0.35	0.72	12.63	76.25	0.84		0.24	7.81	0.89		
F3H	Massive carbonaceous clay	1.61		23.95	39.80	0.99	2.12	0.22	26.55	4.76		
FSH	Fine grained flash-flood sand	0.24	0.44	6.80	88.01	0.46	0.21	0.27	2.54	1.04		
F4H	Upper banded clay	0.36	0.63	12.71	76.76	0.73	0.34	0.25	6.16	2.00	0.08	0.26
FS'H	Fine grained channel sand	0.26	0.48	8.20	85.75	0.47	0.17	0.23	3.31	1.12		
F5H	1st lower banded clay	0.54	1.15	16.79	69.53	1.36	0.45	0.35	8.43	1.33	0.08	
F6H	2nd lower banded clay	0.49	0.81	16.82	71.71	1.31	0.25	0.37	7.32	0.87		
F7H	3rd lower banded clay	0.44	0.70	17.94	71.70	1.19	0.31	0.53	6.62	0.58		
F8H	Alluvial sand	0.20	0.51	9.30	86.08	0.37	0.06	0.38	2.31	0.80		
F9H	Dark carbonaceous clay	0.42	0.69	18.34	72.87	1.20	0.16	0.42	5.18	0.71		
F10H	Very dark peat	0.24	0.92	21.37	70.68	0.63	1.12	0.90	3.24	0.79	0.08	
Total		13.95	32.97	545.38	2257.01	32.25	20.63	11.89	325.21	55.76	1.65	0.74
Avg		0.42	1.00	16.53	68.39	0.98	0.63	0.36	9.85	1.69	0.05	0.02

From the Tables above it can be seen that the average concentration of different major elements generally increases from the surrounding tailings dumps, through the stream sediments to the sediments of the dam deposit, except for SiO_2. Quartz is the major constituent of the Witwatersrand conglomerates, which means that SiO^2 should be the main component of tailings dumps as reflected in Table 3iii above. The analyses shows that the Fleurhof Dam sediments and stream sediments are silica enriched with the average silica abundance (68.39 %) in Fleurhof Dam Close to that of the surrounding tailings dumps (80.77%). Other major elements have a relatively higher average abundance in the Fleurhof Dam sediments, such as Al_2O_3 (16.53%) compared to 11.51% in surrounding tailings dumps and Fe_2O_3 (9.85%) compared to 4.63% in surrounding tailings dumps samples. Highest silica values occur in samples F8A, FSE, F8E, FSH, FS'H and F8H all of which have SiO_2 content of above 80%. F8A, F8E and F8H are samples of the primary alluvial sand layer formed before the deposition of the major sediments of Fleurhof Dam deposit whereas FSE, FSH and FS'H are mainly tailings-rich silt that occur in the partings. Samples F3A, F1E, F3E, F1H and F3H occurring near the top of the profiles (Fig. 8) have very high concentrations of Fe_2O_3 and Al_2O_3, probably due to oxidation of sulphides occurring in the dump materials. These samples are mainly clay-rich with high cation exchange capacities. These samples showed poor XRD results and reflected little or no pyrophylite in their mineralogy (Table 1). Fe^{3+} might have replaced Al^{3+} to give more of amorphous ferric hydroxide than pyrophylite.

Ternary plots were constructed to portray variations amongst SiO_2, Al_2O_3 and K_2O in the Fleurhof Dam samples and are shown in figure 13a) – d) below (Ndasi, 2004). This indicates the relative abundance of silica (quartz), aluminium (pyrophylite) and clay-rich (illite) minerals in the sediments.

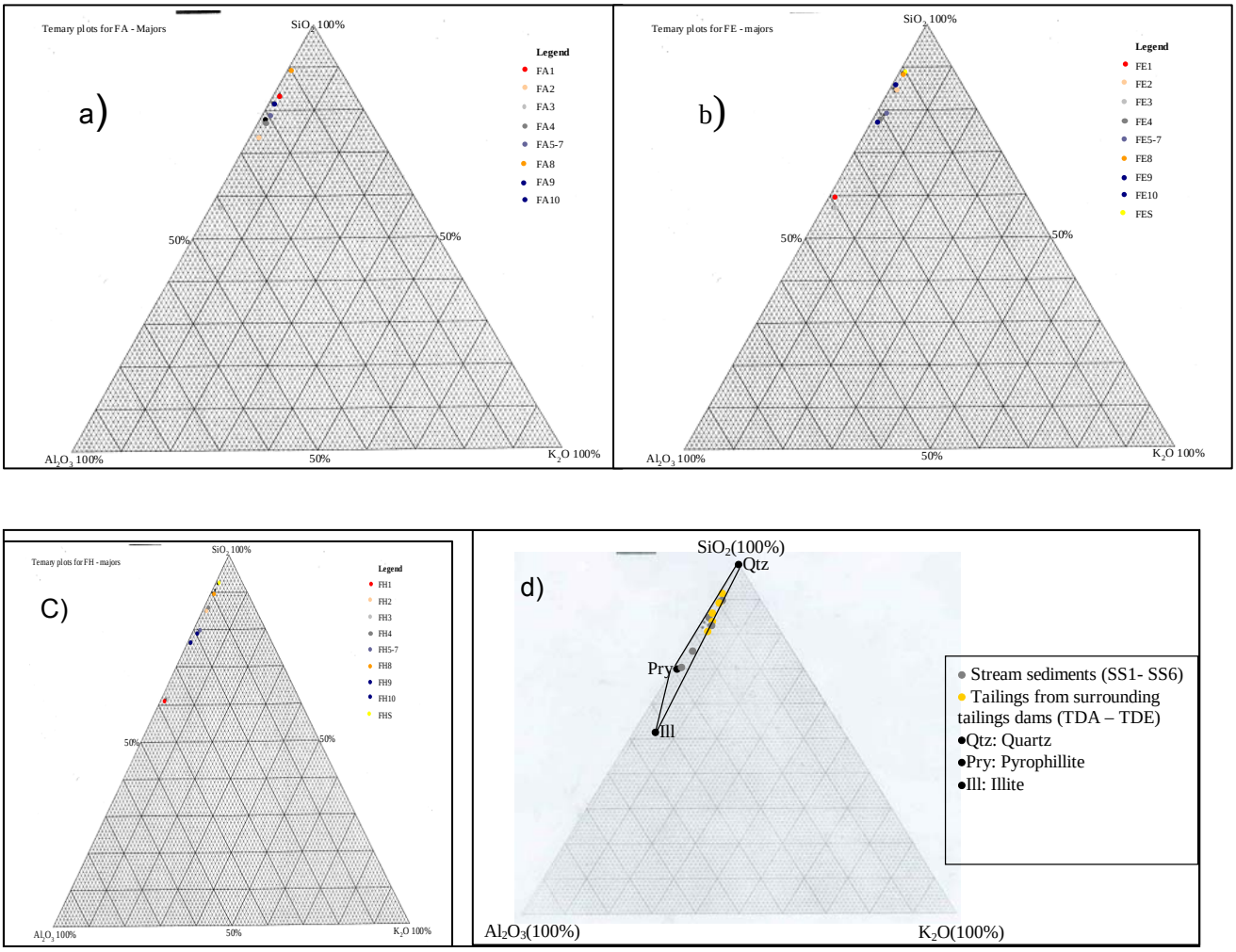


Fig. 13. Ternary plots of major elements for profiles a); A, b): E, c): H and d) stream sediments and tailings from surrounding tailings dams of Fleurhof deposit. See figure 8 for complete description of legend.

From the ternary plots it is evident that SiO_2 is the dominant major element in the sediments as already shown in Table 3iii) above, as most the samples plot toward the SiO_2 pole. The plots also show that Al_2O_3 is relatively more abundant than K_2O. This is further illustrated in the normative calculation in Tables 4 i), ii) and iii) below, which is an expression of the relative abundance of the major minerals namely quartz (SiO_2), pyrophyllite (Al_2O_3), illite (K_2O) and hematite (Fe_2O_3) as a percentage.

Table 4i) Normative calculations of major minerals from surrounding tailings dams samples. TD in column 1 corresponds to 'tailings dump'. For sample localities see figure 1.

Sample	Qtz	Pyroph.	Illite	Hematite	Total
TDA	64.21	23.77	7.52	3.64	99.14
TDB1	49.55	35.47	8.03	6.98	100.03
TDC	49.04	32.2	12.98	5.74	99.96
TDD	70.77	21.38	4.79	2.56	99.5
TDE	52.68	37.57	5.65	4.24	100.14

Table 4ii) Normative calculations of major minerals from stream sediments samples. SS in column 1 corresponds to 'stream sediments'. For sample localities see figure 2.

Sample	Qtz	Pyroph.	Illite	Hematite	Total
SS1	68.57	22.87	5.26	2.71	99.41
SS2	26.24	51.9	14.52	7.63	100.29
SS3	43.62	48.31	4.26	4.13	100.32
SS4	40.92	49.33	5.11	5.66	101.02
SS5	51.94	39.16	6.31	3.49	100.9
SS6	9.61	76.46	10.17	6.72	102.96

Table 4iii). Normative calculations of major minerals from Fleurhof Dam sediments. For sample localities see figure 8.

Sample	Sediment Type	Qtz	Pyroph.	Illite	Hematite	Total
F1A	Reddish brown clay	46.37	37.47	8.49	6.19	98.52
F2A	Brown fragile silt	17.03	50.96	10.83	17.32	96.14
F3A	Massive carbonaceous clay	31.4		10.13	24.83	66.36
F4A	Upper banded clay	26.18	50.57	9.13	12.16	98.04
F5A	1st lower banded clay	37.7	41.49	13.03	7.49	99.71
F6A	2nd lower banded clay	36.36	41.9	13.08	8.45	99.79
F7A	3rd lower banded clay	31.93	49.64	10.8	7.84	100.21
F8A	Alluvial sand	64.15	30.08	3.31	2.5	100.04
F9A	Dark carbonaceous clay	40.61	48.41	6.7	5.08	100.8
F10A	Very dark peat	28.06	53.84	8.81	8.01	98.72
F1E	Reddish brown clay	37.84		5.92	29.1	72.86
F2E	Brown fragile silt	48.89	34.26	8.67	7.58	99.4
F3E	Massive carbonaceous clay	30.34		9.77	27.99	68.1
FSE	Fine grained flash-flood sand	61.89	26.1	5.97	5.24	99.2
F4E	Upper banded clay	29.14	49.48	9.39	10.22	98.23
F5E	1st lower banded clay	41.23	38.96	12.24	6.5	98.93
F6E	2nd lower banded clay	34.05	43.78	12.36	8.45	98.64
F7E	3rd lower banded clay	35.38	42.96	11.22	7.64	97.2
F8E	Alluvial sand	62.01	32.92	3.19	1.72	99.84
F9E	Dark carbonaceous clay	26.83	58.41	9.14	6.04	100.42
F10E	Very dark peat	43.8	36.6	4.38	9.29	94.07
F1H	Reddish brown clay	39.33		5.84	26.11	71.28
F2H	Brown fragile silt	49.72	34.93	7.15	7.81	99.61
F3H	Massive carbonaceous clay	36.58		8.4	26.55	71.53
FSH	Fine grained flash-flood sand	73.77	18.69	3.92	2.54	98.92
F4H	Upper banded clay	49.58	36.58	6.15	6.16	98.47
FS'H	Fine grained channel sand	68.24	23.54	4.01	3.31	99.1
F5H	1st lower banded clay	35.16	43.74	11.49	8.43	98.82
F6H	2nd lower banded clay	37.11	44.31	11.14	7.32	99.88
F7H	3rd lower banded clay	33.98	49.75	10.05	6.62	100.4
F8H	Alluvial sand	65.57	28.63	3.12	2.31	99.63
F9H	Dark carbonaceous clay	34.26	50.98	10.19	5.18	100.61
F10H	Very dark peat	22.73	68.29	5.31	3.24	99.57

The above calculations were completed using the results of XRD. From the table there are similarities in the average abundance of various minerals in the same sedimentary types across the different layers of the sediments. Ternary plots of

quartz, pyrophyllite and illite illustrating normative calculations for profiles A, E and H of the dam sediments above are shown in figures 14 a), b) and c).

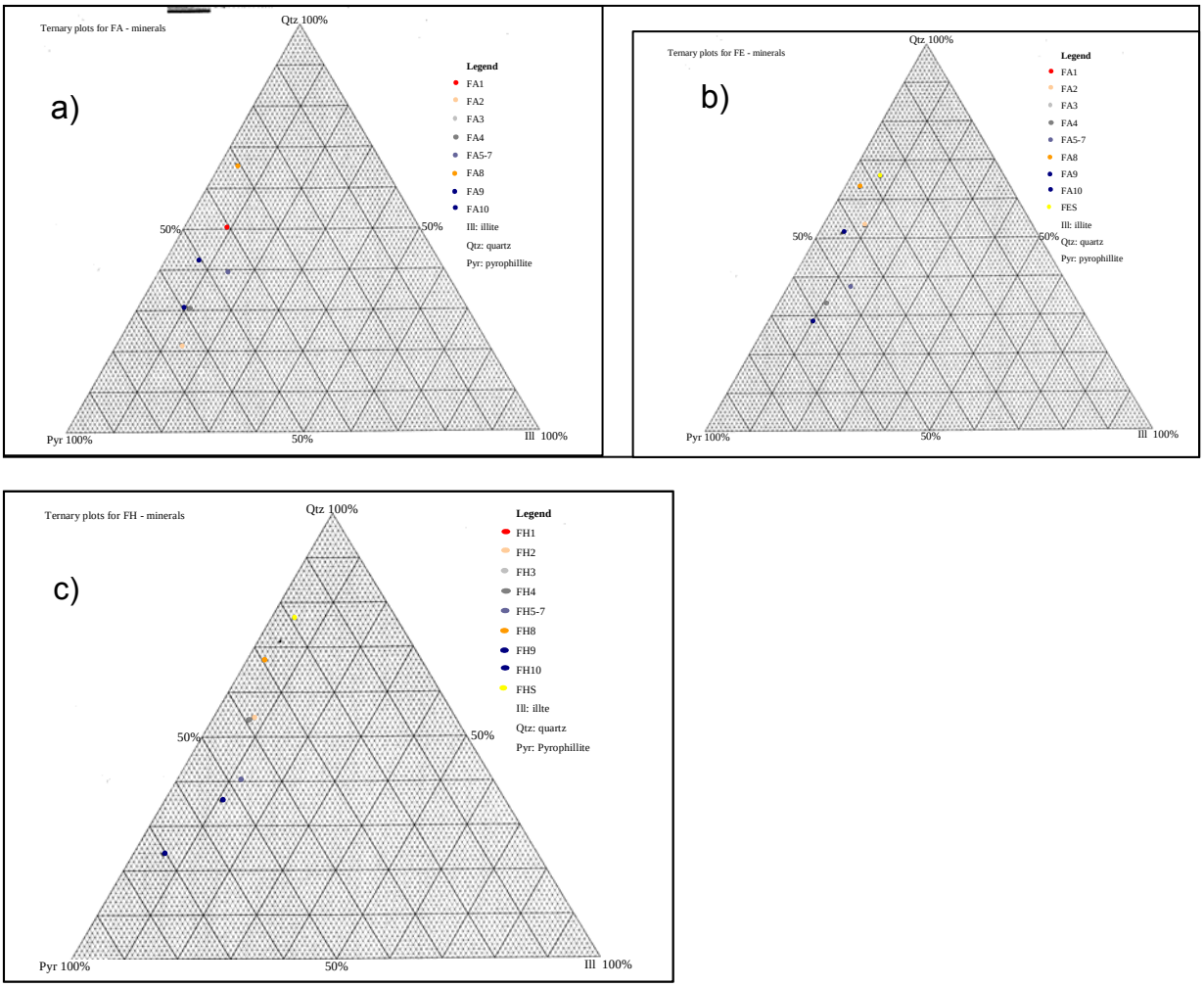


Fig. 14. Ternary plots of major minerals for profiles a); FA, b): FE and c): FH of Fleurhof Dam. See fig 8 for complete description of legend.

As already shown in the normative calculations in Table 4iii) above, quartz is the most abundant mineral as most of the points plot toward the quartz apex, followed by pyrophyllite and this reflects very well the mineralogy of the sediments as shown by XRD.

VI.4.B. TRACE ELEMENTS

VI.4.B.i.). X-Rays Fluorescence (XRF) analysis

The results of trace elements analysis by XRF for surrounding tailings dams, stream sediments and the Fleurhof Dam sediments are shown in Table 5i) – iii) respectively.

Table 5i) Concentration of trace elements by XRF analysis of surrounding tailings dams of Fleurhof. TD in column 1 corresponds to 'tailings dump'. For sample localities see figure 1.

Sample #	**Rb**	**Sr**	**Y**	**Zr**	**Nb**	**Co**	**Ni**	**Cu**	**Zn**	**TiO2**	**V**	**Cr**	**Ba**
	ppm	**ppm**	**ppm**	**ppm**	**ppm**	**Ppm**	**ppm**	**ppm**	**ppm**	**(%)**	**ppm**	**ppm**	**ppm**
LLD	**3**	**3**	**3**	**8**	**3**	**6**	**6**	**6**	**6**	**0.1**	**12**	**12**	**20**
TDA	17	26	10	111	7	9	22	16	28	0.30	47	185	131
TDB1	24	38	14	115	7	11	50	67	44	0.31	57	298	181
TDC	38	56	21	143	8	17	56	135	71	0.41	68	288	256
TDD	8	16	10	126	7	<6	10	<6	19	0.29	35	163	56
TDE	17	31	13	156	6	8	41	23	42	0.31	53	262	109
Avg.	20.8	33.4	13.6	130.07	6.97	11.25	35.8	60.3	40.8	0.324	52	239.2	146.6

Table 5ii) Concentrations of trace elements by XRF analysis of stream sediments samples of Fleurhof. SS corresponds to 'stream sediment'. For sample localities see figure 2.

Sample #	**Rb**	**Sr**	**Y**	**Zr**	**Nb**	**Co**	**Ni**	**Cu**	**Zn**	**TiO2**	**V**	**Cr**	**Ba**
	ppm	**ppm**	**ppm**	**ppm**	**ppm**	**Ppm**	**ppm**	**ppm**	**ppm**	**(%)**	**ppm**	**ppm**	**ppm**
LLD	**3**	**3**	**3**	**8**	**3**	**6**	**6**	**6**	**6**	**0.1**	**12**	**12**	**20**
SS1	12	19	11	129	7	12	38	40	40	0.29	39	178	86
SS2	53	71	48	121	8	173	279	115	447	0.48	115	478	387
SS3	18	104	17	150	8	15	61	65	514	0.50	79	287	226
SS4	16	38	19	182	8	36	76	47	199	0.49	80	318	148
SS5	16	25	12	159	7	6	27	29	34	0.36	56	273	129
SS6	33	50	19	147	8	11	99	48	53	0.55	109	423	212
Avg	24.67	51.17	21	148.1	7.61	42.67	96.67	57.3	214.5	0.445	79.67	326.2	198

Table 5iii) Concentration of trace elements by XRF analysis of Fleurhof Dam sediments. The description of each sample is given in the legend of figure 8.

Sample #	Sediment type	Rb	Sr	Y	Zr	Nb	Co	Ni	Cu	Zn	TiO2	V	Cr	Ba
		ppm	ppm	ppm	Ppm	ppm	ppm	ppm	ppm	ppm	(%)	ppm	ppm	ppm
LLD		**3**	**3**	**3**	**8**	**3**	**6**	**6**	**6**	**6**	**0.1**	**12**	**12**	**20**
F1A	Reddish brown clay	29	39	33	129	8	113	451	154	535	0.32	57	287	177
F2A	Brown fragile silt	57	65	155	84	11	876	3546	738	2076	0.27	61	433	279
F3A	Massive carbonaceous clay	70	72	313	54	14	2105	7825	1306	3464	0.18	58	516	285
F4A	Upper banded clay	52	64	97	113	11	526	2401	529	1321	0.34	73	437	296
F5A	1st lower banded clay	49	60	36	128	9	130	746	229	359	0.39	77	395	322
F6A	2nd lower banded clay	50	65	44	121	9	152	800	224	431	0.38	75	391	299
F7A	3rd lower banded clay	48	56	49	157	11	157	672	581	1071	0.54	94	360	271
F8A	Alluvial sand	8	11	12	161	6	<6	19	13	51	0.33	54	183	58
F9A	Dark carbonaceous clay	28	33	20	178	9	11	58	62	511	0.56	85	318	149
F10A	Very dark peat	34	35	24	114	9	90	333	142	6020	0.61	126	364	249
F1E	Reddish brown clay	34	33	172	78	9	222	710	716	1176	0.38	90	654	209
F2E	Brown fragile silt	29	41	26	124	8	85	264	183	231	0.33	60	291	199
F3E	Massive carbonaceous clay	76	70	305	51	15	2374	8282	1236	4884	0.19	51	509	277
F4E	Upper banded clay	47	59	95	118	10	461	2254	503	1197	0.32	66	390	
F5E	1st lower banded clay	17	25	17	146	7	32	136	71	98	0.30	46	220	256
F6E	2nd lower banded clay	48	61	53	122	9	217	1195	265	569	0.35	72	385	125
F7E	3rd lower banded clay	45	56	43	141	9	138	570	417	865	0.45	78	324	279
F8E	Alluvial sand	7	11	10	102	6	7	18	11	43	0.38	46	137	223
F9E	Dark carbonaceous clay	42	41	26	165	11	33	138	85	1772	0.69	114	366	56
F10E	Very dark peat	14	28	17	60	6	25	81	32	1358	0.42	127	289	257
F1H	Reddish brown clay	38	31	133	79	10	139	514	721	669	0.39	100	464	282
F2H	Brown fragile silt	25	30	47	114	8	93	715	280	391	0.25	47	249	187
F3H	Massive carbonaceous clay	74	68	378	69	16	3178	10207	1446	4954	0.20	56	489	131
FSH	Fine grained flash-flood sand	9	16	18	109	6	54	225	82	232	0.23	32	136	249
F4H	Upper banded clay	23	32	41	113	8	182	899	255	559	0.26	43	239	54
FS'H	Fine grained channel sand	10	17	17	111	7	31	142	108	172	0.24	35	133	123
F5H	1st lower banded clay	39	50	50	131	9	196	1026	245	519	0.34	65	419	72
F6H	2nd lower banded clay	46	58	41	139	9	135	673	317	523	0.44	78	346	250
F7H	3rd lower banded clay	45	49	42	170	11	89	412	379	689	0.59	93	349	266
F8H	Alluvial sand	6	10	11	168	7	12	28	21	147	0.36	53	201	248
F9H	Dark carbonaceous clay	36	44	27	152	9	31	116	86	1201	0.51	96	349	46
F10H	Very dark peat	29	29	19	130	10	13	112	55	206	0.87	142	449	222
Avg		36.4	42.5	74.1	119.8	9.33	384.1	1424	359	1197	0.388	73.44	346	206

Table 5iii) shows generally higher metal values in layers F2A, F2E, F2H, F3A, F3E and F3H along the three profiles of the cross section (Fig. 6). These layers consist of light silty clay with conspicuous silt partings. F3A, F3E and F3H also showed high concentrations of Al_2O_3 and Fe_2O_3 (Table 3iii). The high values could be attributed to a concentration of metals in those layers enriched in tailings. This generates acidity during weathering of tailings materials that contain pyrite. This eases the mobilisation of heavy metals. The concentrations generally

decreased with depth, with the exception of gold in layers F8A and F8E, which consists of coarse-grained primary fluvial sand and grit. The reason for the marked high value of gold concentrations in this layer (Table 6iii, ICP-OES results) could not be understood clearly as sandy soils tend to be easily leached and have low cation exchange capacities. The gold values were greater than 30 ppm which corresponded to the values reported by Crown Gold Recovery (Laing, personal communication, 2005). This could be attributed to the adsorption of gold from water up-rising from the peat layer underneath F8. Higher gold values could also be due to a primary alluvial concentration of gold. Gold forms strong complexes with chlorides ($[Au\ (Cl)_n]^-$) for instance, and these adsorb strongly on silica (Tutu and Cukrowska, 2004). While gold concentrations were observed to be high in the sandy layer F8A and F8E, elevated concentrations were also observed in F9H (consisting mainly of organic matter), F3 and F4. This could be attributed to the adsorption of gold on biomolecules. Sample F8H (common layer with F8A and F8E) is situated on a higher elevation and did not show a high concentration of gold, evidence that the gold in layers F8A and F8E comes from the layer below. The water level at point F8H would likely be below the primary alluvial layer at point F8H. No conclusions have been reached yet about the chemistry of gold transportation and studies are being carried out currently to assess this. The iron concentration varied down the profiles. This could be attributed to changes in its redox equilibrium. Again Tables 5i)-iii) show that metal concentrations increase from surrounding tailings dams through stream sediments to the Fleurhof Dam sediments as already shown in Tables 3i)-4iii). It

therefore appears that there is an enrichment of metals in dam sediments as the dam receives waters from streams and run-offs from surrounding tailings dams and cleans them up.

Comparative graphs were drawn for a number of selected metals to illustrate the relation between metal concentration and stratigraphy along the profiles A, E and H (Fig. 6) as discussed above. These are shown in figures 15, 16, and 17. The results of Au presented in these graphs are from ICP-OES analysis as shown in Tables 6i)-iii).

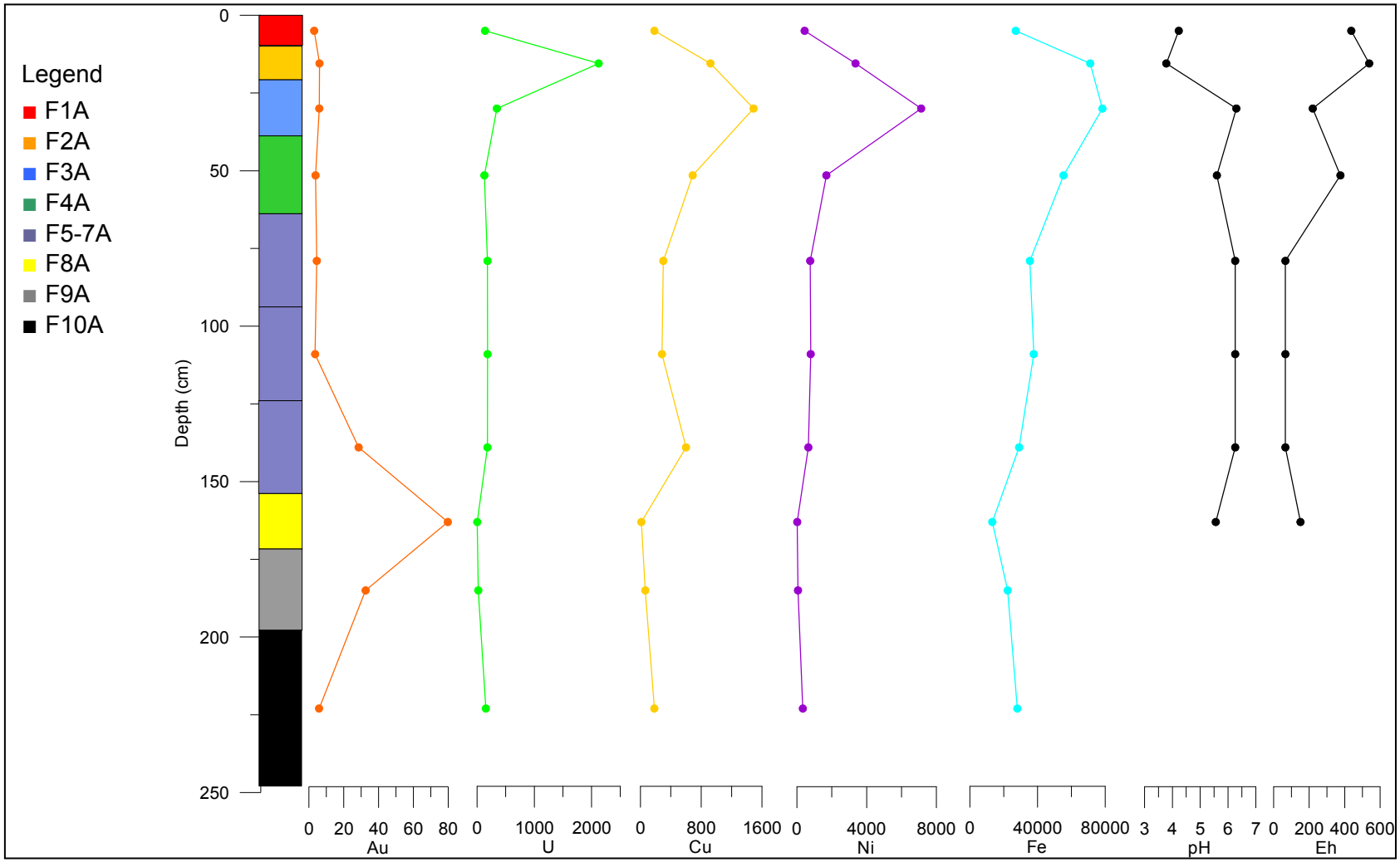


Fig.15. Comparative graphs of metals along profile A (assay values for metals are in ppb). See figure 6 for full description of legend. (after Ndasi, 2004)

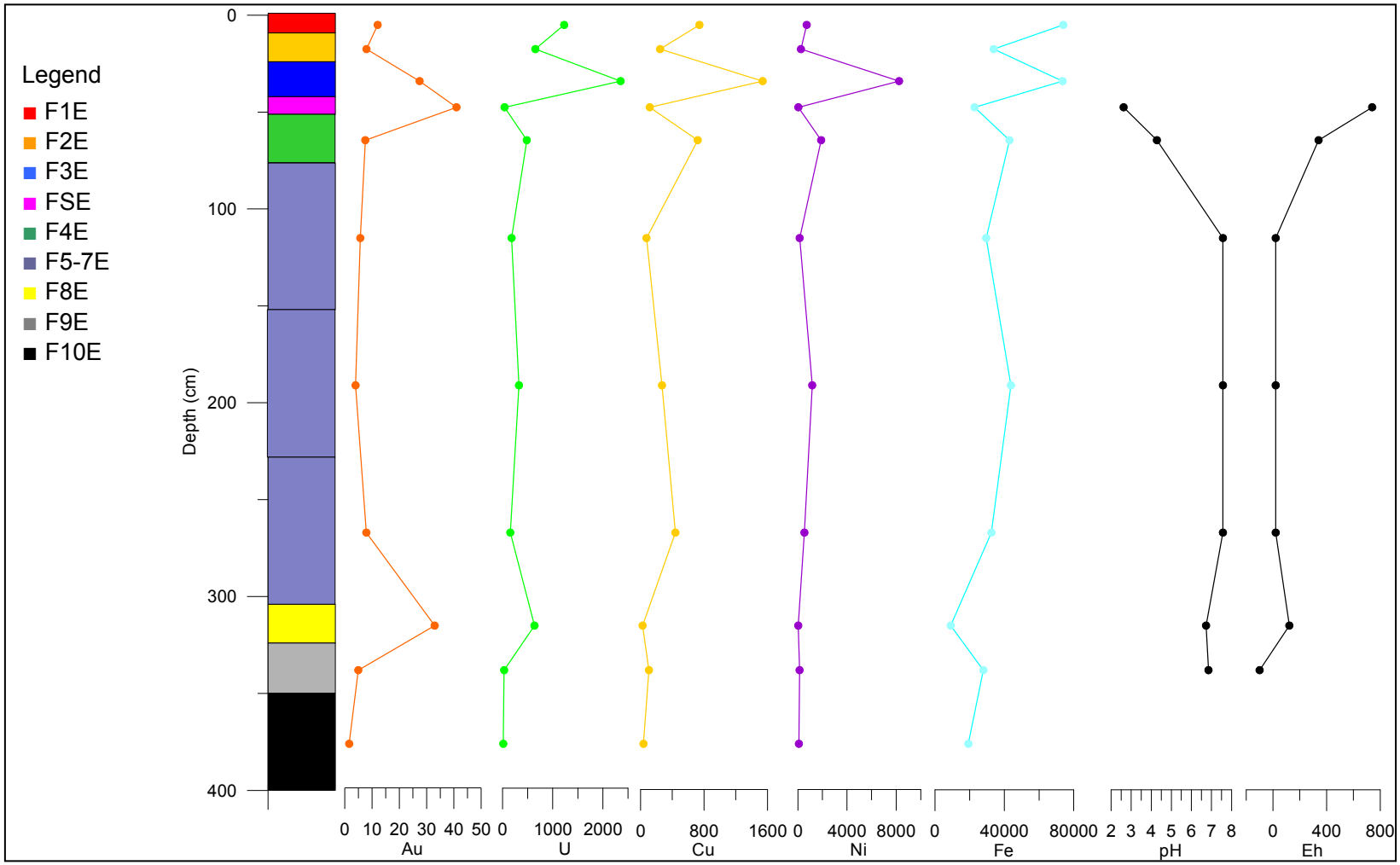


Fig. 16. Comparative graphs of metals along profile E (assay values for metals are in ppb). See figure 6 for full description of legend (after Ndasi, 2004).

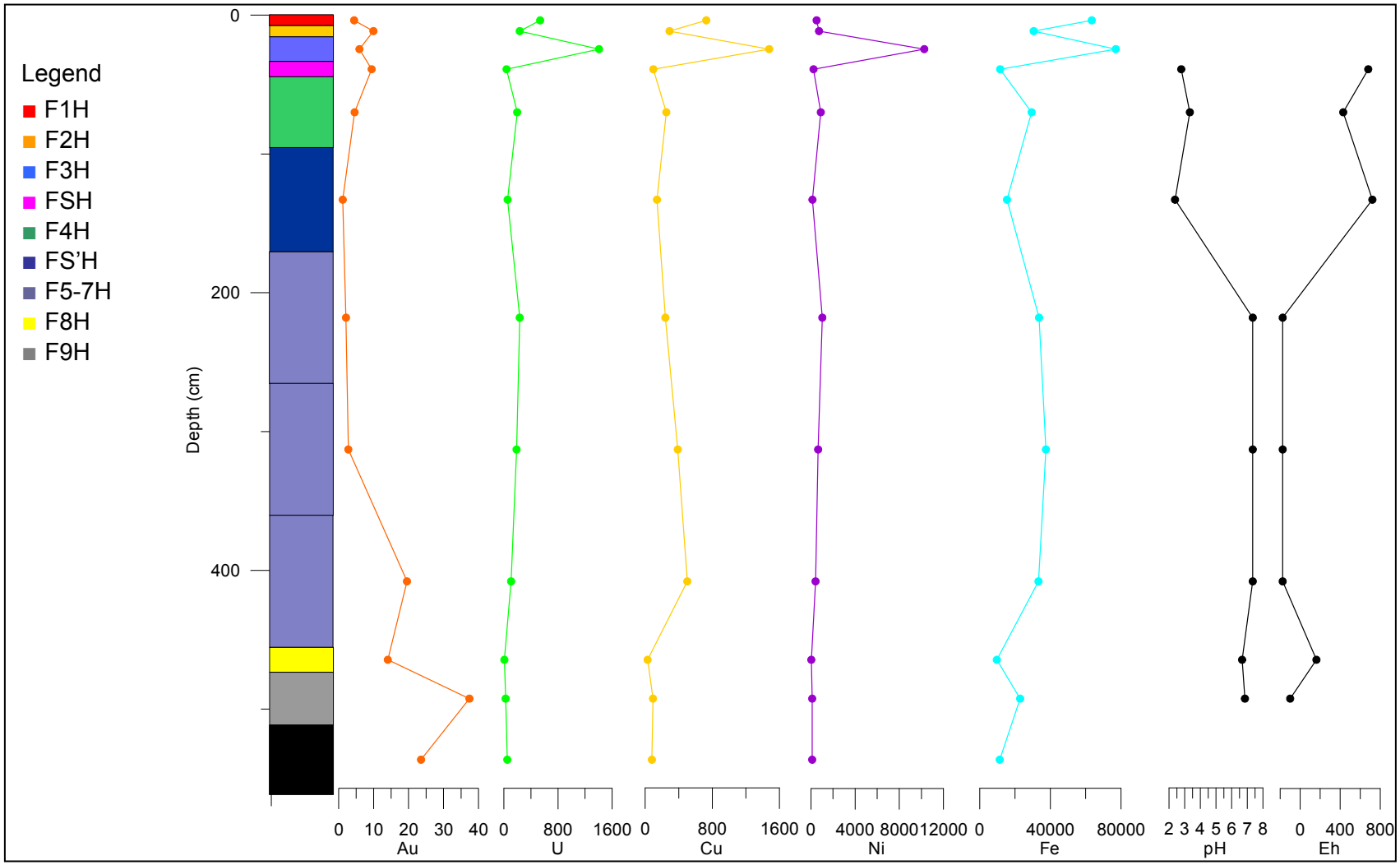


Fig. 17. Comparative graphs of metals along profile H (assay values for metals are in ppb). See figure 6 for full description of legend (Ndasi, 20004).

As seen from the graphs metal concentrations are generally higher in the clays than in the sandy and silt layers. Metal concentrations are generally highest near the top, except for gold where the tendency is for values to be higher near the base of the profiles than those above. Clays absorb metals like Fe, Al and Mn, causing them to precipitate. Some metals, like uranium, undergo some chemical interactions with the clay materials and so are adsorbed onto the clay-rich layers. Uranium for example is initially bound to ligands such as sulphates and these complexes bind tightly to clay materials. Clays have a high cationic exchange capacity and can therefore undergo these chemical-complex interactions more readily than sands. The concentration of these metals is therefore high in the clay-rich layers. Other metals like Ni, Cu and Zn co-precipitate with and Fe, Al, Mn and uranium, and will thus equally have high concentrations with these metals in the clays.

The high concentration of gold in the silty fine-grained sand layers near the top might be due to the entrainment of fine gold from the source (tailings dumps) and concentrated in this top silt layers. The lower coarse grained sand layer with high Au concentration (averaging 100cm thick) is more consistent than gold in the upper silty layer (averaging 35 cm thick).

VI.4.Bii. Inductively Coupled Plasma-Optical Emission Spectroscopy (ICP-OES) analysis of Fleurhof Dam sediments

Because some metals of interest like Au could not be analysed by XRF, ICP-OES analysis was undertaken for the Fleurhof Dam sediments, first to analyse for metals of interest such as Au and secondly to check the accuracy of XRF analysis. The results of trace element analysis of surrounding tailings dumps, stream sediments and the Fleurhof Dam sediments are shown in Tables 6i)-iii) below. High Au values occur in samples F3, F4 (mainly clay near the top of the profiles), F8 (primary alluvial sand) and F9 (mainly organics) (at the bottom), (Fig. 15, 16 and 17). From Tables 6i)-iii) it can be seen that the average concentration of metals (such as Mn, Fe, Co, Ni, Cu and Zn) increases from the surrounding tailings dam through stream sediments to the dam sediments, another evidence that the dam sediments are a sink to heavy metals washed from the tailings dams, as already seen in Tables VI.4.1i)-iii). Unsystematic values are shown by elements like Na, K, Ca, Mg, Al and Au, all of which show lower values in stream sediments than in both tailings dams and dam sediments. This could be attributed to the solubility of those metals. Na, K and Ca for example, which are also part of the fine clay component, are very soluble, so that their molecules would be constantly washed away by flowing waters and hence cannot be held in the stream sediments. Au values are also higher in the sediments than in the tailings dams. In Table VI.4.4iii) high values of Fe (> 70mg/kg) are seen in samples FA2, F3A, F1E, F3E, and F3H as already recorded in Table 3iii) of

major elements. Other elements that show high values in the same samples and which seem to be co-precipitating with Fe are Ni, Cu and Zn.

Table 6i Table showing concentration of trace elements analysis by ICP-OES of surrounding tailings dumps. TD corresponds to 'tailings dump'. For sample localities see figure 1.

Sample	Na	K	Ca	Mg	Al	Cr	Mn	Fe	Co	Ni	Cu	Zn	As	Sr	Ba	Au	U
	mg/kg	mg/kg	mg/kg	mg/kg	mg/kg	mg/kg	mg/kg	mg/kg	mg/kg	mg/kg	mg/kg	mg/kg	mg/kg	mg/kg	mg/kg	mg/kg	mg/kg
TDA	384.8	2454.0	586.4	1988.0	12740.0	156.8	162.8	15380.0	2.9	2.9	20.9	2.8	57.6	22.4	69.9	0.6	2.9
TDB1	455.7	2022.0	7038.0	2154.0	44100.0	156.2	157.0	28780.0	3.1	10.5	33.8	36.5	180.5	24.0	198.1	1.1	14.0
TDC	1278.4	23260.0	1418.0	2162.0	48240.0	214.0	452.4	25540.0	38.1	3.1	176.4	68.1	112.6	51.6	254.8	1.3	8.5
TDD	908.4	1132.0	762.4	1838.0	10420.0	163.8	135.4	11320.0	2.6	9.9	10.1	24.2	2.5	16.3	57.7	1.6	10.8
TDE	785.6	4124.0	1850.0	1384.0	12080.0	302.0	395.4	38680.0	7.6	53.9	27.2	48.2	133.2	38.2	133.6	0.2	12.8
Avg	762.6	6598.4	2331.0	1905.2	25516.0	198.6	260.6	23940.0	10.9	16.1	53.7	35.9	97.3	30.5	142.8	0.96	9.8

Table 6ii Table showing concentration of trace elements analysis by ICP-OES of Fleurhof stream sediments. SS corresponds to 'stream sediment'. For sample localities see figure 2.

Sample	Na	K	Ca	Mg	Al	Cr	Mn	Fe	Co	Ni	Cu	Zn	As	Sr	Ba	Au	U
	mg/kg	mg/kg	Mg/kg	mg/kg	mg/kg	mg/kg	mg/kg	mg/kg	mg/kg	mg/kg	mg/kg	mg/kg	mg/kg	mg/kg	mg/kg	mg/kg	mg/kg
SS1	370.8	1684.0	544.8	2250.0	9434.0	176.8	168.8	13240.0	19.0	35.2	51.0	43.2	34.4	21.3	87.8	0.3	10.6
SS2	370.0	4902.0	1144.0	1030.0	14280.0	487.4	1566.0	37680.0	192.4	217.0	120.4	426.2	155.0	69.5	372.5	0.7	68.9
SS3	263.8	1458.0	2374.0	1138.0	19200.0	290.0	249.0	19960.0	17.2	57.1	78.7	496.4	45.2	95.5	127.8	0.9	8.8
SS4	305.4	1614.0	888.6	2362.0	14380.0	314.8	246.0	27940.0	25.0	77.7	58.1	195.8	129.8	32.4	147.9	0.7	15.6
SS5	417.3	2060.0	511.4	1544.0	17660.0	271.4	128.8	17160.0	14.4	102.7	38.0	42.5	82.2	47.2	214.9	0.7	10.8
SS6	372.7	3640.0	495.6	880.6	22540.0	333.4	152.0	32800.0	1.0	61.2	63.9	65.1	61.2	24.3	102.8	0.1	3.9
Avg	350.0	2559.7	993.1	1534.1	16249.0	312.3	418.4	24796.7	44.8	91.8	68.3	211.5	84.6	48.4	175.6	0.6	19.8

Table 6iii Table showing concentration of trace elements analysis by ICP-OES of Fleurhof Dam sediments.

Sample	Sediment type	Na	K	Ca	Mg	Al	Cr	Mn	Fe	Co	Ni	Cu	Zn	As	Sr	Ba	Au	U
		mg/kg	mg/kg	Mg/kg	mg/kg	mg/kg	mg/kg	mg/kg	mg/kg	mg/kg	mg/kg	Mg/kg	mg/kg	mg/kg	mg/kg	mg/kg	mg/kg	mg/kg
F1A	Reddish brown clay	499.8	3026.0	1084.0	3206.0	18000.0	219.2	434.8	27080.0	117.8	441.8	183.4	566.2	196.0	37.6	176.7	0.3	138.0
F2A	Brown fragile silt	544.6	11420.0	3166.0	7022.0	8982.0	287.0	2138.0	71120.0	751.6	3362.0	922.0	1770.0	954.2	1.4	202.2	6.0	2122.0
F3A	Massive carbonaceous clay	2200.0	13100.0	5078.0	12280.0	9800.0	334.2	3338.0	78320.0	1750.0	7126.0	1490.0	3326.0	1282.0	1.7	219.6	12.9	344.0
F4A	Upper banded clay	696.5	11680.0	3122.0	4572.0	36680.0	338.6	820.0	55340.0	411.4	1692.0	687.4	1144.0	636.4	51.9	222.2	3.8	126.6
F5A	1st lower banded clay	890.7	7584.0	1680.0	2268.0	52140.0	392.8	257.8	35440.0	137.7	761.8	300.6	396.0	348.5	56.4	329.4	1.5	181.4
F6A	2nd lower banded clay	1570.0	11140.0	1136.0	1696.0	26020.0	393.2	266.8	37720.0	146.8	791.0	283.0	441.2	339.0	64.9	304.4	1.5	182.0
F7A	3rd lower banded clay	466.2	9695.0	760.5	882.7	13154.0	208.2	112.4	29076.0	133.3	658.5	599.7	1058.5	222.0	61.1	277.1	1.8	180.8
F8A	Alluvial sand	309.2	13120.0	980.5	1000.7	29980.0	190.0	142.0	13200.0	6.0	18.8	11.5	48.3	15.5	1106.0	60.9	13.9	2.4
F9A	Dark carbonaceous clay	1230.0	17760.0	237.0	1174.0	20344.0	315.2	179.6	22300.0	16.8	60.0	63.7	493.8	83.6	27.0	202.8	3.6	20.3
F10A	Very dark peat	660.4	13140.0	322.4	530.0	14360.0	348.6	251.0	28000.0	127.2	339.4	182.6	5966.0	62.4	17.0	243.3	5.8	152.2
F1E	Reddish brown clay	529.6	4470.0	459.4	660.2	18300.0	277.6	310.4	73980.0	203.6	718.2	741.4	1166.0	442.0	29.0	203.9	1.2	1228.0
F2E	Brown fragile silt	1032.0	7070.0	2352.0	1730.0	33460.0	227.6	540.0	33820.0	105.6	246.2	245.8	250.0	281.4	43.7	193.8	8.0	653.0
F3E	Massive carbonaceous clay	899.2	48760.0	3786.0	8665.0	45876.0	522.4	3058.0	73600.0	2298.0	8240.0	1538.0	4860.0	1894.0	65.5	239.6	14.4	2352.0
F4E	Upper banded clay	1580.0	44960.0	3396.0	12840.0	89900.0	392.6	665.2	42960.0	529.6	1894.0	719.8	1274.0	687.0	82.2	240.0	7.5	482.0
F5E	1st lower banded clay	595.7	15280.0	744.6	2058.0	33300.0	257.2	365.6	29500.0	166.0	142.0	73.8	103.8	267.8	27.0	129.6	5.7	179.2
F6E	2nd lower banded clay	969.4	5288.0	1474.0	3150.0	30740.0	323.6	357.4	43800.0	230.8	1166.2	269.8	590.4	390.6	57.1	257.8	4.0	326.8
F7E	3rd lower banded clay	349.6	1096.0	887.8	19840.0	77960.0	345.8	660.6	32540.0	165.6	533.0	438.2	964.0	217.8	54.6	229.2	7.9	153.8
F8E	Alluvial sand	446.2	1634.0	613.2	996.6	13233.0	111.8	137.2	9098.0	24.0	28.0	25.2	54.7	13.8	11.4	93.4	13.0	635.6
F9E	Dark carbonaceous clay	444.8	2766.0	927.4	696.4	15120.0	370.2	214.2	27900.0	29.1	136.4	105.2	1802.0	69.4	42.2	261.2	5.0	32.0
F10E	Very dark peat	556.8	3166.0	683.0	2572.0	34080	292.7	325.0	19260	25.9	82.9	36.4	1516.	20.2	21.8	290.6	1.7	14.1

Sample	Sediment type	Na	K	Ca	Mg	Al	Cr	Mn	Fe	Co	Ni	Cu	Zn	As	Sr	Ba	Au	U
		mg/kg	mg/kg	Mg/kg	mg/kg	mg/kg	mg/kg	mg/kg	mg/kg	mg/kg	mg/kg	Mg/kg	mg/kg	mg/kg	mg/kg	mg/kg	mg/kg	mg/kg
						.0			.0				0					
FSH	Reddish brown clay	883.7	977.2	1146.0	1812.0	10420.0	130.0	179.6	11560.0	67.7	232.5	97.4	229.4	31.1	14.7	50.2	1.4	38.8
F1H	Brown fragile silt	776.2	9290.0	705.4	993.4	26520.0	456.4	183.6	63420.0	133.6	509.8	728.2	673.6	239.8	20.9	188.2	1.4	536.6
F2H	Massive carbonaceous clay	647.3	18680.0	3700.0	12380.0	42780.0	209.4	263.8	30540.0	143.8	732.0	290.2	390.6	317.0	27.5	186.4	3.9	233.8
F3H	Fine grained flash-flood sand	708.9	37920.0	3708.0	18760.0	47540.0	475.8	2612.0	77000.0	3174.0	10262.0	1478.0	4972.0	1195.0	85.0	254.0	12.9	1406.8
F4H	Upper banded clay	988.4	2172.0	1900.0	2288.0	17280.0	200.6	393.2	29400.0	206.4	891.8	252.2	536.2	255.8	29.5	95.7	1.6	196.4
FS'H	Fine grained channel sand	216.2	1186.0	627.8	1672.0	10320.0	125.2	186.6	15440.0	31.3	137.4	140.6	161.2	68.3	16.2	73.4	0.2	54.9
F5H	1st lower banded clay	247.5	8880.0	884.4	4266.0	30420.0	271.6	450.4	33560.0	190.0	1028.8	240.8	524.6	338.5	48.8	254.6	1.1	233.8
F6H	2nd lower banded clay	456.8	4216.0	1350.0	1450.0	18840.0	355.4	314.6	37460.0	140.3	648.6	388.4	596.6	260.5	58.0	246.2	0.8	187.0
F7H	3rd lower banded clay	1122.0	6190.0	921.6	876.4	83680.0	356.6	337.8	33260.0	133.0	416.4	502.0	735.2	137.2	47.0	226.2	0.9	106.4
F8H	Alluvial sand	756.5	621.2	509.0	1018.0	16360.0	210.4	83.7	9696.0	8.0	30.8	29.2	138.2	16.4	11.5	48.2	1.1	7.3
F9H	Dark carbonaceous clay	356.3	23960.0	758.8	800.6	43040.0	299.8	244.4	22880.0	27.6	114.8	93.2	1222.0	79.3	47.0	230.0	1.7	25.8
F10H	Very dark peat	416.8	1029.0	804.3	447.4	10080.0	444.6	372.6	11340.0	42.3	111.4	80.0	240.2	12.2	17.0	259.2	1.6	50.3
Avg		739.8	11476.3	1550.2	4151.5	31260.3	298.4	620.3	35830.6	355.8	1320.9	404.6	1160.5	349.8	69.2	202.2	4.6	382.6

Correlation graphs were drawn for the ICP-OES data to observe the general relationship between heavy metals. R-squared values from 0.5 –1 are considered to show correlation of some extent.

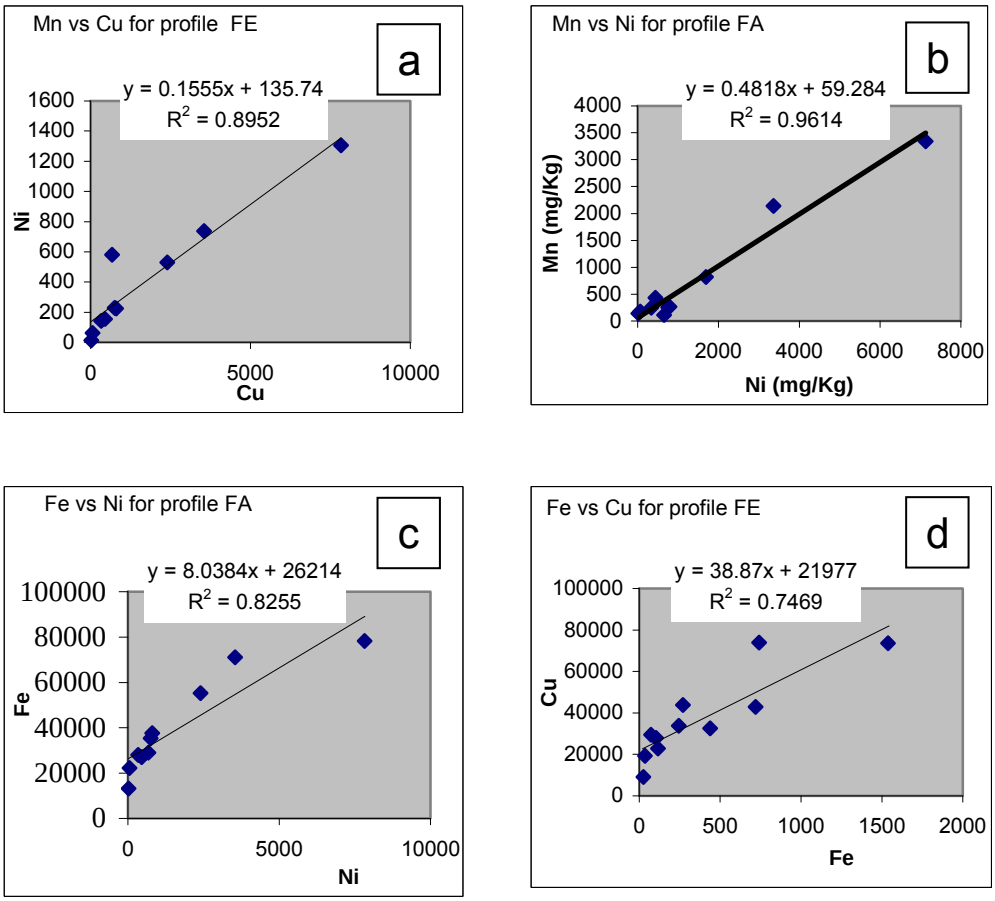


Fig. 18. Correlation plots of a) Mn vs Cu for profile FE; b) Mn vs Ni for profile FE; c) Fe vs Ni for profile FA; d) Fe vs Cu for profile FE.

This means that all metal that makes an R-squared value from 0.5 – 1 with another metal will co-precipitate, to some extent, with that metal. This relationship for a few selected metals are shown in figures 18a) – d).

In general, there is correlation in the concentration of most of the heavy metals. There is, for example correlation in the concentration of Fe and Cu; Fe and Ni; Ni and Mn; Ni and Cu. This explains the high values for those metals (Fe, Ni, Mn, Cu, Zn, Al etc) in similar samples that co-precipitate and so their concentration increases almost proportionally. This is further illustrated in the matrix in Table 7 below. Again values from 0.5 –1 are considered to show correlation of some extent. These are highlighted in bold. Negative values imply an inverse interdependence.

Comparative graphs and a correlation matrix to check the accuracy (analytical quality) of XRF and ICP-OES analyses are shown in Appendix A.1.

Table 7. Correlation matrix for trace elements from ICP-OES analysis of Fleurhof Dam sediments. Concentrations of elements are in mg/kg.

	Na	K	Ca	Mg	Al	Cr	Mn	Fe	Co	Ni	Cu	Zn	As	Se	Sr	Cd	Sn	Ba	Pt	Au	Hg	Pb	Bi	Th	U
Na	**1**	0.49	**0.64**	0.13	0.19	-0.02	0.16	0.12	0.14	0.15	0.16	0.05	0.2	0.27	-0.07	0.39	0.01	0.05	0.47	0.27	-0.3	0.09	0.2	0.1	0.02
K	0.49	1	**0.61**	0.41	0.47	0.26	0.42	0.35	**0.53**	**0.5**	0.46	0.43	**0.6**	0.33	0.1	0.42	0.21	0.27	0.31	0.41	-0.5	0.47	0.19	**0.59**	0.42
Ca	**0.64**	**0.61**	**1**	0.34	0.25	-0.03	0.35	0.28	0.33	0.34	0.3	0.16	0.4	0.21	-0.01	0.41	-0.02	0.11	0.32	0.18	-0.2	0.13	0.15	0.25	0.21
Mg	0.13	0.41	0.34	**1**	**0.5**	0.31	**0.61**	**0.5**	**0.67**	**0.67**	**0.64**	0.45	**0.6**	0.05	-0.04	-0.12	0.3	0.22	0.03	-0.1	-0.3	0.36	0.07	**0.59**	0.41
Al	0.19	0.47	0.25	**0.5**	**1**	0.29	0.09	0.21	0.19	0.17	0.27	0.12	0.25	0.23	0.08	0.23	0.34	0.38	0.19	0.15	-0.4	0.48	0.08	0.49	0.11
Cr	-0.02	0.26	-0.03	0.31	0.29	**1**	**0.5**	**0.6**	0.49	0.49	**0.56**	**0.5**	**0.5**	-0.05	-0.04	0.1	0.02	**0.7**	-0.2	-0.3	-0.1	**0.6**	-0.1	0.4	0.39
Mn	0.16	0.42	0.35	**0.6**	0.09	**0.5**	**1**	**0.8**	**0.88**	**0.91**	**0.85**	**0.7**	**0.9**	0.04	-0.05	-0.06	0.1	0.33	-0	-0.1	-0.3	0.3	-0	0.47	**0.69**
Fe	0.12	0.35	0.28	**0.5**	0.21	**0.62**	**0.75**	**1**	**0.72**	**0.75**	**0.89**	**0.6**	**0.8**	-0.06	-0.1	0.08	0.13	0.47	-0.1	-0.3	-0.2	**0.5**	0.01	0.45	**0.73**
Co	0.14	**0.53**	0.33	**0.7**	0.19	0.49	**0.88**	**0.7**	**1**	**0.99**	**0.87**	**0.7**	**0.9**	0.03	-0.02	-0.02	0.04	0.26	0.06	-0.1	-0.3	0.45	-0	**0.65**	**0.7**
Ni	0.15	**0.5**	0.34	**0.7**	0.17	0.49	**0.91**	**0.8**	**0.99**	**1**	**0.9**	**0.7**	**0.9**	-0.01	-0.02	-0.03	0.04	0.27	0.04	-0.1	-0.3	0.4	-0	**0.64**	**0.72**
Cu	0.16	0.46	0.3	**0.6**	0.27	**0.56**	**0.85**	**0.9**	**0.87**	**0.9**	**1**	**0.7**	**0.9**	-0.05	-0.07	0.07	0.19	0.38	-0	-0.1	-0.3	0.45	0.04	**0.59**	**0.76**
Zn	0.05	0.43	0.16	0.45	0.12	**0.54**	**0.67**	**0.6**	**0.74**	**0.74**	**0.7**	**1**	**0.7**	-0.04	-0.06	0.09	0.18	0.39	-0.1	-0.1	-0.3	0.32	-0.1	0.43	**0.57**
As	0.2	**0.55**	0.4	**0.6**	0.25	**0.51**	**0.9**	**0.8**	**0.88**	**0.92**	**0.92**	**0.7**	**1**	0.06	-0.06	0.07	0.12	0.34	0.08	-0.1	-0.3	0.42	0.04	**0.64**	**0.81**
Se	0.27	0.33	0.21	0.05	0.23	-0.05	0.04	-0.1	0.03	-0.01	-0.05	-0	0.06	**1**	-0.1	0.49	0.13	0.02	0.67	0.36	-0.3	0.1	0.32	0.16	0.08
Sr	-0.07	0.1	-0.01	-0	0.08	-0.04	-0.05	-0.1	-0.02	-0.02	-0.07	-0.1	-0.1	-0.1	**1**	-0.01	-0.12	-0.1	-0	**0.6**	0.01	-0.1	0.47	0.05	-0.06
Cd	0.39	0.42	0.41	-0.1	0.23	0.1	-0.06	0.08	-0.02	-0.03	0.07	0.09	0.07	0.49	-0.01	**1**	-0.01	0.21	0.46	0.28	-0	0.19	0.39	0.15	0.04
Sn	0.01	0.21	-0.02	0.3	0.34	0.02	0.1	0.13	0.04	0.04	0.19	0.18	0.12	0.13	-0.12	-0.01	**1**	0.18	-0	0.17	**-0.6**	0.17	-0.1	0.17	0.13
Ba	0.05	0.27	0.11	0.22	0.38	**0.72**	0.33	0.47	0.26	0.27	0.38	0.39	0.34	0.02	-0.13	0.21	0.18	**1**	-0.2	-0.2	-0.2	**0.6**	0.08	0.27	0.22
Pt	0.47	0.31	0.32	0.03	0.19	-0.24	-0.01	-0.1	0.06	0.04	-0.02	-0.1	0.08	**0.67**	-0.01	0.46	-0.01	-0.2	**1**	0.42	-0.3	0.05	0.27	0.08	0.05
Au	0.27	0.41	0.18	-0.1	0.15	-0.28	-0.1	-0.3	-0.07	-0.09	-0.12	-0.1	-0.1	0.36	**0.6**	0.28	0.17	-0.2	0.42	**1**	-0.4	-0.1	0.48	0.1	-0.03
Hg	-0.27	-0.47	-0.21	-0.3	-0.41	-0.08	-0.27	-0.2	-0.26	-0.25	-0.28	-0.3	-0.3	-0.31	0.01	-0.02	**-0.6**	-0.2	-0.3	-0.4	**1**	-0.2	-0	-0.3	-0.33
Pb	0.09	0.47	0.13	0.36	0.48	**0.58**	0.3	**0.5**	0.45	0.4	0.45	0.32	0.42	0.1	-0.06	0.19	0.17	**0.6**	0.05	-0.1	-0.2	**1**	0	**0.53**	0.32
Bi	0.2	0.19	0.15	0.07	0.08	-0.09	-0.01	0.01	-0.02	-0.01	0.04	-0.1	0.04	0.32	0.47	0.39	-0.08	0.08	0.27	0.48	-0	0	**1**	0.16	-0.03
Th	0.1	**0.59**	0.25	**0.6**	0.49	0.4	0.47	0.45	**0.65**	**0.64**	**0.59**	0.43	**0.6**	0.16	0.05	0.15	0.17	0.27	0.08	0.1	-0.3	**0.5**	0.16	**1**	**0.53**
U	0.02	0.42	0.21	0.41	0.11	0.39	**0.69**	**0.7**	**0.7**	**0.72**	**0.76**	**0.6**	**0.8**	0.08	-0.06	0.04	0.13	0.22	0.05	-0	-0.3	0.32	-0	**0.53**	**1**

CHAPTER SEVEN

STUDY METHODOLOGY OF RUSSEL STREAM DAM

VII.1. MAPPING AND SAMPLING OF RUSSEL STREAM DAM

The sediments in the Russel Stream dams B and C have not yet been reprocessed for their gold content, except for bulk sampling carried out by Crown Gold Recovery on the far western end of Dam C. The sediments of the Russel Stream are called the “Valley Silt” by Crown Gold Recovery and the dams are labelled A, B and C (Fig. 19). Dam A has been completely mined out, dams B and C are still unmined, except for a small trial mine operation conducted close to the far western boundary of Dam C. An excellent exposure of the stratigraphy of the old dam sediments is seen along a recent erosion channel in Dam B where a 150m longitudinal east-west section through the northern part of the sediments has been studied, approximately 100 m north-east of the old dam wall. The studied section of the exposed face of the sediment was mapped by extrapolation of five vertical profiles as shown in figure 22. Mapping and sampling procedures were the same as described in section V.1 for the Fleurhof Dam deposit.

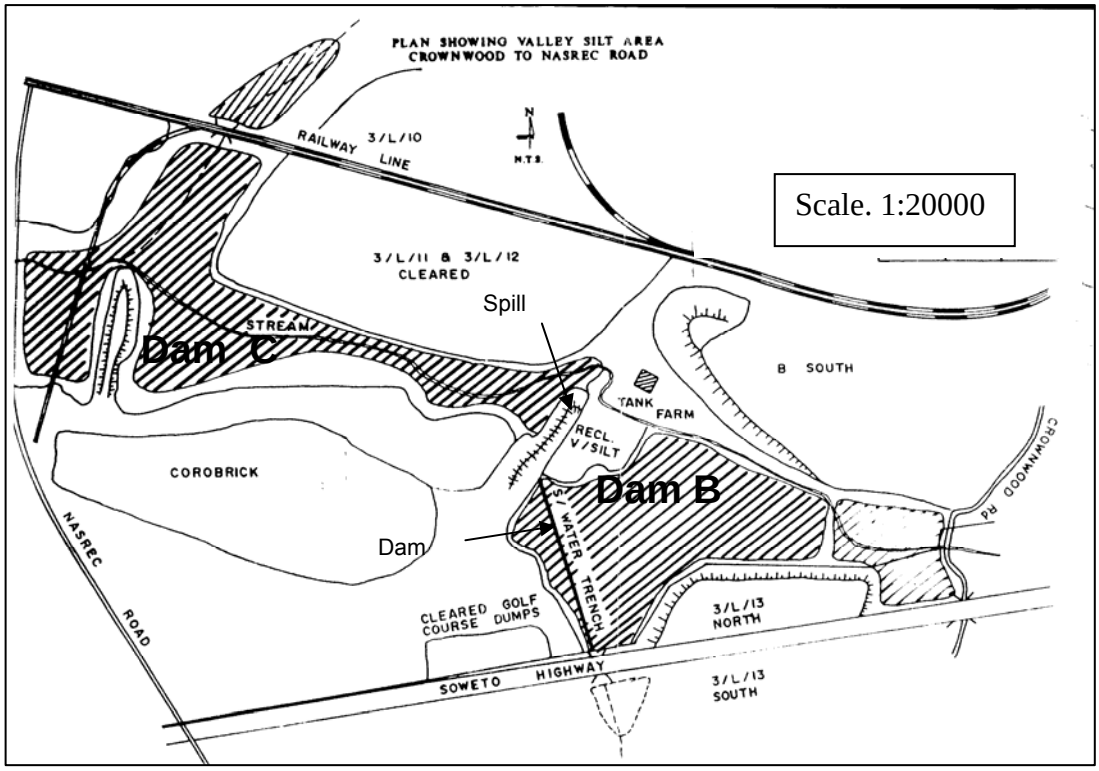


Fig.19. Diagram showing valley silt deposit of dams A, B and C on Russel Stream. (Figure obtained and modified from Crown Gold Recovery).

VII.2. SEDIMENT THICKNESS ISOPACH AND GOLD VALUE ISOCHON

Drilling data obtained from Crown Gold Recoveries prior to mining were used to model sediment thickness shown in the isopach maps in figures 20 and 21, and gold value distribution in figures 24 and 25 of the Russel Stream dams B and C. From these models an estimate of the gold resource of the deposit at Russel Stream, was determined by calculations.

VII.3. STRATIGRAPHIC LOGGING AND PROFILING OF RUSSEL STREAM DAM SEDIMENTS

Stratigraphic logging and profiling was based on physical observation of the sediments and the main criteria used to differentiate between different layers were colour, texture and layering. Based on these criteria the different layers were described and stratigraphic profiles drawn.

VII.4. MINERALOGICAL ANALYSIS OF RUSSEL STREAM DAM SEDIMENTS

VII.4.A. X-RAY DIFFRACTION (XRD) ANALYSIS

Mineralogical analysis was conducted at the School of Geosciences at the University of the Witwatersrand, Johannesburg, by the same procedures as described in section V.4.A. of Fleurhof Dam.

VII.5. GEOCHEMICAL ANALYSIS OF RUSSEL STREAM DAM SEDIMENTS

VII.5.A. X-RAY FLUORESCENCE (XRF) ANALYSIS

Geochemical analysis by XRF for the Russel Stream sediments was carried out at the School of Geosciences at the University of the Witwatersrand, Johannesburg, by Mrs Sharon Farrel by the same procedure as described in section V.5.A. of Fleurhof Dam.

VII.5.B. INDUCTIVELY COUPLED PLASMA-MASS SPECTROSCOPY (ICP-MS) ANALYSIS

Inductively Coupled Plasma-Mass Spectroscopy (ICP-MS) was carried out for the Russel Stream samples by the Council for Geosciences in Pretoria. Specific ICP-MS methods were used for different groups of metals: Ni, Cu, Zn, Cd, Hg and Pb were analysed by Aqua Regia-leach; Bi, Th, and U by $HF/HClO_4$ decomposition; As and Se by HNO_3 leach while Co, Pt and Au were done by fire assay and atomic absorption.

VII.6. NORMATIVE CALCULATIONS ON RUSSEL STREAM DAM SEDIMENTS

Normative calculations on the Russel Stream samples were done in the same manner as described in section V.6. of Fleurhof Dam, and portrayed on ternary plots.

CHAPTER EIGHT

RESULTS AND DISCUSSION OF RUSSEL STREAM DAM STUDY

VIII.1. SEDIMENTOLOGY OF RUSSEL STREAM DAM

VIII.1i. SEDIMENT THICKNESS.

In the Russel Stream deposits, the maximum thickness is defined by a region of greater than 12 m of sediment fill just below and behind the dam wall in Dam B (Fig. 20). An axial zone following the original river course contains sediments in excess of 10m over a distance of 250 m. Dam C downstream of Dam B shows a similar pattern with an axial zone of greater than 8m thickness (Fig. 21). Sediments below the dam wall of Dam B came from a leakage of the golf course dumps (Fig. 19), (Laing, 2005, personal communication). Not many distributaries are seen, but there is a major diversion of the original river channel at the river mouth in Dam B due to sediment infill.

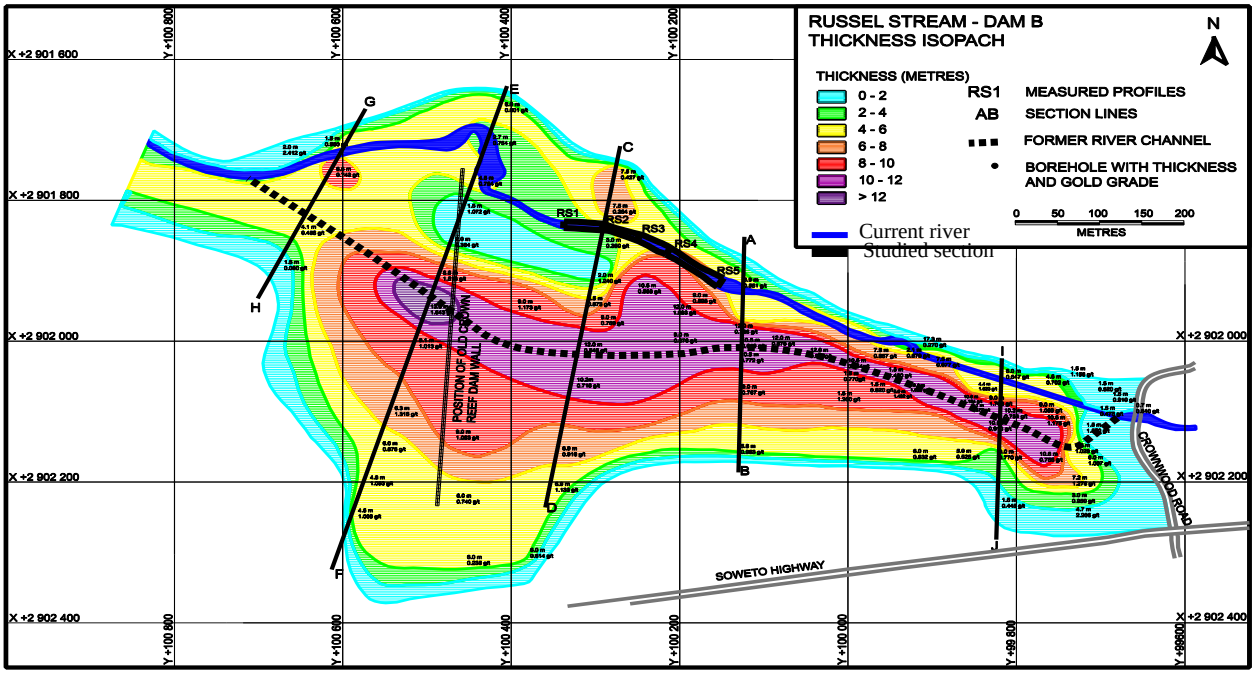


Fig. 20, Isopach of sediment thickness (m) in the Russel Stream Dam B. Map was obtained from Crown Gold Recovery, 2005, hand-contoured. Marco of Uramin Inc digitised the hand-contoured map using Geostation software.

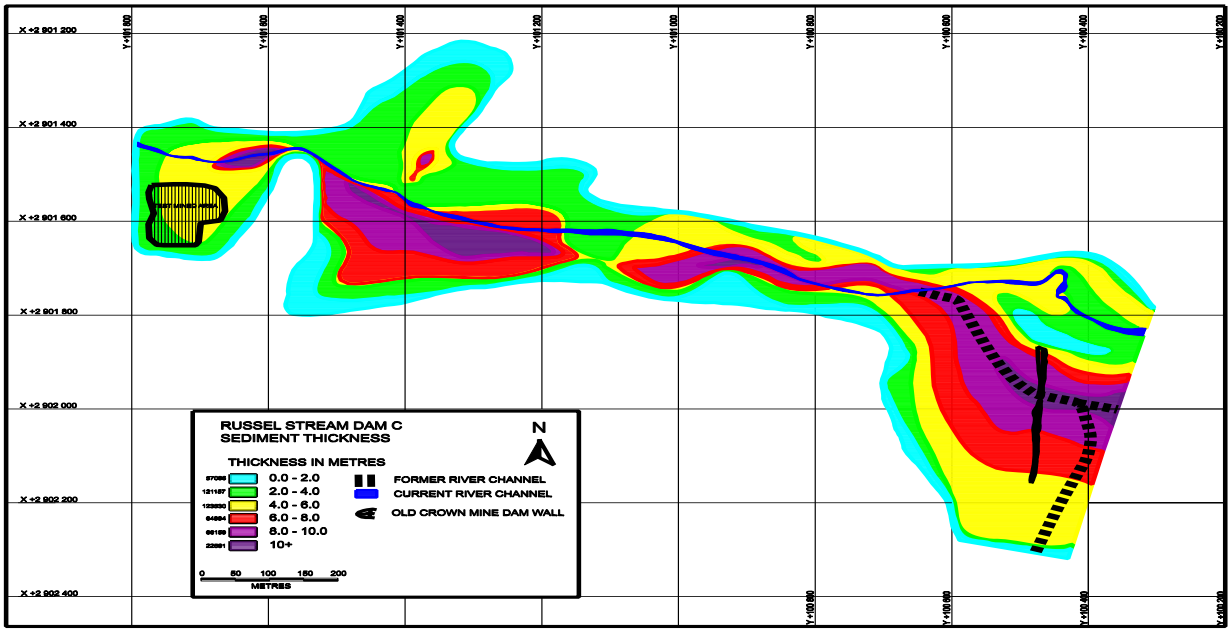


Fig. 21, Isopach of sediment thickness (m) in the Russel Stream Dam C. Map was obtained from Crown Gold Recovery, 2005, hand-contoured. Marco of Uramin Inc digitised the hand-contoured map using Geostation software.

In general the zone of highest thickness occurs along the main river channel and thins out on both sides toward the edges of the dams, as is the case in the Fleurhof Dam. Sediments are generally thicker in Dam B than in Dam C.

VIII.1.ii. LONGITUDINAL SECTION OF RUSSEL STREAM DAM.

The section mapped and studied on the Russel Stream sediments is a 150 m long east-west oblique section of Dam B approximately 100 m north-east of the dam wall where a concrete wall was built. This section has been exposed by the recent erosion channel of the Russel Stream. The studied section of the exposed face of the sediment was mapped to correlate the stratigraphic columns shown in figure 21 above. The section varies in thickness along the river course from the concrete wall toward the edge of the dam. The quartzitic bedrock rises in the section as it is oblique to the axis of the dam, causing an on-lapping of the layers. The top of layer RSF represents the original water level when it was covered with water by analogy with the Fleurhof deposit. Lines RS1, RS2, RS3, RS4 and RS5 are the stratigraphic profiles from where samples were collected (Fig. 23).

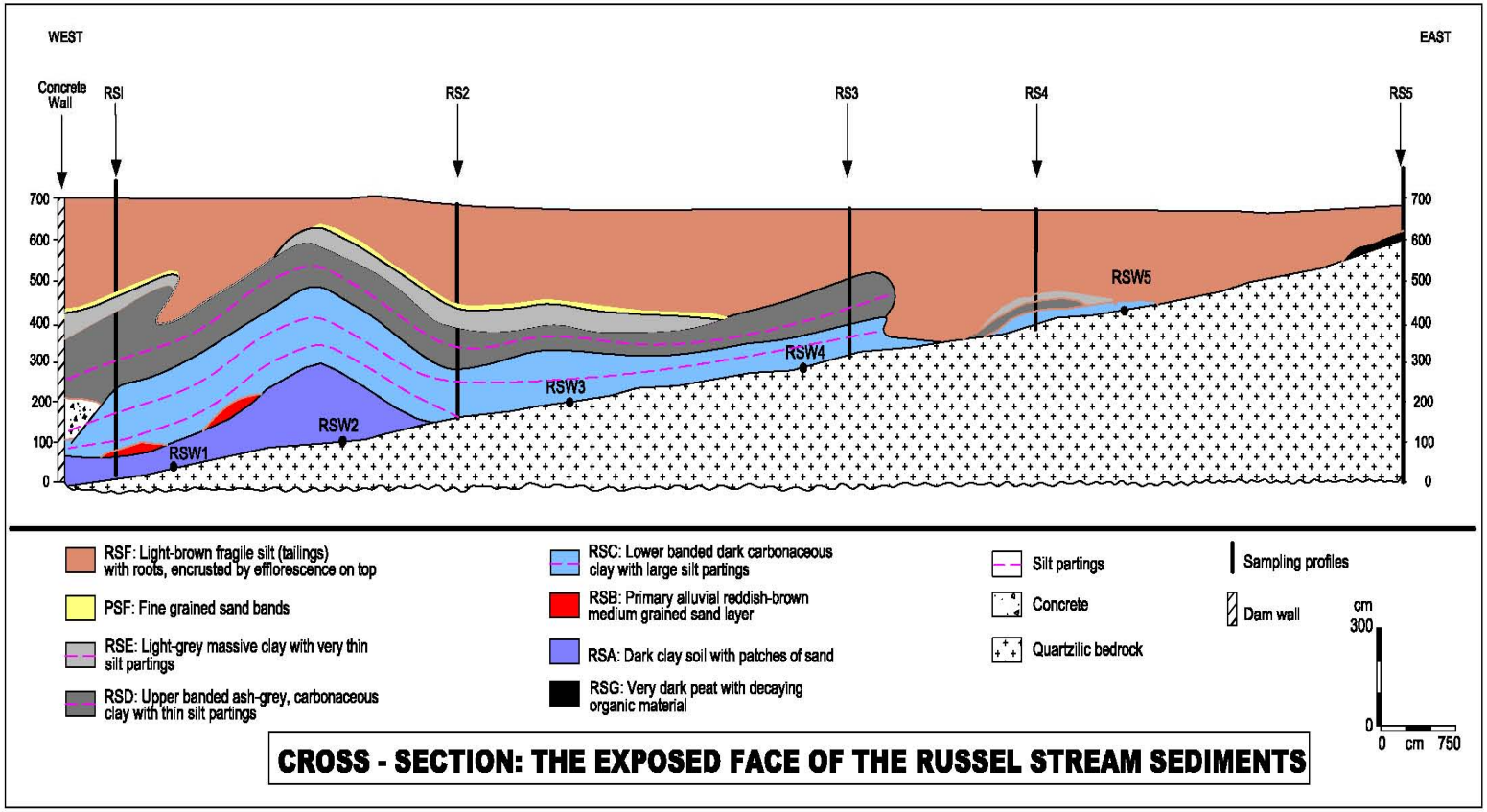


Fig. 22 Stratigraphic section of exposed face of unmined sediment in the Russel Stream dam.

VIII.1.iii. STRATIGRAPHIC COLUMNS OF RUSSEL STREAM DAM

Five vertical profiles labelled RS1, RS2, RS3, RS4 and RS5 were logged and described using the same criteria (colour, texture and layering) as for the Fleurhof Dam, and are portrayed in figure 23. The manner in which Samples as represented in figure 8 have been collected from the dam is as follows: samples RS1F, RS2F, RS3F, RS4F and RS5F are taken from the same layer RSF in such a way that each sample is a representative of the entire layer within the corresponding profile. The continuous stratigraphic section of the studied area of the Russel Stream deposit exposed by the current river channel is shown in figure 22. The stratigraphic columns reveal the following layers from top to bottom:

RSF: Light-brown silt with grass roots, encrusted with efflorescence.

RSF': Yellowish fine grained sand bands.

RSE: Light-grey mud with very thin silt partings.

RSD: Upper banded ash-grey carbonaceous mud with thin silt partings.

RSC: Lower banded dark carbonaceous mud with large silt partings.

RSB: A primary alluvial reddish-brown medium grained sand.

RSA: Dark muddy soil with patches of sand.

RSG: Very dark peat with decaying organic material.

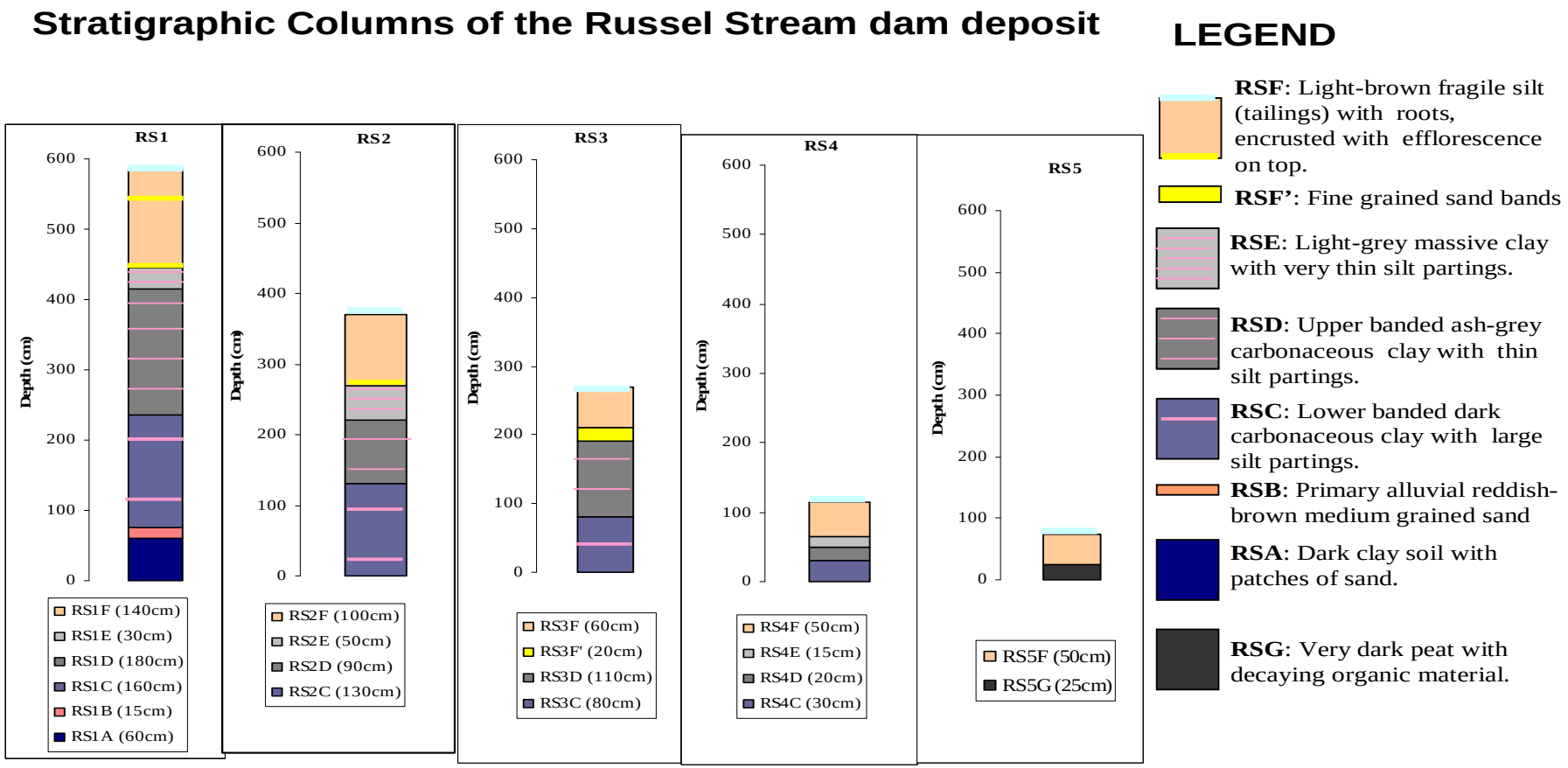


Fig. 23. Stratigraphic columns of profiles RS1, RS2, RS3, RS4 and RS5 of Russel Stream dam. Profiles were drawn using power point. Sample number (e.g. RS1A) represents an entire layer within the corresponding profile from which it is collected.

VIII.1.iv. DEPOSITIONAL STYLE AND SEDIMENTATION OF RUSSEL STREAM DAM

Russel Stream dam was fed by the Russel Stream. Sediments eroded from surrounding tailings dams of the Crown Mines were washed down directly into the Russel Stream and deposited into three dams stretching over a distance of about 2km east-west and connected to one another, some 500m south and southwest of the present Crown Gold Recovery plant. The depositional style is also deltaic with progadational sedimentation, similar to that of the Fleuhof dam. Few metres north of the dam wall a spill gate was built, but subsequently broken down by pressure from in-coming water and sediment accumulation and the river's course was diverted to go around the dam wall. Sediments were then washed down into Dam C. Sediments behind the dam wall in Dam B were eroded from the Crown Mines Golf Course dump (Fig. 19).

VIII.2. GOLD VALUE DISTRIBUTION IN RUSSEL STREAM DAM

The vertical profiles for gold occurrence in the Russel Stream sediment are shown in figures 28, 29 and 30. The highest gold peaks occur in layers RSE and RSC. These layers consist mainly of mud. The map of gold grade distribution for Russel Stream Dams B and C are shown in isochon maps in figures 24 and 25. Data obtained from Crown Gold Recovery were hand-contoured and digitised. The average gold grade in the sediments is 0.8g/t Au. The areas of highest gold

grade occurrence (>1.2g/t Au), define ore shoots, which closely follow the former river channel in the proximal part of Dam B and extends over a length of about 300m with an average width of 50m, from the river mouth in an east-west direction. A short break then occurs before the higher grade shoot continues for another distance of 300m up to the dam wall. High Au values occur on both sides of the dam wall. West of the dam wall the high values are in part due to leakage of tailings from the Crown Mines Golf Course dumps (W. Laing, 2005, personal communication). An area averaging 1g/t Au and trending north – south straddles the dam wall and runs over a distance of about 300m with an average width of 100m. These are in close association with areas of maximum sediment thickness.

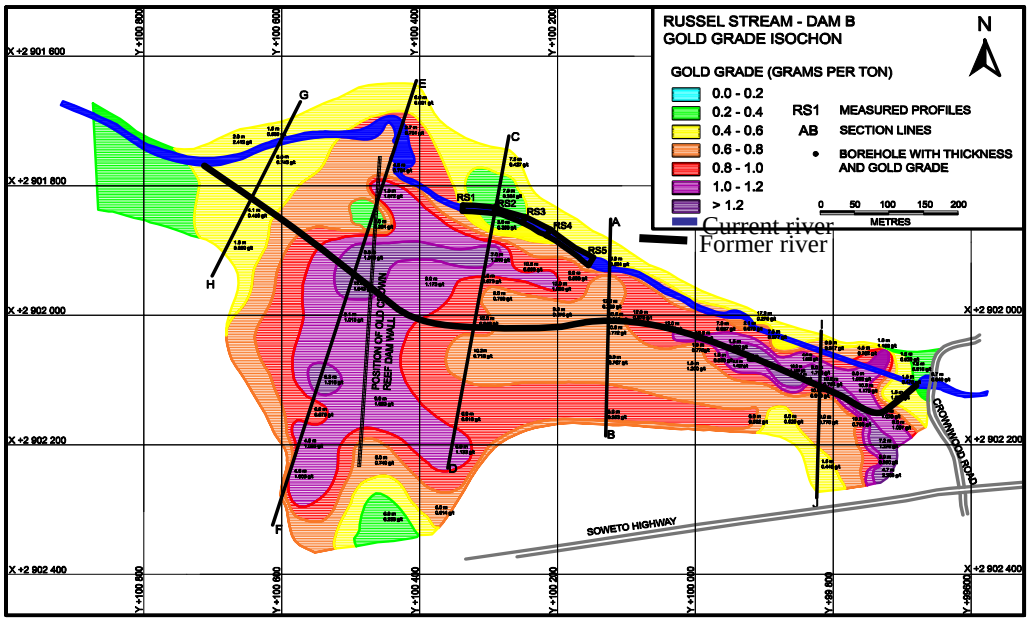


Fig. 24: Isochon of gold grade (g/t Au) in the Russel Stream sediments (Dam B). Data obtained from Crown Gold Recovery, 2005, was hand-contoured. Marco of Uramin Inc. digitised the hand-contoured map using Geostation software.

Lower gold grade characterises Dam C (Fig. 25). Most of the areas average 0.4g/t Au and the distribution pattern is not well defined and differs from that of Dam B. Two small high grade areas of about 50m long and 10m wide occur at the proximal most part of Dam C, immediately south of the dam wall in Dam B and in the distal most part near the bulk mine area.

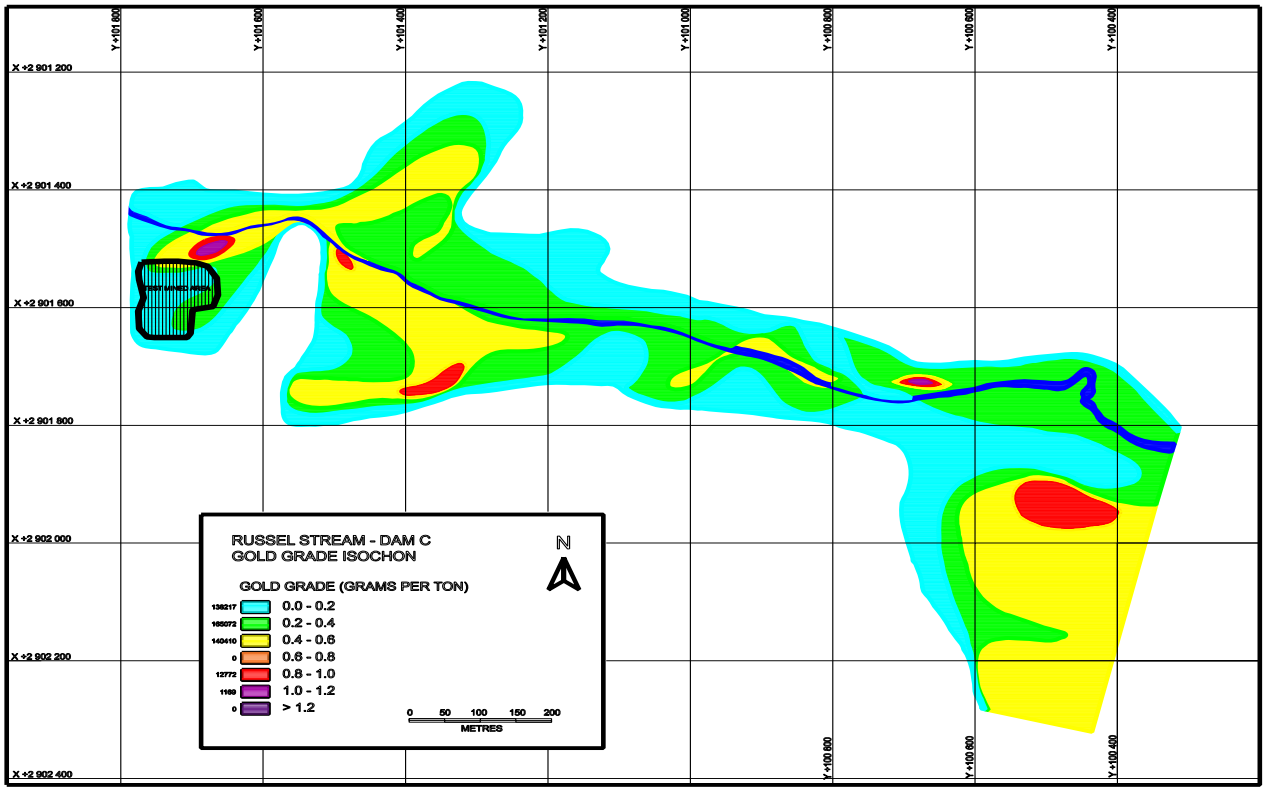


Fig. 25 Isochon of gold grade (g/t Au) in the Russel Stream sediments (Dam C). Map obtained from Crown Gold Recovery, 2005, was hand-contoured. Marco S. of Uramin Inc. digitised the hand-contoured map using Geostation software.

The sediments in Dams B and C of the Russel Stream deposit are almost totally unmined except for a bulk sample area on the far western boundary of Dam C, which was carried out by Crown Gold Recovery. Calculations were thus done in

an effort to estimate the gold resource in these dams as shown in Tables 8i) and 8ii) below.

Table 8i and 8ii Calculations of the volume of sediment and gold content in the Russel Stream Dams B and C on Crown Mines

Table 8.i. Dam B

Thickness Range (m)	Colour index	Avg thickness (m)	Area	Volume (m3)	Tonnage
0-2		1	62694	62694	106580
2-4		3	54449	163347	277690
4-6		5	119037	595185	1011815
6-8		7	53655	375585	638495
8-10		9	65732	591588	1005700
10-12		11	57116	628276	1068069
>12		13	3302	42926	72974.2
Total					**4,181,322**

Table 8.ii. Dam C

Thickness Range (m)	Colour index	Avg thickness (m)	Area	Volume (m3)	Tonnage
0-2		1	57086	57086	97046.2
2-4		3	121157	363471	617901
4-6		5	123530	617650	1050005
6-8		7	64994	454958	773429
8-10		9	66159	595431	1012233
>10		11	22581	248391	422265
Total					**3972878**
Test mined area		4	11686	46745.2	79466.8

Grand total = 4181322 (Dam B) + 3972878 (Dam C) = **8,154,200 tons.** If the test mined area is taken out, then the total volume of sediment in the Russel Stream deposit at present is estimated to be 8,154,200 - 79466.8 (Test mined area) = **8,074,733 tons at 0.8g/t Au.** The average grade, 0.8g/t Au, is determined from data provided by Crown gold Recovery and the density of tailings d = 1.7. From this the total gold content in this deposit (inferred resource) has been estimated to be **6.4 tons of gold (≈ 206,452 ounces).**

VIII.3. MINERALOGY OF RUSSEL STREAM DAM

VIII.3. A. X-Ray Diffraction (XRD)

The minerals obtained from XRD analysis for samples from the Russel Stream Dam are shown in Table 9.

Table 9, XRD results from Russel Stream. For sample localities see figure 22.

Samples points	**Sediment type**	**Minerals present**
RS1A	Dark clay soil	Quartz, Pyrophylite
RS1B	Primary alluvial sand	Quartz, Pyrite.
RS1C'	Flash-flood sand	Quartz, Muscovite, Pyrophylite, Pyrite
RS1C	Lower banded carbonaceous clay	Quartz, Muscovite, Pyrophylite.
RS1D	Upper banded carbonaceous clay	Quartz, Pyrophylite, Muscovite
RS1E	Massive clay	Quartz, Muscovite, Pyrophylite.
RS1F	Fragile silt	Quartz, Gypsum
RS2C'	Flash-flood sand	Quartz, Muscovite, Chloritoid
RS2C	Lower banded carbonaceous clay	Quartz, Potassium
RS2D	Upper banded carbonaceous clay	Quartz, Muscovite.
RS2E	Massive clay	Quartz, Muscovite
RS2F	Fragile silt	Quartz, Muscovite, Pyrophylite.
RS3C'	Flash-flood sand	Quartz, Pyrite, Muscovite, Pyrophylite.
RS3C	Lower banded carbonaceous clay	Quartz, Muscovite, Pyrite, Chloritoid, Pyrophylite
RS3D	Upper banded carbonaceous clay	Quartz, Muscovite, Pyrophylite, Pyrite.
RS3F'	Massive clay	Quartz, Muscovite, Pyrophylite, Chloritoid, biotite
RS3F	Fragile silt	Quartz, Pyrite.
RS4C	Lower banded carbonaceous Clay	Quartz, Muscovite, Pyrite.
RS4D	Upper banded carbonaceous clay	Quartz, Muscovite, Pyrite, Orthoclase
RS4F	Fragile silt	Quartz, Muscovite, Biotite, Pyrite, Pyrophylite, Chloritiod,
RS5F	Fragile silt	Quartz, Muscovite, Pyrite
RS5G	Dark peat	Quartz, Muscovite, Pyrophylite, Pyrite, Orthoclase
RD1	Tailings	Quartz, Muscovite, Pyrophylite
RD2	Tailings	Quartz, Muscovite, biotite, Orthoclase

Quartz represents the most abundant mineral and also occurs in all samples of the Russel Stream sediments. Muscovite is the second most abundant mineral. Other minerals that occur in smaller proportions are pyrophylite, illite, pyrite, uranite. Muscovites is a flaky minerals and is easily trapped by organic matters in comparison to pyrophylite. The Russel Stream sediments show very low or no illite content. RD1 and RD2 are samples from tailings dams close to the Russel Stream dams and contain little or no illite.

VIII.4. GEOCHEMISTRY OF RUSSEL STREAM DAM

VIII.4.i. MAJOR ELEMENTS

VIII.4.i.a. X-Ray Fluorescence (XRF) analysis

Major element abundance obtained from XRF analysis of the Russel Stream deposits are shown in Table 10.

Table 10. Major elements abundance (wt %) in Russel Stream sediments. For sample localities see figure 22.

Sample #	Sediment type	%Na2O	%MgO	%Al2O3	%SiO2	%K2O	%CaO	%TiO2	%Fe2O3	%LOI	%MnO	%P2O5
RS1A	Dark clay soil	0.04	0.00	8.55	82.55	0.28	0.11	0.45	2.11	5.15	0.01	0.02
RS1B	Primary alluvial sand	0.03	0.00	3.92	87.60	0.16	0.14	0.27	3.28	3.46	0.02	0.01
RS1C	Lower banded clay	0.23	0.00	10.51	71.51	1.19	0.13	0.44	5.25	9.30	0.06	0.07
RS1C`	Flash-flood sand	0.12	0.00	6.42	83.38	0.60	0.03	0.37	3.69	4.55	0.03	0.03
RS1D	Upper banded clay	0.33	0.11	13.53	76.96	2.13	0.06	0.48	6.49	0.00	0.05	0.10
RS1E	Massive	0.37	0.15	12.44	70.86	2.16	0.76	0.38	4.80	8.65	0.03	0.16

Sample #	Sediment type	%Na2O	%MgO	%Al2O3	%SiO2	%K2O	%CaO	%TiO2	%Fe2O3	%LOI	%MnO	%P2O5
	clay											
RS1F	Fragile silt	0.16	0.00	6.61	71.90	0.81	1.96	0.34	7.03	11.57	0.05	0.06
RS2C`	Flash-flood sand	0.17	0.00	6.86	82.39	0.78	0.03	0.36	4.51	4.30	0.03	0.03
RS2C	Lower banded clay	0.32	0.24	13.18	72.07	1.68	0.40	0.45	3.66	8.50	0.04	0.06
RS2D	Upper banded clay	0.32	0.03	14.00	76.09	1.92	0.07	0.45	5.88	0.00	0.04	0.09
RS2E	Massive clay	0.33	0.40	12.84	70.45	1.90	0.21	0.41	5.03	10.15	0.04	0.13
RS2F	Fragile silt	0.19	0.00	7.55	82.31	0.92	0.09	0.39	4.15	4.34	0.04	0.06
RS3C	Lower banded clay	0.28	0.06	13.10	69.77	1.66	0.20	0.47	6.09	8.38	0.05	0.10
RS3D	Upper banded clay	0.34	0.07	11.61	74.39	1.61	0.17	0.39	4.98	6.95	0.04	0.05
RS3F`	Massive clay	0.11	0.00	3.26	90.81	0.36	0.06	0.32	2.13	1.65	0.02	0.00
RS3F	Fragile silt	0.14	0.00	5.40	86.90	0.62	0.08	0.35	3.35	3.53	0.03	0.02
RS4C	Lower banded clay	0.27	0.03	11.53	73.52	1.45	0.10	0.43	5.97	6.67	0.03	0.08
RS4D	Upper banded clay	0.29	0.00	10.35	77.67	1.42	0.06	0.36	2.83	7.45	0.03	0.03
RS4F	Fragile silt	0.13	0.00	4.52	87.03	0.55	0.10	0.32	3.35	4.25	0.03	0.05
RS5F	Fragile silt	0.13	0.00	3.58	88.92	0.44	0.06	0.30	2.61	2.66	0.03	0.02
RS5G	Dark peat	0.18	0.00	5.81	77.33	0.73	3.44	0.32	4.46	6.18	0.03	0.08
Average		0.21	0.05	8.62	79.26	1.08	0.38	0.38	4.29	5.45	0.03	0.06

SiO_2 has an average abundance of above 79.26. Highest silica values occur in samples RS1A, RS1B, RS1C', RS3C'', RS3F', RS3F, RS4F and RS5F, which all have a SiO_2 content of above 80%. These represent the very silty and/or sandy layers. The high content of SiO_2 in layer RS1A (the dark peat) is probably due to SiO_2 and carbonaceous material being the main components of RS1A. RS1A also contains patches of sand. Other major elements that occur in less abundance are Al_2O_3, Fe_2O_3, S and K_2O. Highest values of these elements occur in samples RS1D, RS1E, RS1F, RS2C, RS2D, RS2E, RS3C, and RS4C which are mainly mud with high adsorbing capacity. Ternary plots were drawn to

portray variations in SiO_2, Al2O3 and K_2O for profiles RS1-RS5 of the studied section of Russel Stream Dam B are shown in figures 26a) – e).

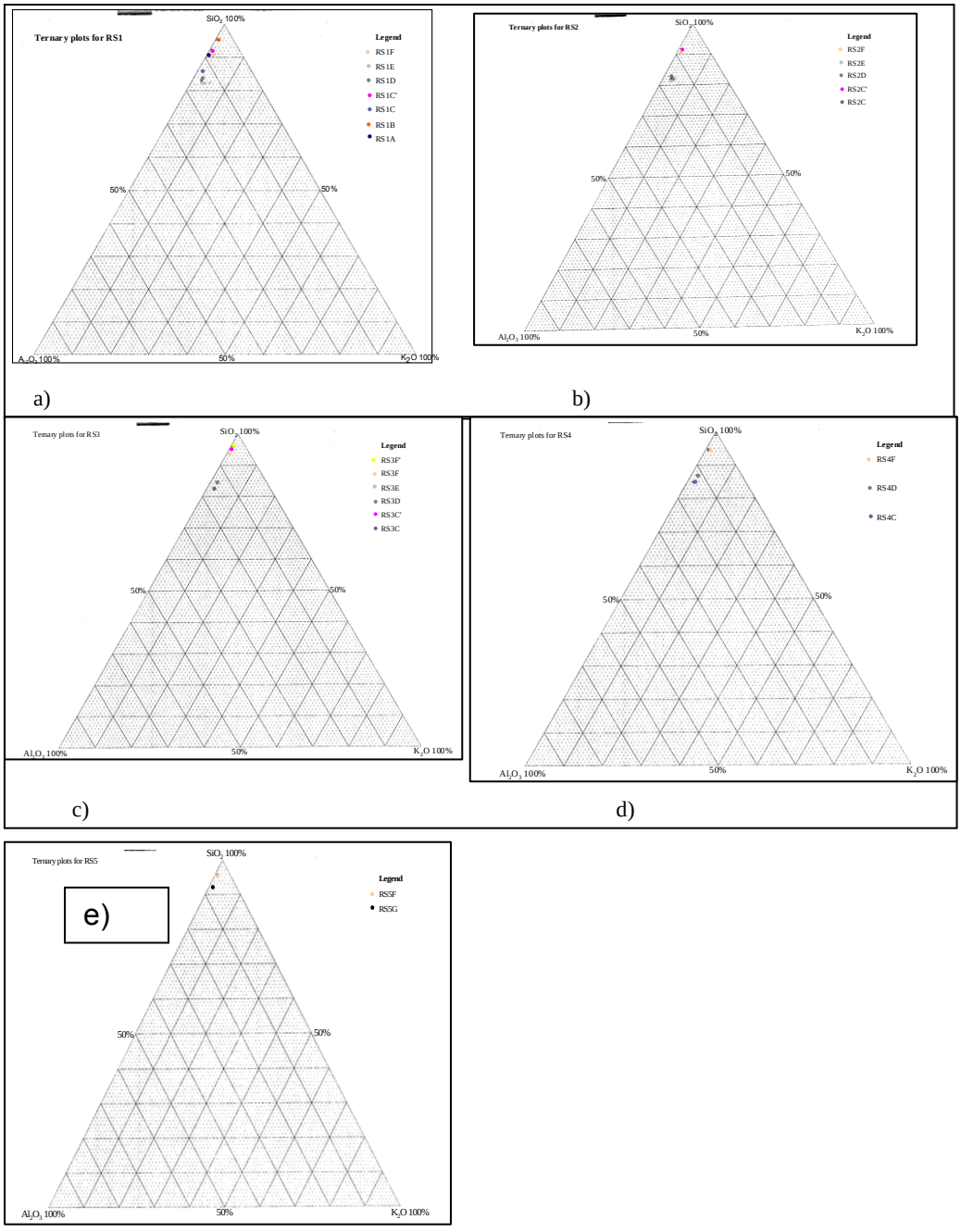


Fig. 26: Ternary plots of major elements abundance (wt %) for profiles a):RS1; b): RS2; c): RS3; d): RS4 and e): RS5 of Russel Stream Dam B. See fig. 23 for complete description of legend.

The ternary plots indicate the dominance of quartz in the samples as seen in the average concentration of major elements in Table 10 above. This is further portrayed in the normative calculations shown in Table 11.

Table 11. Table showing normative calculations of major minerals of Russel Stream sediments. For sample localities see figure 22.

Sample	Sediment type	Quartz	Pyrophyllite	Illite	Hematite	Total
RS1A	Dark clay soil	63.47	26.99	2.37	2.11	94.95
RS1B	Primary alluvial sand	78.98	12.01	1.36	3.28	95.62
RS1C	Flash-flood sand	51.31	23.45	10.08	5.25	90.10
RS1C`	Lower banded clay	70.55	15.79	5.08	3.69	95.11
RS1D	Upper banded clay	53.25	23.32	18.05	6.49	101.11
RS1E	Massive clay	49.83	19.12	18.31	4.8	92.06
RS1F	Fragile silt	59.43	14.04	6.86	7.03	87.37
RS2C`	Flash-flood sand	69.22	15.27	6.61	4.51	95.61
RS2C	Lower banded clay	47.46	27.25	14.24	3.66	92.61
RS2D	Upper banded clay	50.47	27.39	16.27	5.88	100.01
RS2E	Massive clay	47.48	23.52	16.10	5.03	92.14
RS2F	Fragile silt	68.05	16.10	7.80	4.15	96.09
RS3C``	Flash-flood sand	81.24	9.68	3.64	2.83	97.40
RS3C	Lower banded clay	45.27	27.20	14.07	6.09	92.63
RS3D	Upper banded clay	53.21	22.51	13.64	4.98	94.34
RS3F`	Massive clay	84.51	7.38	3.05	2.13	97.07
RS3F	Fragile silt	76.55	11.95	5.25	3.35	97.11
RS4C	Lower banded clay	51.91	24.07	12.29	5.97	94.24
RS4D	Upper banded clay	58.73	20.24	12.03	2.83	93.84
RS4F	Fragile silt	78.49	9.65	4.66	3.35	96.15
RS5F	Fragile silt	82.17	7.59	3.73	2.61	96.10
RS5G	Dark peat	66.44	12.14	6.19	4.46	89.22

Samples that have quartz values above 70% include RS1B, RS1C', RS3C'', RS3F', RS3F, RS4F and RS5F. RS1B is the primary sand layer, RS1C', RS3C'', RS3F', RS3F, RS4F and RS5F either contain silt or are silt partings (Fig. 23). These samples also have relatively low values of Al_2O_3, Fe_2O_3, S and K_2O. Where the values of these elements (Al_2O_3, Fe_2O_3, S and K_2O) are high such as

in samples RS4C, RS4D, RS3C, RS3D, RS2C, and RS2D (which are more clay rich layers), the values of quartz are low. Thus the clay content of the sediment decreases as the sand or silt content increases. Ternary plots further illustrating the abundance of quartz, pyrophylite and illite are shown in figures 27 a) – e).

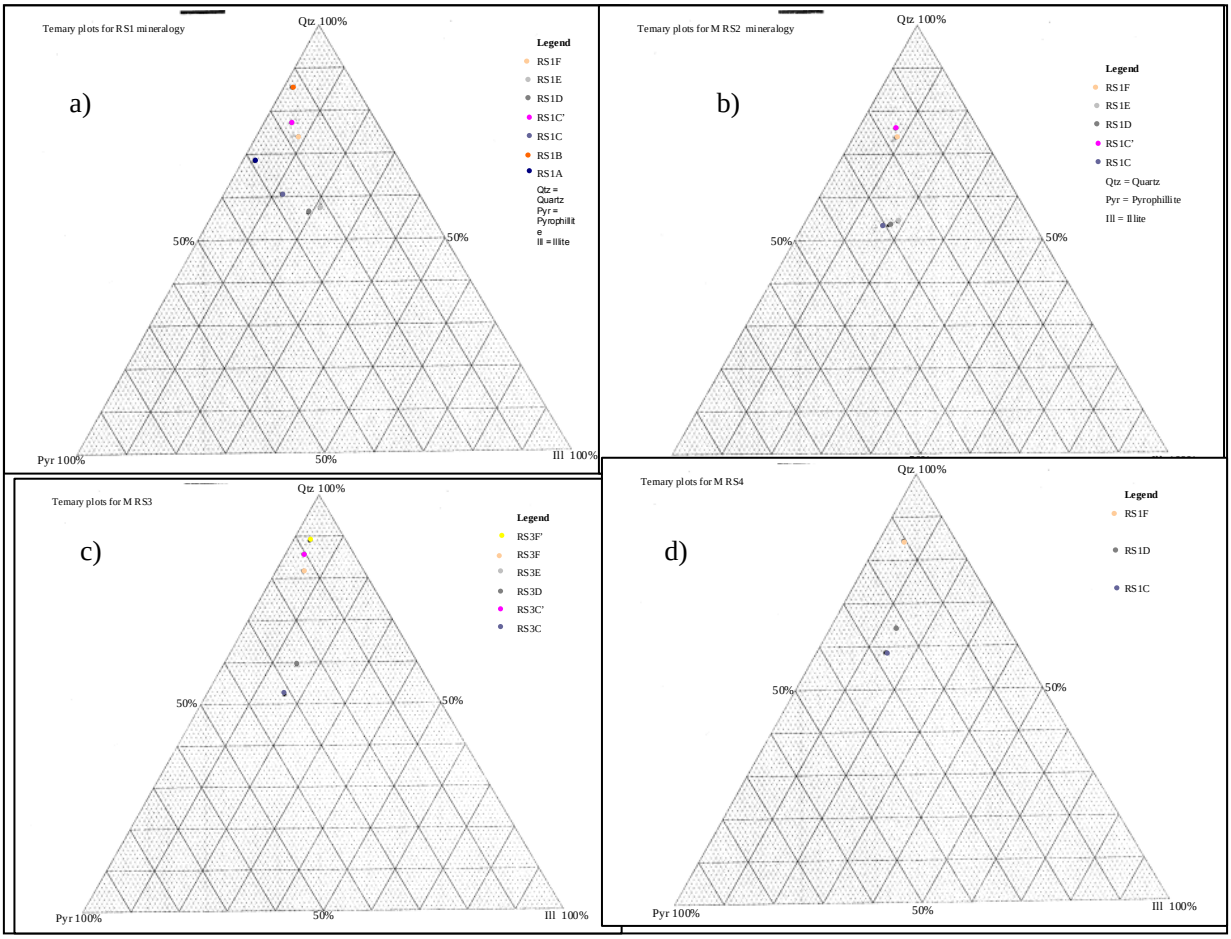


Fig. 27. Ternary plots of major minerals for profiles a):RS1; b): RS2; c): RS3; d): RS4 and e): RS5 of Russel Stream Dam B. See figure 23 for complete description of legend.

The results of major elements analysis as shown in the ternary plots and normative calculations are in conformity with the mineralogy of the samples as indicated by the result of XRD results. Samples reflect abundance in silica. Silica abundance increases from bottom to top of the profiles and longitudinally from the dam wall upstream-ward.

VIII.4.ii. TRACE ELEMENTS

VIII.4.ii.a. X-Rays Fluorescence (XRF) analysis

The results of trace elements analysis by XRF for the Russel Stream samples are shown in Table 12.

Table 12. Results of trace elements analysis by XRF for the Russel Stream sediments. The description of each sample is given in the legend of figure 22.

Sample #	Sediment type	Rb	Sr	Y	Zr	Nb	Co	Ni	Cu	Zn	TiO2	V	Cr	Ba
		ppm	Ppm	ppm	ppm	Ppm	Ppm	Ppm	ppm	ppm	Ppm	ppm	ppm	ppm
LLD		**3**	**3**	**3**	**8**	**3**	**6**	**6**	**6**	**6**	**0.01**	**12**	**12**	**20**
RS1A	Dark clay soil	30	18	19	168	7	35	145	34	385	0.26	120	299	162
RS1B	Primary alluvial sand	16	22	12	132	5	16	59	28	174	0.46	65	196	147
RS1C	Flash-flood sand	28	36	13	170	6	16	73	37	73	0.38	64	230	216
RS1C'	Lower banded clay	29	64	15	184	5	45	92	107	124	0.42	58	269	294
RS1D	Upper banded clay	45	61	32	166	6	115	385	104	463	0.48	91	328	381

RS1E	Massive clay	61	67	22	153	7	48	217	77	171	0.4	87	362	478
RS1F	Fragile silt	64	92	19	137	6	58	233	88	152	0.44	80	357	467
RS2C	Lower banded clay	61	67	34	162	7	235	961	124	910	0.5	90	361	425
RS2C'	Flash-flood sand	30	45	13	174	5	15	68	50	65	0.43	60	240	269
RS2D	Upper banded clay	62	71	18	152	6	30	135	100	124	0.49	97	382	522
RS2E	Massive clay	65	74	23	140	6	42	173	72	167	0.41	87	371	455
RS2F	Fragile silt	34	43	12	174	5	20	86	52	110	0.36	62	287	277
RS3C		62	68	27	166	7	80	241	278	613	0.52	85	359	439
RS3C'	Flash-flood sand	17	32	11	181	5	14	59	17	41	0.37	41	185	172
RS3D	Lower banded clay	51	60	20	143	6	76	306	69	268	0.4	77	309	414
RS3F	Upper banded clay	23	34	11	161	5	10	40	34	44	0.38	47	212	202
RS3F'	Massive clay	16	25	9	159	5	6	26	18	25	0.42	38	177	143
RS4C	Lower banded clay	50	64	16	167	6	25	99	72	159	0.41	86	320	394
RS4D	Upper banded clay	50	58	14	152	6	24	94	69	103	0.34	75	303	379
RS4F	Fragile silt	21	31	9	155	5	8	33	60	51	0.36	53	238	211
RS5F	Fragile silt	17	28	8	145	4	8	27	22	26	0.33	41	168	162
RS5G	Dark peat	31	36	22	193	6	100	348	60	119	0.35	65	293	250
Avg		39.23	49.82	17.227	160.6	5.73	46.64	177.3	71.46	199	0.41	71.32	284	311.77

High metal concentrations occur in layers RS1A, RS1C, RS2C, RS3C, RS1E, RS2E and RS3E. Layer RSA is the very dark clay on top of the peat layer. RSC is the carbonaceous mud. Layer RSE is the massive light grey mud with very fine silt partings. In general, the tendency is for metal concentration to be higher in the bottom layers than in the layers near the surface. The concentration of gold in layer RSB is very low. Comparative graphs of metal correlation were drawn for profiles RS1, RS2 and RS3 of the Russel Stream sediments and are shown in figures 28, 29 and 30. The Au values presented on these graphs are from ICP-MS results shown in Table 13ii.

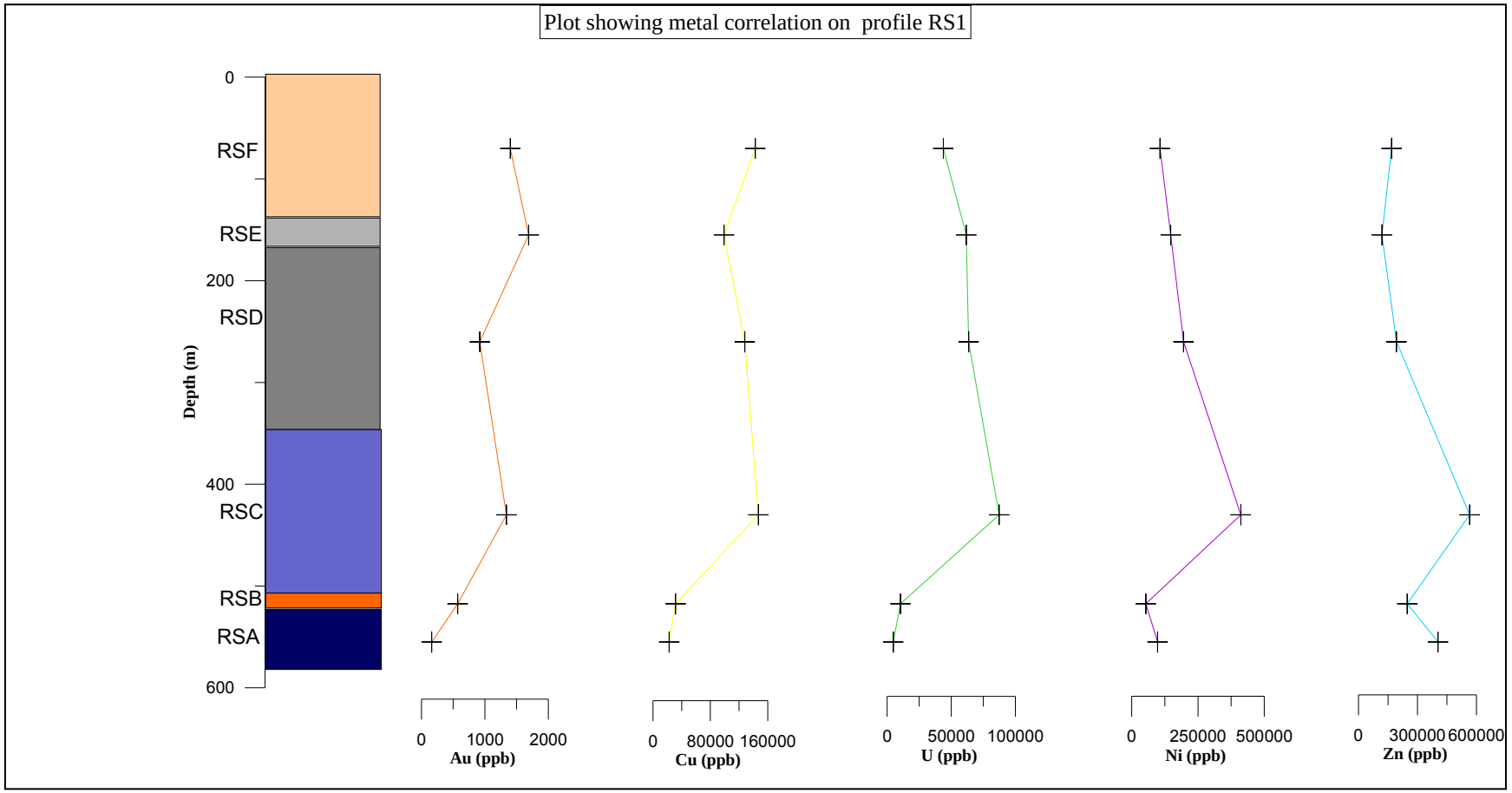


Fig. 28. Comparative graphs of metal concentration along profile RS1 on Russel Stream. See figure 23 for full description of stratigrapgy.

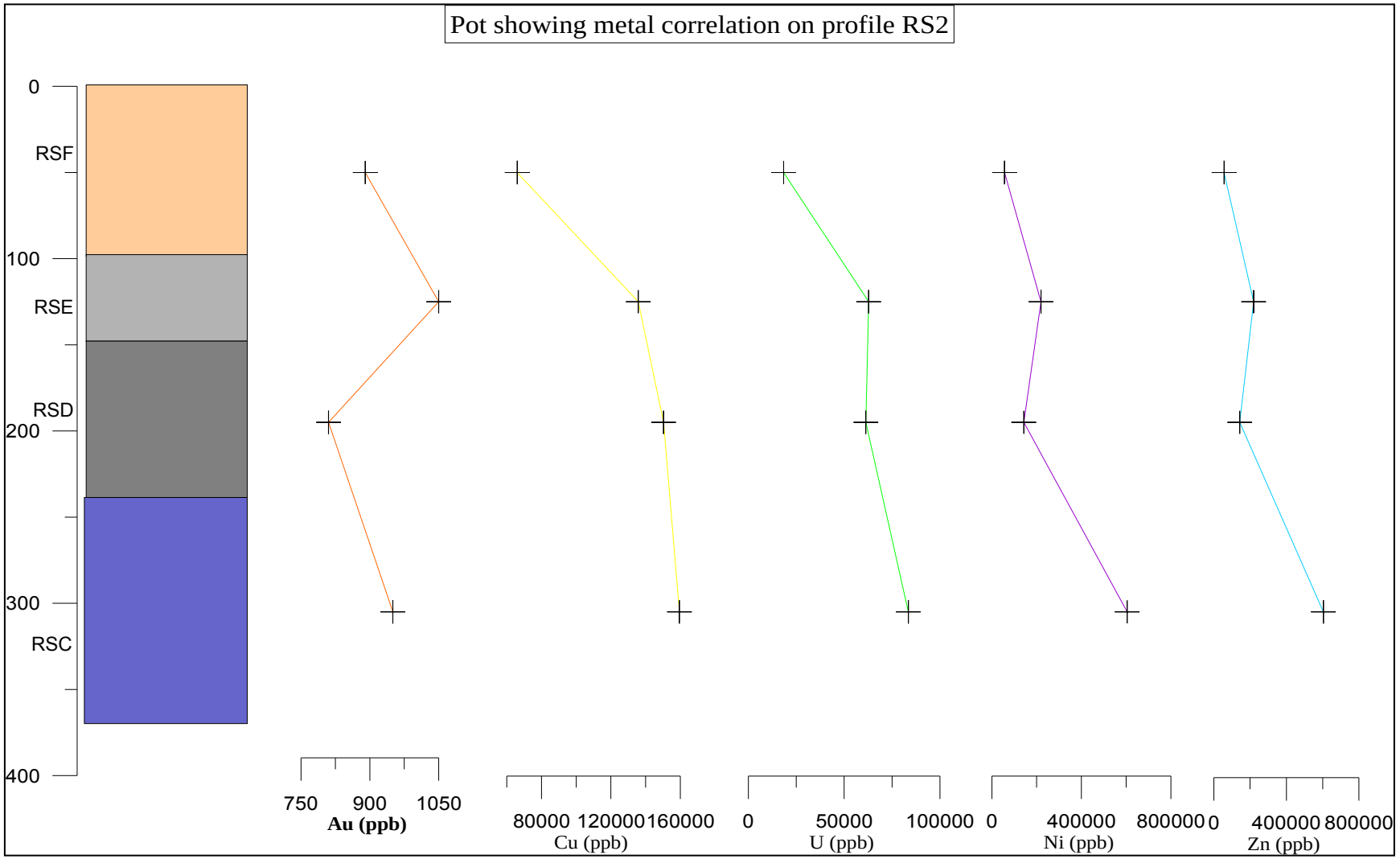


Fig.29. Comparative graphs of metals along profile RS2 on Russel Stream. See figure 23 for full description of stratigraphy.

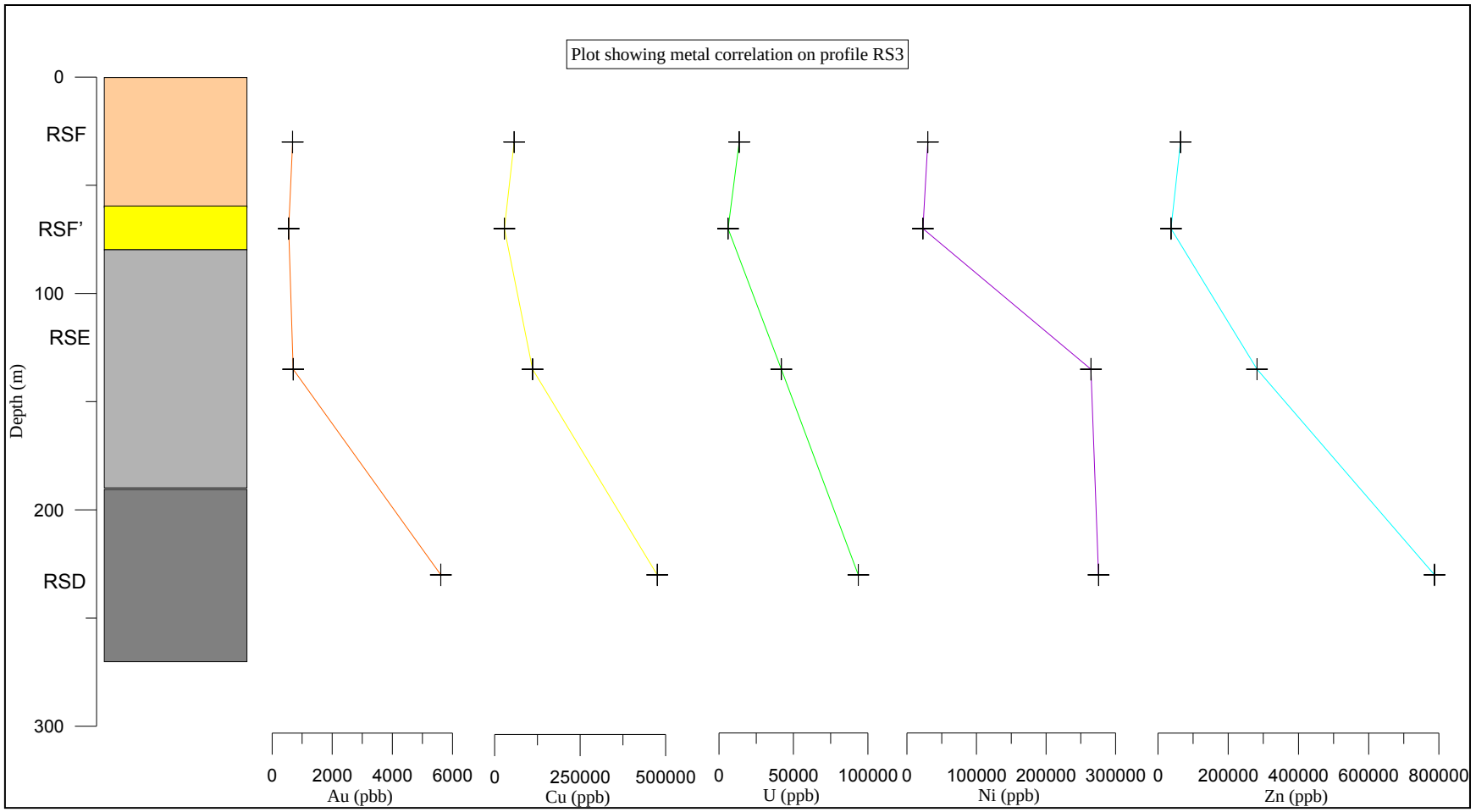


Fig.30. Comparative graphs of metals along profile RS3 on Russel Stream. See figure 23 for full description of stratigraphy.

VIII.4.ii.b. Inductively Coupled Plasma-Mass Spectroscopy (ICP-MS) analysis of Russel Stream sediments

The results of ICP-MS analysis for the Russel Stream sediments are shown in Tables 13i)-iv). Different analytical methods were used for different elements.

Table 13.i) ICP-MS analysis by HNO_3 leach for As and Se. Table 13.ii) ICP-MS analysis by gold mehtod for Co, Pt and Au.

Table 13. a) ICP-MS analysis by HNO_3 leach for As and Se; b) ICP-MS analysis by gold method for Co, Pt and Au; c) ICP-MS analysis by Aqua Regia – leach for Ni, Cu, Cd, Hg and Pd; d) ICP-MS analysis by HF/ $HClO_4$ decomposition for Bi, Th and U. The description of each sample is given in the legend of figure 22.

Table 13a

Samples	Sediment type	As (75) ppb	Se (82) ppb
RS 1A	Dark clay soil	2 900	400
RS 1B	Primary alluvial sand	8 500	200
RS 1C'	Flash-flood sand	79 200	400
RS 1C	Lower banded clay	113 200	700
RS 1D	Upper banded clay	175 400	1 200
RS 1E	Massive clay	120 300	900
RS 1F	Fragile silt	93 900	700
RS 2C'	Flash-flood san	143 200	500
RS 2C	Lower banded clay	127 300	1 000
RS 2D	Upper banded clay	183 100	1 000
RS 2E	Massive clay	183 200	1 400
RS 2F	Fragile silt	100 600	500
RS 3C'	Flash-flood sand	48 600	300
RS 3C	Lower banded clay	140 800	1 400
RS 3D	Upper banded clay	106 100	800
RS 3F'	Flash-flood sand	38 600	200
RS 3F	Massive clay	58 300	400
RS 4C	Lower banded clay	150 300	800
RS 4D	Upper banded clay	94 300	1 000
RS 4F	Fragile silt	41 500	400
RS 5F	Fragile silt	53 500	600
RS 5G	Dark peat	98 600	1 200

Table 13b

Samples	Co (59) ppb	Pt (194) ppb	Au (197) ppb
RS 1A	24 800	< 10	160
RS 1B	9 500	< 10	570
RS 1C'	7 800	20	650
RS 1C	80 300	< 10	1 340
RS 1D	25 800	15	920
RS 1E	28 300	11	1 690
RS 1F	38 200	11	1 400
RS 2C'	6 700	12	810
RS 2C	105 700	< 10	950
RS 2D	19 100	< 10	810
RS 2E	27 400	15	1 050
RS 2F	8 900	12	890
RS 3C'	5 700	< 10	660
RS 3C	52 800	< 10	5 610
RS 3D	40 500	11	700
RS 3F'	4 100	< 10	550
RS 3F	4 300	< 10	680
RS 4C	11 900	< 10	1 040
RS 4D	9 800	< 10	570
RS 4F	4 500	< 10	470
RS 5F	3 500	< 10	380
RS 5G	72 400	19	1 060

Table 13c

Samples	Sediment type	Ni (60) ppb	Cu (63) ppb	Zn (66) ppb	Cd (111) ppb	Hg (202) ppb	Pb (208) ppb
RS 1A	Dark clay soil	97 700	22 600	404 300	70	100	11 000
RS 1B	Primary alluvial sand	53 300	31 600	248 000	130	500	31 400
RS 1C'	Flash-flood sand	52 300	49 000	79 000	120	2 500	57 800
RS 1C	Lower banded clay	411 500	147 000	565 900	1 010	5 500	126 800
RS 1D	Upper banded clay	195 600	128 000	193 000	340	9 600	162 300
RS 1E	Massive clay	147 400	99 000	119 200	290	8 500	169 400
RS 1F	Fragile silt	106 700	142 600	168 100	310	2 400	201 100
RS 2C'	Flash-flood san	47 500	67 800	61 200	90	4 100	97 100
RS 2C	Lower banded clay	604 400	159 400	651 600	970	7 900	130 900
RS 2D	Upper banded clay	142 500	150 300	150 400	380	8 500	181 600
RS 2E	Massive clay	219 600	135 700	248 600	460	13 700	212 800
RS 2F	Fragile silt	56 200	66 000	97 600	190	4 100	325 200
RS 3C'	Flash-flood sand	41 600	23 300	44 100	80	1 300	43 600
RS 3C	Lower banded clay	275 600	475 700	787 600	1 650	12 200	147 000
RS 3D	Upper banded clay	264 700	110 900	282 100	570	8 000	156 900
RS 3F'	Flash-flood sand	22 900	28 400	37 100	50	400	36 300
RS 3F	Massive clay	29 900	56 900	64 300	100	1 600	77 000
RS 4C	Lower banded clay	70 000	93 600	141 100	1 900	6 600	126 500
RS 4D	Upper banded clay	68 100	89 000	84 500	1 340	6 200	92 800
RS 4F	Fragile silt	28 100	84 500	76 000	300	900	258 800
RS 5F	Fragile silt	23 700	26 600	34 900	50	700	81 800
RS 5G	Dark peat	312 400	75 300	140 200	280	2 100	78 600

Table 13d

Samples	Sediment type	Bi (209) ppb	Th (232) ppb	U (238) ppb
RS 1A	Dark clay soil	370	5 500	4 800
RS 1B	Primary alluvial sand	440	5 500	10 400
RS 1C'	Flash-flood sand	770	5 400	20 800
RS 1C	Lower banded clay	1 920	12 200	87 300
RS 1D	Upper banded clay	2 630	9 700	63 600
RS 1E	Massive clay	3 270	9 200	61 700
RS 1F	Fragile silt	1 310	7 700	43 800
RS 2C'	Flash-flood san	1 660	7 100	32 200
RS 2C	Lower banded clay	2 260	9 200	83 500
RS 2D	Upper banded clay	2 730	14 000	61 300
RS 2E	Massive clay	4 430	11 500	62 800
RS 2F	Fragile silt	1 160	5 400	18 400
RS 3C'	Flash-flood sand	580	4 300	7 900
RS 3C	Lower banded clay	1 680	12 000	93 600
RS 3D	Upper banded clay	2 610	9 700	41 900
RS 3F'	Flash-flood sand	450	4 100	6 100
RS 3F	Massive clay	960	4 900	13 600
RS 4C	Lower banded clay	2 060	9 200	46 200
RS 4D	Upper banded clay	1 790	7 600	25 300
RS 4F	Fragile silt	540	4 000	17 100
RS 5F	Fragile silt	550	4 200	8 200
RS 5G	Dark peat	1 230	6 500	54 500

ICP-MS was carried out on Russel Stream sediments to analyze Au and other elements that could not be analyzed by XRF. The analytical quality of XRF was also checked by a correlation matrix as presented in Appendix A.2. High Au values occur in samples RS1C, RS1E, RS1F, RS2E, RS3C, RS4C (mud) and RS5G (organics) (fig 22). Ni, Cu and Zn have relatively very high values in samples RS1C, RS2C, RS3C and RS3D.

It's already been shown in Section VI.4.B.i. that these metals co-precipitate. Table 14 is a correlation matrix drawn from the results of ICP-MS. From the Table it can be seen that except for Pb, almost all of the trace elements show

considerable correlation with one another with R-square values above 0.5 (highlighted in bold).

Table 14: Correlation matrix for the trace elements from ICP-MS (Russel Stream). Concentrations of elements are in ppb.

	As	Se	Co	Au	Ni	Cu	Zn	Cd	Hg	Pb	Bi	Th	U
As	**1.00**	**0.78**	0.31	0.36	0.42	**0.52**	0.21	0.45	**0.86**	0.49	**0.85**	**0.82**	**0.76**
Se		**1.00**	**0.53**	**0.53**	**0.58**	**0.67**	0.44	**0.53**	**0.85**	0.35	**0.76**	**0.75**	**0.80**
Co			**1.00**	0.34	**0.97**	0.47	**0.76**	0.38	0.37	0.07	0.32	**0.51**	**0.77**
Au				**1.00**	0.31	**0.93**	**0.63**	**0.54**	**0.54**	0.19	0.21	0.48	**0.62**
Ni					**1.00**	0.48	**0.77**	0.40	**0.51**	0.12	0.46	**0.59**	**0.81**
Cu						**1.00**	**0.73**	**0.63**	**0.68**	0.32	0.37	**0.67**	**0.76**
Zn							**1.00**	**0.53**	0.47	0.02	0.22	**0.56**	**0.69**
Cd								**1.00**	**0.55**	0.14	0.34	**0.56**	**0.58**
Hg									**1.00**	0.45	**0.90**	**0.85**	**0.79**
Pb										**1.00**	0.45	0.33	0.34
Bi											**1.00**	**0.80**	**0.70**
Th												**1.00**	**0.87**
U													**1.00**

CHAPTER NINE

DISCUSSION AND CONCLUSSIONS

Fleurhof Dam (on Rand Leases) and Russel Stream dam (on Crown mines were built at the turn of the 20th century on boggy wetlands and vleis to serve mines of the Central Rand. The dams have accumulated tailings material eroded from surrounding tailings dams for over 100 years, trapping the heavy metals in them. Although the sediments in Fleurhof Dam have been partly removed by Crown Gold Recovery, an exposed unmined face of the sediments upstream of the dam revealed a well layered stratigraphy that is comparable to an exposure of sediment in the Russel Stream Dam made by a relatively recent erosion channel of the stream.

IX.1. STUDY METHODOLOGY

Study methodology and experimental procedures were similar for both deposits and include mapping and sampling of sediments, modelling, stratigraphic logging and profiling, mineralogical analysis and geochemical analysis. However, whereas ICP-OES was done on Fleurhof Dam sediments, ICP-MS was done on Russel Stream sediments to analyze for Au, and to check the accuracy of XRF analysis. These geochemical analyses all point to heavy metal concentrations higher in dam sediments than in the surrounding tailings dumps from where they were washed-off by running waters. Correlation matrixes show considerable closeness in the analytical quality of these different methods.

IX.2. SEDIMENTOLOGY

The depositional styles of both deposits are similar to a Mississippi type delta, with Fleurhof Dam Being fed by the upper Klipspruit while the Russel Stream dam is fed by the Russel Stream. In general the zone of greatest thickness of sediments occurs along the main river channels and their tributaries and decreases outward on both sides toward the edges of the dams. The maximum thickness of sediments in Fleurhof Dam is obtained upstream at the bar back (Fig. 4). This is the normal deltaic depositional style as illustrated in figure 10. In Russel Stream dam the known maximum thickness is at the dam wall in Dam B (Figs. 24 and 25). Behind the dam wall sediments are mostly entrained from the Golf Course dump as already explained above.

The layers of sediments in Fleurhof Dam are generally similar to those of the Russel Stream dam with much of the sediments being mud and silt.

Characteristic silt (tailings) partings are present in both deposits. These parting are probably caused by seasonal flash-floods, and their frequency of occurrence and size portray some climatic cycles. The peat at the bottom of the deposits probably represents the original surface before younger sedimentary accumulations began. In the Fleurhof Dam this layer occurs consistently along the studied section (Fig. 8). In Russel Stream it is only observed at profile RS5, (Fig. 23). Fleurhof Dam occurs in a wetland covered with reeds. It's probable that more peat would have been formed in Fleurhof Dam than in Russel Stream. The

primary alluvial sand. Layer RSB that only occurs in patches in Russel Stream dam is a counterpart of F8 in the Fleurhof Dam.

IX.3. MINERALOGY

There is close similarity in the mineralogy of both deposits. The same mineral assemblages occur in both deposits although in different proportions, and these mineral assemblages are strongly related to the geology of the Central Rand conglomerate reefs. Quartz represents the most abundant mineral and also occurs in all samples of the Russel Stream sediments as is the case of the Fleurhof Dam sediments. In the Russel Stream sediments, muscovite is the second most abundant mineral. This is contrary to the situation for the Fleurhof Dam sediments where pyrophyllite is more abundant in the dam sediments than muscovite. Muscovites is a flaky mineral more easily trapped by organic matter than pyrophyllite, making the mineralogy of the Russel Stream sediments more comparable with that of the stream sediments immediately north of the Fleurhof Dam deposit than with the actual dam sediments. The Russel Stream sediments show very low or no illite content as is the case with samples SS1-SS6 (stream sediments) of the Fleurhof Dam. Clay minerals are more easily washed away by water.

IX.4. GEOCHEMISTRY

IX.4i. MAJOR ELEMENTS

Major elements analyses of both studies were done by XRF at the School of Geosciences at the University of the Witwatersrand, Joannesburg. The analyses show that the sediments of both dams are silica enriched. Ternary plots indicate the dominance of quartz in the samples of both dams. The samples from Fleurhof Dam, however seem to contain slightly more Al_2O_3 than their Russel Stream counterparts. Fleurhof Dam is situated in a wetland and on a slightly lower elevation than the Russel Stream dams. It is possible that more clay material would accumulate in this depression (Fleurhof Dam) than in the Russel Stream dams which are situated on an inclined topography. In-coming water would stay for a longer period in Fleurhof Dam, giving enough time for more very fine material (clay) to settle than it will in the Russel Stream dams.

IX.4II. TRACE ELEMENTS

The trend is generally similar with high heavy metal concentrations in the carbonaceous mud layers of both dams. However the pattern of metal concentration is slightly different. Whereas metal concentration is higher in the layers near the surface of the Fleurhof Dam sediments, the tendency is for metal concentration to be higher in the bottom layers than in the layers near the surface for the Russel Stream sediments. This difference in pattern (Figs. 15, 16 and 17 for Fleurhof Dam and figures 28, 29 and 30 for Russel Stream), is not well understood. Layer RSE of the Russel Stream dam is the massive light grey mud

with very fine silt partings and is a counterpart of layer F2 of the Fleurhof Dam in which high concentrations of metals were noticed. The concentration of gold in layer RSB in Russel Stream, which is a counterpart of layer F8 in the Fleurhof Dam (where high gold concentration was noticed), is very low. This is evidence that the gold in layer F8 of Fleurhof Dam might be coming from water rising from the layer below or occurring as primary alluvial gold.

Modelling of sediment thickness and gold grade distribution in both deposits showed that the concentration of gold in dam sediments can be of great economic importance, as has been demonstrated by Crown Gold Recovery operations at Fleurhof Dam.

REFERENCES

Anthony, M., 1998. Introduction to mineral exploration. Oxford Blackwell Science, 396 p.

Blatt, H., 1980. Origin of sedimentary rocks. Englewood Cliffs, N.J.: prentice-hall, 2nd ed., 782 p.

Burke K., Kidd W.S.F. and Kusky T.M., (1986). Archaean foreland basin tectonics in the Witwatersrand, South Africa. Tectonics, 5, 406-433.

Colella, A. and David, B., 1990. Coarse-grained deltas, Oxford Blackwell Scientific, 357 p.

Dag, N. et al., 1982. Deltaic sedimentation on the Louisiana Coast. A collection of papers prepared in connection with the GCS-SEPM Spring Field Trip, April, pp 10-11, 1982, pp 36-37.

Department of Minerals and Energy, 2005. South Africa's Mineral Industry 2004/2005, pp 4-9.

Down, C.G. and Stocks, J., 1977. Environmental Impact of Mining. London: Applied Science Publishers, 371 p.

Galloway, W.E., 1989. Depositional systems and shelf-slope relationships in Upper Pennsylvanian rocks, North-Central Texas. Austin: Texas univ., 62 p.

Gordon, K., 2004. Introducing the Terraspec ^{Tm}. Terraspec ^{Tm} handouts, pp 1-3.

Hallbauer, D.K., 1986. The mineralogy and geochemistry of Witwatersrand pyrite, Gold, Uranium and carbonaceous matter'. In: Anhaeusser, C.R. and Maske, S (ed). Mineral deposits of South Africa, Johannesburg, pp 1,731 –752.

Hatch, F.H. and Chalmers, J.A., 1895. The gold mines of the Central Rand, London: Macmillan, 306 p.

Mphephu, N.F., 2001.Enviromental issues related to the underground workings of the central Rand goldfields, Johannesburg, South Africa. MSc degree thesis, Faculty of Science, University of the Witwatersrand, Johannesburg, pp 1, 40–43.

Mphephu, N.F., Viljoen, M.J. and Anne garn, H.J., 2003.Geochemistry of mine tailings and contribution to soil and water pollution on the Central Rand, pp 3 – 4.

Ndasi, M.B., 2004. The geochemistry and mineralogy of mine tailings sediments in the Fleurhof Dam and their contribution to pollution in the Fleurhof Wetland, Central Rand. BSc with Honours degree thesis, Faculty of Science, University of the Witwatersrand, Johannesburg, pp 1, 2, 26 – 28, 40-51.

Pretorius, D.A, 1964."The geology of the Central Rand Goldfield". In: Hanton, S.H.(ed), The geology of some ore deposits in Southern Africa. Vol 1.Geol.Soc.S.Africa, Johannesburg, pp 27 – 30.

Robb, L.J. and Meyer, F.M., 1995. The Witwatersrand Basin, South Africa: Geological framework and mineralization processes. Ore Geology Reviews, pp 10, 67 – 94.

Tankard, A.J., Jackson, M.P.A, Erickson, K.H., Hobday, D.K., Hunter, D.R and Minter, W.E.L., 1982. Crustal Evolution of Southern Africa. Spinger-Verlog, Berlin, pp 231 – 333.

Tutu, H., E. Cukrowska, 2004. Transport and fate of uranium from gold tailings dams based on computer modelling of its speciation. Proceedings to the adances in mineral resources management and environmental geotechnology conference, Hania, Greece, pp 559-563.

Werdmuller, V.W., 1986."The central Rand". In: E.S.A. Antrobus(ed). Witwatersrand gold-100years.Geol.Soc.S.Afr, Johannesburg, pp 7 – 31.

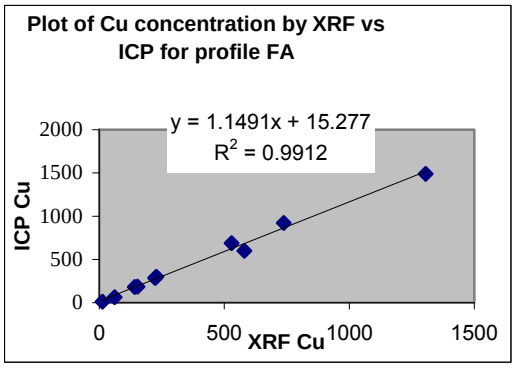
Laing, W., 20 Nov. 2005. Personal communication.

Appendix

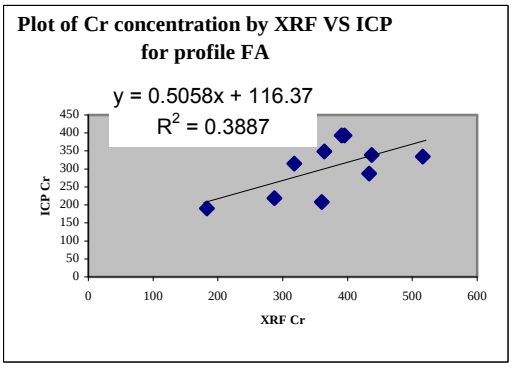
A. Analytical quality

A.1. XRF and ICP-OES analyses of Fleurhof Dam sediments

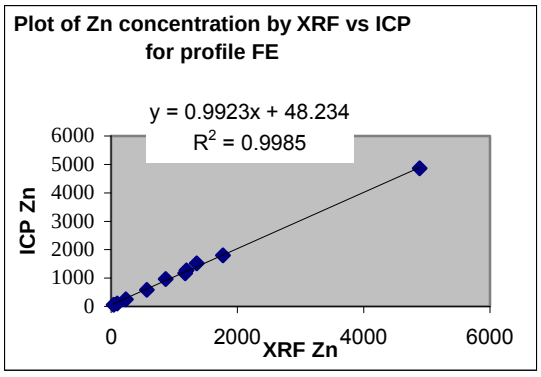
Comparative graphs for XRF and ICP analyses for selected metals of the Fleurhof Dam deposit were drawn to check accuracy of the above two methods used. Figures A.1.1 a) – d) are comparative graphs for the two methods.



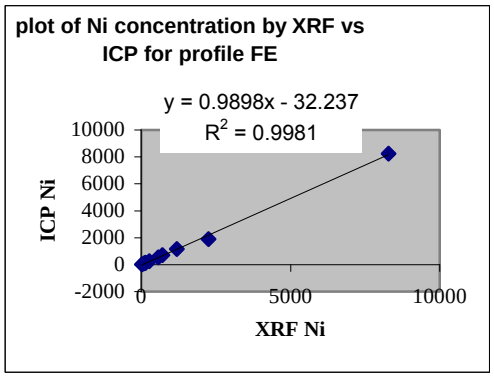
(a)



(b)



(b)



(d)

Figs. A.1.1 a) – d): graphs of comparison between XRF and ICP analyses for trace elements.

From the graphs above it is seen that there is a close correlation in the results of the two methods. Exceptions in accuracy may be due to errors from instruments, calibration or sample contamination during sample preparations. R-squared values from 0.5 –1 are considered to show correlation or closeness in results to some extent. This means that all metal from ICP that makes an R-squared value from 0.5 – 1 with another metal from XRF was accurately analysed, to some extent, by both methods. Such values are highlighted in bold in Table I1.1, which is a ccorrelation matrix showing a further comparison of the two methods, considering only those elements analysed by both methods. This Table also shows that, except for Sr (R-square value highlighted in blue), which shows no correlation in the two methods, all the other metals have considerably similar measurements for both methods (R-square values highlighted in red).

Table I1.1: Correlation matrix for the XRF and ICP-OES analyses

	Pb-X	As-X	U-X	Th-X	Sr-X	Co-X	Ni-X	Cu-X	Zn-X	Cr-X	Ba-X	Co-I	Ni-I	Cu-I	Zn-I	As-I	Sr-I	Ba-I	Th-I	U-I	Pb-I	Cr-I
Pb-X	**1.00**	**0.70**	**0.67**	**0.58**	**0.76**	**0.58**	**0.60**	**0.69**	**0.58**	**0.67**	0.43	**0.59**	**0.59**	**0.69**	**0.57**	**0.66**	-0.10	**0.61**	0.43	**0.51**	**0.80**	**0.59**
AS-X	**0.70**	**1.00**	**0.95**	**0.64**	**0.50**	**0.89**	**0.93**	**0.91**	**0.86**	**0.62**	0.35	**0.87**	**0.91**	**0.93**	**0.84**	**0.98**	-0.08	0.37	0.35	**0.76**	0.35	0.49
U-X	**0.67**	**0.95**	**1.00**	**0.66**	0.44	**0.95**	**0.96**	**0.96**	**0.92**	**0.61**	0.30	**0.94**	**0.96**	**0.96**	**0.91**	**0.95**	-0.05	0.31	0.41	**0.77**	0.41	**0.53**
Th-X	**0.58**	**0.64**	**0.66**	**1.00**	**0.62**	**0.66**	**0.66**	**0.58**	**0.60**	0.20	0.11	**0.64**	**0.65**	**0.60**	**0.58**	**0.65**	0.00	0.12	**0.78**	**0.50**	0.37	0.18
Sr-X	**0.76**	**0.50**	0.44	**0.62**	**1.00**	**0.41**	0.43	0.47	0.45	**0.51**	0.42	0.40	0.42	0.49	0.44	**0.48**	-0.09	0.55	0.47	0.30	**0.57**	**0.50**
Co-X	**0.58**	**0.89**	**0.95**	**0.66**	0.41	**1.00**	**0.99**	**0.89**	**0.94**	**0.50**	0.19	**1.00**	**1.00**	**0.88**	**0.93**	**0.90**	-0.03	0.27	0.43	**0.69**	0.39	0.48
Ni-X	**0.60**	**0.93**	**0.96**	**0.66**	0.43	**0.99**	**1.00**	**0.91**	**0.94**	**0.52**	0.22	**0.99**	**1.00**	**0.91**	**0.93**	**0.93**	-0.03	0.29	0.41	**0.70**	0.36	0.49
Cu-X	**0.69**	**0.91**	**0.96**	**0.58**	0.47	**0.89**	**0.91**	**1.00**	**0.89**	**0.68**	0.37	**0.88**	**0.90**	**0.99**	**0.88**	**0.89**	-0.07	0.39	0.38	**0.74**	0.45	**0.55**
Zn-X	**0.58**	**0.86**	**0.92**	**0.60**	0.45	**0.94**	**0.94**	**0.89**	**1.00**	**0.60**	0.23	**0.93**	**0.94**	**0.89**	**1.00**	**0.88**	-0.05	0.40	0.40	**0.73**	0.39	**0.57**
Cr-X	**0.67**	**0.62**	**0.61**	0.20	**0.51**	**0.50**	**0.52**	**0.68**	**0.60**	**1.00**	**0.50**	0.48	**0.51**	**0.68**	**0.60**	**0.60**	-0.11	**0.73**	0.04	**0.51**	0.44	**0.82**
Ba-X	0.43	0.35	0.30	0.11	0.42	**0.19**	0.22	0.37	0.23	**0.50**	**1.00**	0.18	0.20	0.41	0.22	0.33	-0.19	**0.53**	-0.01	0.27	0.27	**0.52**
Co-I	**0.59**	**0.87**	**0.94**	**0.64**	0.40	**1.00**	**0.99**	**0.88**	**0.93**	0.48	0.18	**1.00**	**0.99**	**0.87**	**0.93**	**0.88**	-0.02	0.27	0.46	**0.70**	0.43	0.49
Ni-I	**0.59**	**0.91**	**0.96**	**0.65**	0.42	**1.00**	**1.00**	**0.90**	**0.94**	**0.51**	0.20	**0.99**	**1.00**	**0.90**	**0.93**	**0.92**	-0.03	0.28	0.43	**0.71**	0.38	0.49
Cu-I	**0.69**	**0.93**	**0.96**	**0.60**	0.49	**0.88**	**0.91**	**0.99**	**0.89**	**0.68**	0.41	**0.87**	**0.90**	**1.00**	**0.88**	**0.92**	-0.07	0.40	0.38	**0.76**	0.42	**0.56**
Zn-I	**0.57**	**0.84**	**0.91**	**0.58**	0.44	**0.93**	**0.93**	**0.88**	**1.00**	**0.60**	0.22	**0.93**	**0.93**	**0.88**	**1.00**	**0.87**	-0.05	0.41	0.41	**0.71**	0.40	**0.58**
As-I	**0.66**	**0.98**	**0.95**	**0.65**	0.48	**0.90**	**0.93**	**0.89**	**0.88**	**0.60**	0.33	**0.88**	**0.92**	**0.92**	**0.87**	**1.00**	-0.07	0.36	0.42	**0.81**	0.39	**0.52**
Sr-I	-0.10	-0.08	-0.05	0.00	-0.09	-0.03	-0.03	-0.07	-0.05	-0.11	-0.19	-0.02	-0.03	-0.07	-0.05	-0.07	**1.00**	-0.13	0.05	-0.06	-0.05	-0.05
Ba-I	**0.61**	0.37	0.31	0.12	**0.55**	0.27	0.29	0.39	0.40	**0.73**	**0.53**	0.27	0.28	0.40	0.41	0.36	-0.13	**1.00**	0.12	0.23	**0.53**	**0.73**
Th-I	0.43	0.35	0.41	**0.78**	0.47	0.43	0.41	0.38	0.40	0.04	-0.01	0.46	0.43	0.38	0.41	0.42	0.05	0.12	**1.00**	0.36	**0.53**	0.15
U-I	**0.51**	**0.76**	**0.77**	**0.50**	0.30	**0.69**	**0.70**	**0.74**	**0.73**	**0.51**	0.27	**0.70**	**0.71**	**0.76**	**0.71**	**0.81**	-0.06	0.23	0.36	**1.00**	0.30	0.39
Pb-I	**0.80**	0.35	0.41	0.37	**0.57**	0.39	0.36	0.45	0.39	0.44	0.27	0.43	0.38	0.42	0.40	0.39	-0.05	**0.53**	**0.53**	0.30	**1.00**	**0.51**
Cr-I	**0.59**	0.49	**0.53**	0.18	**0.50**	0.48	0.49	**0.55**	**0.57**	**0.82**	**0.52**	0.49	0.49	**0.56**	**0.58**	**0.52**	-0.05	**0.73**	0.15	0.39	**0.51**	**1.00**

X = XRF

I = ICP-OES

A.2. XRF and ICP-MS analyses of Russel Stream sediments

Co, Ni, Cu and Zn are the few elements of the Russel Stream sediments that were analysed by both XRF and ICP-MS. A correlation matrix was done for these elements as shown in Table A.2.1. This Table shows considerably similar measurements of the same elements for both methods (R-square values highlighted in red).

Table A.2.1: Correlation matrix for the XRF and ICP-MS analyses

	Co(ICP)	Ni(ICP)	Cu(ICP)	Zn(ICP)
Co(XRF)	**0.77**	**0.81**	0.37	**0.56**
Ni(XRF)	**0.78**	**0.82**	0.32	**0.55**
Cu(XRF)	0.39	0.41	**0.92**	**0.63**
Zn(XRF)	**0.65**	**0.71**	**0.56**	**0.78**

X-XRF
MS-ICPMS